**CHARLES UNIVERSITY IN PRAGUE**

**FACULTY OF SCIENCES**

**Ph.D. Thesis**

**2013** **Elvia Amparo Rosero Alpala**

**CHARLES UNIVERSITY IN PRAGUE, FACULTY OF SCIENCES**

**Department of Experimental Plant Biology**

**Ph.D. study program: Plant Anatomy and Physiology**

## Ph.D. Thesis

# ROLE OF FORMINS IN THE ORGANIZATION AND DYNAMICS OF INTRACELLULAR STRUCTURES IN *Arabidopsis thaliana*

**Elvia Amparo Rosero Alpala**

**Thesis Supervisors:**

**Doc. RNDr. Fatima Cvrčková, Dr.rer.nat. and**

**RNDr. Viktor Žárský, CSc.**

**Prague, 01.08. 2013**

## ACKNOWLEDGEMENTS

I would like to thank Fatima Cvrčková and Viktor Žárský to give me the oportunity to work in their research team, for the guidance, advice and support they have provided throughout my studies. I would also like to thank all members of the Department of Experimental Plant Biology-Charles University in Prague who taught me different methods used in my experiments, specially Anatomy lab members.

Definitely, I would like to thank my colleagues and latin friends who have made great my stay in Czech Republic and at University. To my loved ones who always have given me support, encourage and joy to my life.

Finally, after five years that I have been in Czech Republic and consider it as my second home I would like to thank Czech Government-Ministry of Education, Youth and Sport- for giving us the oportunity to know this beautiful country and study by the scholarship offered to members of developing countries.

**CONTENT**

## ABSTRACT

On the basis of detailed phenotypic examination of *fh1* and *fh2* mutants we observed that the main housekeeping *Arabidopsis thaliana* formin AtFH1 (At3g25500) and its closest relative, *AtFH2* (At2g43800) are involved in both actin filaments and microtubule dynamics. *fh1* mutants showed increased sensitivity to the actin polymerization inhibitor Latrunculin B (LatB). Formin mutants had cotyledon pavement cells which exhibited more pronounced lobes compared to the wild type, and alterations in vascular tissue patterning were found. The double *fh1 fh2* homozygote was not obtained, suggesting that at least one functional formin gene is required for proper gametophyte development. Methods used to observe and quantify both architecture and dynamics of the cortical cytoskeleton from confocal laser scanning microscopy (CLSM) and variable angle epifluorescence microscopy (VAEM) were standarized and allowed to find that mutants exhibited more abundant but less dynamic F-actin bundles and more dynamic microtubules than wild type seedlings, *fh1* mutant phenotype observed in roots was further aggravated by a (heterozygous) *fh2* mutation. The formin inhibitor SMIFH2 mimicked the alterations observed in *fh1* mutants in plants, it has been the first report of this inhibitor in plants. Defects in membrane trafficking were observed in formin mutants and confirmed by SMIFH2 inhibitor which slowed down the movement of CLC-GFP dots.

# 1. INTRODUCTION

Plant growth, development and morphogenesis are processes influenced by the organization and dynamics of cytoskeletal components. Two important polymeric macromolecules have been considered to be the major components in the cytoskeleton, microtubules and microfilaments. Their essential role on cell growth and shape determination is due to their influence on both coordinated expansion/recycling of plasma membrane and on cell wall assembly by controlling matrix materials deposition and cellulose microfibrils arrangement (for review see Szymanski and Cosgrove, 2009; Hussey et al., 2006; Smith and Oppenheimer, 2005; Mathur, 2004; Zarsky et al., 2009).

## 1.1. Overview of actin cytoskeleton role in cellular processes

Actin cytoskeleton is a highly dynamic network essential for a wide variety of basic cellular processes (see Schmidt and Hall, 1998; Dobrak et al., 2004; Hussey et al., 2006). The actin filaments turnover depends of accessory proteins activity which maintain the balance of actin monomers, initiate polymerization, restrict the length of actin filaments, regulate the assembly and turnover of actin filaments, and cross-link filaments into networks or bundles (see Pollard and Cooper, 2009; Chen et al., 2000). These events conform the known actin stochastic dynamic model which generate flexibility in the actin filament network (Smertenko et al., 2010; Staiger et al., 2009).

Actin filaments arrangement and dynamics modulate the membrane trafficking (see Pollard and Cooper, 2009; Mooren et al., 2012). In mammalian and yeast cells, F-actin dynamics are required for multiple distinct stages of clathrin-coated vesicle formation, including coated pit formation, constriction, and internalization (Yarar et al., 2005), "actin patches" assembled by actin nucleators such as Arp2/3 provide force to form and internalize an endocytic vesicle from the plasma membrane (Ferguson et al., 2009; see Pollard and Cooper, 2009) and endosomes motility can be modulated by stabilizing their association with the actin cytoskeleton through Diaphanous-related Formin, hDia2C (RhoD effector) (Gasman et al., 2003). In migrating cells, the formation of lamellipodium and fillopodium extension are produced by Rho GTPases activation of WASP/WAVE proteins- ARP2/3 complex and Diaphanous-related formins (DRFs) which induce nucleation and extension of branching and non-branching actin filaments, respectively, and then plasma membrane protrusion is stimulated (see Ridley, 2006, Vaskovicova et al., 2013).

On the other hand, actin cables are involved in the transport of secretory vesicles (see Pruyne and Bretscher, 2000); localization of components of exocytic machinery and secretory vesicles are affected by disruption of cytoskeleton (Zhang et al., 2001); however, vesicle tethering at the plasma membrane by the exocyst seems to be cytoskeleton- independent mechanism (Bendezu and Martin, 2011). In yeast, actin cables formation and stabilization is directed by formins, for example Bni1p and Bnr1p, which are activated by Rho proteins and their loss of function rapidly depolarizes vesicular targeting and misorients the mitotic spindle (Dong et al., 2003; Evangelista et al., 2002). Double mutant of formin –for3- and

its activator –Rho3- not only displayed abnormal F-actin cytoskeleton but also in cytoplasmic microtubules organization affecting the normal delivery of vesicles (Nakano et al., 2002) and at the same time Rho3 showed strong genetic interactions with exocyst component, Exo70, involved during docking and fusion of secretory vesicles at the plasma membrane (Adamo et al., 1999). Cell shape changes are induced by the turnover between branched and unbranched filaments, according to the presence of the dense network of short, branched actin filaments assembled by Arp2/3 complex or formins-assembled polarized filaments which form bundles that serve as tracks for vesicle-organelle movement (see Pollard and Cooper, 2009).

In plant cells; the Arp2/3 complex and formin family play an essential role during *De novo* actin polymerization; profilin, ADF/Cofilin and CAP proteins maintaining control over the subunit pool; capping protein and villin/gelsolin regulating and creating ends; fimbrins, formins, LIMs and villins involved in actin filaments bundling (see Blanchoin et al., 2010; Staiger and Blanchoin, 2006). The absence or reduced level of these proteins induces alterations in actin organization and dynamics, thereby AtFH1 formin mutation caused reduction of microfilament density and increase of actin bundling (Rosero et al., 2013), similar to some Arabidopsis mutants with altered balance between fine actin filaments and bundles, such as adf4 (Henty et al., 2011) or aip1 (Ketelaar et al., 2004), the knockdown capping mutants showed more dynamic activity at filament ends and enhanced filament-filament annealing (Li et al., 2012) and mutation in the ARP2/3 subunits genes affected the spatial distribution of diffuse F-actin and bundles (Li et al., 2003).

The alterations of actin cytoskeleton architecture and dynamics affect different intracellular processes suggesting several functions for actin including delivery of secretory vesicles to the tip, maintenance of clear zone structure and/or support of endocytic vesicle uptake (see Samaj et al., 2006), microfilaments balance the membrane homeostasis by determination of growth site, Golgi-derived vesicles movement and, in endosomes movement and morphology (Voigt et al., 2005; Guimil and Dunand, 2007), disruption of F-actin by cytochalasin affects the number and distribution of vesicles slowing-down the endocytotic process (Parton et al., 2001).

### 1.2. Cytoskeleton in plant morphogenesis: microtubule - actin crosstalk

Plant cytoskeleton plays important roles in cell shape determination (see Szymanski and Cosgrove, 2009; Smith and Oppenheimer, 2005; Mathur, 2004), microtubules are associated with the cellulose microfibrils arrangement as a key determinant of cell expansion pattern (Bibikova et al., 1999) while microfilaments promote and regulate growth by controlling intracellular trafficking affecting cell wall composition and membrane homeostasis (see Smith and Oppenheimer, 2005; Hussey et al., 2006).

In roots, the growth is result of both controlled cell divisions in the apical meristem and regulated anisotropic cell expansion, and differentiation into the distinct cell types in the elongation zone to create the mature section of a root (Vaughn et al., 2010). Anisotropic cell expansion is modulated by the organization of cortical microtubules and actin filaments. Mutation of genes

associated with microtubule and microfilament network show significant effects on cytoskeleton architecture, stability, density, and often produces deffects in the root growth such as increased root twisting and waving, retarded root growth, left or right-handed helical growth or deffects in root hairs (Thitamadee et al., 2002; Gilliland et al., 2003; Abe and Hashimoto, 2005). The role of the cytoskeleton also has been observed by using inhibitors; LatB induces shorter and thicker roots as response of altered cell expansion rather than cell division (Rosero et al., 2013; Baluska et al., 2001). The effect of LatB on cytoskeleton also disrupt intracellular membrane trafficking (Zhang et al., 2010), crucial for polar auxin transport and root growth (Rahman et al., 2007).

Development of leaf pavement cells might involve a combination of localized tip growth and diffuse growth to produce strangely shaped interlocking cells (see Mathur, 2004). In the stage I, elongated polygons are generated from small and pentagonal or hexagonal initials cells which expand preferentially along the leaf long axis. The stage I cells initiate multiple outgrowths or localized lateral expansion from their anticlinal walls into adjacent cells, producing stage II cells with multiple shallow lobes alternating with indentations or necks. The lobes expand while lobe and neck formation continues, resulting in highly lobed interlocking cells regulated by cell-to-cell signaling (stage III) (Fu et al., 2005). In highly lobed pavement cells, there is no global orientation of microtubules but rather local and periodic patches of parallel polymers that are correlated with the interlocking cells (Fu et al., 2005). Thus, formation of neck regions is dependent on microtubule banding while lobe formation depends on patches of

microfilaments (Fu et al., 2005; Xu et al., 2010; Zhang et al., 2011b; see Kotzer and Wasteneys, 2006).

Many proteins have been identified to be related with the pavement cells morphogenesis by regulation of actin–microtubule arrangement and dynamics (see Mathur, 2006). The pathway of Rho of plant (ROP) GTPase signaling cascades was reported to play an important role in interdigitating cell growth. The Rho of plant (ROP) GTPases and their RIC family interactors play an important role in cell growth by controlling cytoskeleton arrangement and membrane trafficking (see Smith and Oppenheimer, 2005; Hussey et al., 2006; Yalovsky et al., 2008). Microtubule bands in neck regions are induced by the RIC1/ROP6 pathway which antagonizes the RIC4/ROP2 pathway, promoting microfilament assembly in the lobes (Fu et al., 2005; Fu et al., 2009). The ROP6 GTPase signalling pathway induce microtubule severing through Katanin activity for organizing paralleled cortical microtubule arrays (Lin et al., 2013). ROP2 is activated by auxin; it also inhibits PIN1 endocytosis via promoting accumulation of cortical actin filaments, resulting thus in local positive-feedback enhancement of the growth-promoting pathway in lobes (Xu et al., 2010; Nagawa et al., 2012).

The use of mutant lines have shown to be a useful tool to understand the genes involves on cell shape, the T-DNA insertion mutants (*spike1, clasp1-1, distorted, wrm*) expressed a misdirected cell expansion, trichome expansion was randomized, hypocotyl cells curl out of the normal epidermal plane, root hairs are sinuous and pavement cells were smaller and fail to produce lobes, exhibiting a significant reduction in mean lobe length and a corresponding increase in mean neck width (Ambrose et al., 2007; Mathur et al., 2003; Qiu et al., 2002).

Mutations in the Arp2/3 subunit genes (*arp2-1, arp2-2, arp3-1*, and *arpc5-1*) affect the spatial distribution, but not the assembly, of either cortical diffuse F-actin or actin bundles in Arabidopsis leaf pavement cells; neck width was not affected, whereas the lobe height was dramatically reduced (Li et al., 2003).

Actin filaments and microtubules are involved in cell development, their constant remodelling (Staiger et al., 2009; Blanchoin et al., 2010) and crosstalk (Collings et al., 2006; Smertenko et al., 2010; Sampathkumar et al., 2011) may be mediated by bifunctional proteins or protein complexes (see Petrasek and Schwarzerova, 2009), from this side, formins seems to play important role in both actin filaments and microtubules organization and dynamics (Rosero et al., 2013) and their mutations can affect the normal interdigitating cell growth (Rosero et al., 2013 submitted).

### 1.3. Formins and their role in cytoskeleton organization

Formins have been recognized as key molecular regulators of cytoskeletal assembly and organization, because of its ability to promote rapid assembly of actin filaments and in animals some of them interact with microtubules. Formins are the more important nucleator along Arp2/3 complex, Spire and Cordon-bleu, formin proteins stimulate the *de novo* polymerization of actin filaments, are keys for diverse cellular and developmental processes, especially those dependent on polarity establishment (Aspenstrom, 2010; Cheung and Wu, 2004).

The formin family is conformed by 21 *Arabidopsis* genes that are predicted to contain FH2 domain (Deeks et al., 2002). A subset of plant formins, referred to as

group I, is distinct from formins from other species in having evolved a unique N-terminal structure with a signal peptide, a Pro-rich domain, potentially glycosylated extracellular domain, and a transmembrane domain (Banno and Chua, 2000; Cheung and Wu, 2004). Group-II plant formins have FH1 and FH2 domains, no known protein motif has yet been identified in group-II N-termini (Deeks et al., 2002).

Recently, studies show that formin proteins are associated with actin nucleation but also interact with the organization and stability of microtubule cytoskeleton (Palazzo et al., 2001; Wen et al., 2004; reviewed by DeWard and Alberts, 2008; Chesarone et al., 2010). In plant formins, recent studies suggest that formins in plants are important links between the plasma membrane and actin remodeling, and also good candidates in cortical actin and microtubule crosstalk (see van Gisbergen and Bezanilla, 2013; Cvrckova, 2012). AtFH4 formin showed a plant specific region (named the GOE domain) that mediates an association with the microtubule cytoskeleton. Overexpressed AtFH4 accumulates at the endoplasmic reticulum membrane and co-aligns the endoplasmic reticulum with microtubules (Deeks et al., 2010). AtFH14, a type II formin, was found to regulate both microtubule and microfilament arrays. Expression, knockdown and mutation of AtFH14 showed its important role on microtubule and microfilament interaction during plant cell division, its absence showed abnormalities in microtubule arrays, altered interactions between microtubules and microfilaments, resulting in the formation of an abnormal mitotic apparatus or meiosis-associated process (Li et al., 2010).

AtFH1 formin protein, the main housekeeping of formin family, contains a putative signal peptide and a transmembrane domain suggesting its association with membrane Banno and Chua, 2000. Its overexpression of AtFH1 resulted in an abundance of membrane-associated actin cables, induced tube broadening, growth depolarization, and growth arrest in transformed pollen tubes (Cheung and Wu, 2004). Recently, the extracellular domain of AtFH1 formin was studied, AtFH1 forms a bridge that provides stable anchor points for the actin cytoskeleton, across the plasma membrane and is anchored within the cell wall. Proline-rich extracellular domain of AtFH1 has homology with cell-wall extensins (Martiniere et al., 2011).

## 2. AIMS OF THE THESIS

The main aim of this thesis was:

**To study the effect of formin mutations on the organization and dynamics of intracellular structures**

This aim was addressed through the following particular aims:

1. To evaluate phenotypes of knockout AtFH1 and AtFH2 lines (Paper 1 and 2).
2. To investigate the possibility of using cytoskeletal inhibitors in order to uncover the effect of formin mutations (Paper 1 and 2).
3. To observe the effect of formin mutation in *in vivo* fluorescent protein-tagged cytoskeletal markers (GFP-FABD for actin and GFP-MAP4 for microtubules) using CSLM and VAEM microscopy (Paper 1 and 2).
4. To identify different intracellular processes affected by alterations in cytoskeleton organization and dynamics (Paper 2).
5. To optimize methods for quantifying actin filament and microtubule organization and dynamics (Paper 1, 2 and 3).

# 3. THESIS OUTLINE

## 3.1. *Paper 1.* Rosero A, Zarsky V, Cvrckova F. 2013. AtFH1 formin mutation affects actin filament and microtubule dynamics in Arabidopsis thaliana. *J Exp Bot.* 64: 585-597

On the basis of detailed phenotypic examination of *fh1* mutants we observed that AtFH1 is involved in both actin filaments and microtubule dynamics, *fh1* mutants showed increased sensitivity to the actin polymerization inhibitor Latrunculin B (LatB). LatB-treated mutants had thicker and shorter roots than wild type plants which were consistent with deffects in cell expansion. Mutants exhibited more abundant but less dynamic F-actin bundles and more dynamic microtubules than wild type seedlings. Treatment of wild type seedlings with a formin inhibitor, SMIFH2, mimicked the root growth and cell expansion phenotypes and cytoskeletal structure alterations observed in *fh1* mutants. It has been the first report of SMIFH2 inhibitor in plants.

**My contribution:** Phenotypic characterization of *fh1* mutants grown in standard medium and supplemented with inhibitors (LatB, Oryz and SMIFH2). Detailed observations by optical, confocal and VAEM microscopy. Analysis of cytoskeleton organization and dynamics using reported methods. Writing the draft of the manuscript.

*Journal of Experimental Botany*, Vol. 64, No. 2, pp. 585–597, 2013
doi:10.1093/jxb/ers351 Advance Access publication 1 December, 2012
This paper is available online free of all access charges (see http://jxb.oxfordjournals.org/open_access.html for further details)

Journal of Experimental Botany
www.jxb.oxfordjournals.org

RESEARCH PAPER

# AtFH1 formin mutation affects actin filament and microtubule dynamics in *Arabidopsis thaliana*

**Amparo Rosero[1], Viktor Žárský[1,2] and Fatima Cvrčková[1,*]**

[1] Department of Experimental Plant Biology, Faculty of Sciences, Charles University, Viničná 5, CZ 128 44 Praha 2, Czech Republic
[2] Institute of Experimental Botany, Academy of Sciences of the Czech Republic, Rozvojová 135, CZ 160 00 Prague 6, Czech Republic

* To whom correspondence should be addressed. E-mail: fatima.cvrckova@natur.cuni.cz

Received 30 April 2012; Revised 8 November 2012; Accepted 9 November 2012

## Abstract

**Plant cell growth and morphogenesis depend on remodelling of both actin and microtubule cytoskeletons. AtFH1 (At5g25500), the main housekeeping *Arabidopsis* formin, is targeted to membranes and known to nucleate and bundle actin. The effect of mutations in AtFH1 on root development and cytoskeletal dynamics was examined. Consistent with primarily actin-related formin function, *fh1* mutants showed increased sensitivity to the actin polymerization inhibitor latrunculin B (LatB). LatB-treated mutants had thicker, shorter roots than wild-type plants. Reduced cell elongation and morphological abnormalities were observed in both trichoblasts and atrichoblasts. Fluorescently tagged cytoskeletal markers were used to follow cytoskeletal dynamics in wild-type and mutant plants using confocal microscopy and VAEM (variable-angle epifluorescence microscopy). Mutants exhibited more abundant but less dynamic F-actin bundles and more dynamic microtubules than wild-type seedlings. Treatment of wild-type seedlings with a formin inhibitor, SMIFH2, mimicked the root growth and cell expansion phenotypes and cytoskeletal structure alterations observed in *fh1* mutants. The results suggest that besides direct effects on actin organization, the *in vivo* role of AtFH1 also includes modulation of microtubule dynamics, possibly mediated by actin–microtubule cross-talk.**

**Key words:** Actin, *Arabidopsis*, At5g25500, LatB, microtubules, SMIFH2, VAEM.

## Introduction

Plant growth, development, and morphogenesis are intimately associated with the dynamics of both microtubule and actin microfilament cytoskeletons (see, for example, Smith and Oppenheimer, 2005). Plant cell morphogenesis depends on mechanical properties of the cell wall, determined by organization of the cellulose microfibrils, interlinked with cortical microtubules (Emons *et al.*, 2007). Microfilaments contribute less directly, for example via participation in membrane recycling (Bannigan and Baskin, 2005), though they are important in tip-growing cells such as root hairs (Peremyslov *et al.*, 2010).

Root growth results from regulated cell divisions in the meristem, and anisotropic cell expansion and differentation in the elongation and differentiation zones. Mutations affecting the cytoskeleton often affect root growth or root hair development (Thitamadee *et al.*, 2002; Gilliland *et al.*, 2003; Abe and Hashimoto, 2005).

Formins (FH2 proteins) are key eukaryotic cytoskeletal regulators. Their hallmark FH2 domain can dimerize and nucleate actin (Blanchoin and Staiger, 2010). Seed plants have two formin clades with numerous paralogues (Deeks *et al.*, 2002; Grunt *et al.*, 2008); *in vitro* studies of several proteins demonstrated microfilament nucleation, capping, and binding (e.g. Ingouff *et al.*, 2005; Yi *et al.*, 2005). Metazoan formins also participate in remodelling the microtubular cytoskeleton (Bartolini and Gundersen, 2010). Similar observations were also reported for plant formins—*Arabidopsis* AtFH4 and AtFH14 (Deeks *et al.*, 2010; Li *et al.*, 2010) and rice FH5 (Yang *et al.*, 2011; Zhang *et al.*, 2011), which interact with microtubules using diverse mechanisms (see also Wang *et al.*, 2012).

AtFH4 is a class I formin, exhibiting the clade-specific structure with a signal peptide, a proline-rich extracellular domain, and a transmembrane domain in front of the conserved FH1 and FH2 domains (Cvrčková, 2000). It binds microtubules via a motif shared by a subgroup of class I formins, the GOE domain (Deeks *et al.,* 2010). AtFH14 and rice FH5 are typical class II formins with a PTEN-related domain in front of FH1 and FH2 (Grunt *et al.,* 2008); since they lack the GOE motif, they obviously bind microtubules by other means.

AtFH1 is the main housekeeping class I formin in *Arabidopsis thaliana*, as judged from its gene expression pattern (Zimmermann *et al.,* 2004). It has the typical class I structure, associates with membranes (Banno and Chua, 2000; Cheung and Wu, 2004), and its extracellular domain may anchor the actin cytoskeleton across the plasmalemma into the cell wall (Martiniere *et al.,* 2011). AtFH1 can nucleate and bundle actin (Michelot *et al.,* 2005, 2006); it contains no known microtubule-binding motifs, and no discernible phenotype was described so far in mutants lacking AtFH1, although its transient overexpression caused loss of pollen tube polarity (Cheung and Wu, 2004).

Here the characterization of seedling root development in mutants harbouring T-DNA insertions in the *AtFH1* locus is reported. While under normal conditions mutants exhibited no obvious phenotypic alterations, they were hypersensitive towards an anti-actin drug (alone or together with a microtubule inhibitor). Organization of microfilaments and microtubules in the mutant root cortex, as well as their dynamics, documented by variable-angle epifluorescence microscopy (VAEM; see Wan *et al.,* 2011), differed from those of wild-type (wt) plants. The growth and cytoskeletal organization phenotypes were mimicked by treatment with a specific inhibitor of FH2 domain function (Rizvi *et al.,* 2009). Thus, AtFH1 appears to participate in regulation of cytoskeletal dynamics *in vivo* by a mechanism involving cross-talk between actin and microtubules.

## Materials and methods

### *Plants*

Two T-DNA insertional mutants (*fh1-1*, SALK-032981; and *fh1-2*, SALK-009693) in the *AtFH1* gene (At5g25500) were obtained from the SALK Institute (Alonso *et al.,* 2003). To determine *AtFH1* allelic status, PCR using primers *fh1-1*-LP (5'GTCTCCGTCACTGTCGTTAGC3') with *fh1-1*-RP (5'TTGTTGTTTAACGACTTCGCC3') was employed to detect the wt allele in crosses involving *fh1-1*, and *fh1-2*-LP (5'TG TTTGTGTAGGCTGCTTGTG3') with *fh1-2*-RP (5'ATTCTTTCGTG GTACACACGG3') for the wt allele in crosses of *fh1-2*. For mutant alleles, the RP primers were combined with the SALK primer LBb1.3: 5'ATTTTGCCGATTTCGGAAC3' for the T-DNA insertion.

Mutants were crossed with green fluorescent protein (GFP)–MAP4 and GFP–FABD reporter lines (Marc *et al.,* 1998; Ketelaar *et al.,* 2004) as described (Cole *et al.,* 2005). Media with kanamycin and BASTA® were used to select GFP–MAP4- and GFP–FABD-carrying plants, respectively, and fluorescence was evaluated microscopically. Genotyping to select *fh1* homozygotes was done in the second and third generation.

### *RT–PCR*

RNA was isolated from 7-day-old seedlings using the RNeasy Plant kit (Qiagen). First-strand cDNA synthesis and semi-quantitative reverse transcription–PCR (RT–PCR; with β-actin-specific primers for control) were performed according to Dvořáková *et al.* (2007) using 30 cycles, DreamTaq polymerase (Fermentas), and AtFH1-specific primers (5'GGATCCAGAAGAAAGAAGAAGATAACACAATGC3' and 5'CTGAGCCTTCTTCGGGTCCAGG3'). The 2042 bp product was visualized by agarose gel electrophoresis.

### *Growth conditions and inhibitor treatments*

Inhibitor treatment experiments were performed according to Collings *et al.* (2006). Seed germination was synchronized by several days at 4 °C, followed by growth on vertical Murashige and Skoog (MS) plates for 4–5 d at 22 °C with a 16 h light/8 h dark cycle prior to transfer on inhibitor-containing media, which were then incubated under the same conditions for 72 h, unless stated otherwise. Inhibitor stock solutions were prepared in dimethylsulphoxide (DMSO), stored at −20 °C [latrunculin B (LatB), oryzalin (Oryz), taxol, and jasplakinolide] or 4 °C (SMIFH2), and added to liquid agar to the desired concentrations; the DMSO concentration was adjusted to 0.2% (v/v). All inhibitors were purchased from Sigma. Effective doses were calculated using the R statistical software (http://www.r-project.org/index.html) according to Knezevic *et al.* (2007) from two or three replications of ~20 plants for each concentration.

### *Morphometric analyses*

Root diameter and root growth (defined as increment in length in a specified interval of time) was determined from photographs taken at 24, 48, and 72 h after transfer with a digital camera (Olympus C5050), measuring the distances between the root tips and marks made on the rear of the plates at tip locations at transfer time. To determine root hair density, root hairs were counted under a light microscope (BX-51, Olympus) at ×10 magnification in a 2 mm region at the midpoint of the portion of root grown after transfer. Lengths of 10 root hairs from the midpoint of each measured region were measured at ×20 magnification. From the same zone, root diameter and the lengths of 10 trichoblasts and 10 atrichoblasts per root were estimated. In all experiments, 2–3 replicates of ~20 plants were used per data point. Measurements were performed using the ImageJ software (http://rsbweb.nih.gov; Abramoff *et al.,* 2004).

### *Confocal microscopy and image analysis*

GFP-tagged cytoskeleton was observed in roots of 5-day-old seedlings using a confocal laser scanning microscope (LCS 510; Leica) with a ×63/1.2 water immersion objective and 488 nm argon laser (25 mW) excitation. Images were acquired as z-series with a 0.7–1 μm interval. Microfilament bundling and density were quantified according to van der Honing *et al.* (2012) and Higaki *et al.* (2010). Profiles of fluorescence intensity were divided into four classes of grey level (arbitrary units) to generate plots documenting microfilament bundling (low intensity represents weakly labelled bundles or single filaments; high intensity corresponds to brightly labelled bundles). Skewness of fluorescence intensity distribution (correlated with microfilament bundling because bundles exhibit brighter fluorescence) and occupancy (i.e. fraction of pixels constituting the skeletonized microfilaments relative to the total pixel number of the analysed region, proportional to the overall microfilament density) were determined using the ImageJ plugins and macros from Higaki's laboratory (http:/hasezawa.ib.k.u-tokyo.ac.jp/zp/Kbi/HigStomata). Microtubule density was determined as the number of microtubules in an area of 500 $\mu m^2$ from confocal images in five cells from several plants.

### *VAEM*

To evaluate cytoskeletal dynamics, we used the Leica AF6000 LX fluorescence platform with integrated TIRF module, the HCX PL APO ×100/1.46 oil immersion objective, 400 nm peak excitation, and 210 ms exposure time. Plants were mounted in water on chambered slides; images were captured with a Leica DFC350FXR2 digital camera at 0.5 s intervals over the course of 2 min and analysed with Leica Application

Suite (LAS) and ImageJ software. Kymographs were generated using the Multiple Kymograph ImageJ plug-in from a time-lapse image series collected from well-focused 30 µm long 'optical transects' parallel to the longitudinal axis of the root (Sampathkumar *et al.*, 2011). The distribution of microtubule growth and shrinkage rates was estimated from at least 250 microtubule ends from at least 50 atrichoblasts in each genotype or treatment.

## Results

### *Cytoskeletal inhibitors differentially affect root growth in* fh1 *mutant and wild-type seedlings*

Two *Arabidopsis* T-DNA mutant lines, *fh1-1* and *fh1-2*, with corresponding wt controls were characterized. The T-DNA insertion interrupts the *AtFH1* gene in the third exon in *fh1-1* and in the 5' untranslated region (UTR; 27 bp before start codon) in *fh1-2* (Fig. 1A). In homozygous seedlings, AtFH1 mRNA was undetectable in *fh1-1*, while *fh1-2* had a reduced transcript level (Fig. 1B).

Under standard growth conditions in soil or *in vitro*, *fh1-1* and *fh1-2* plants do not differ noticeably from the wt. The *in vitro* growth media were thus supplemented with anti-cytoskeletal drugs LatB and/or Oryz to enhance expected subtle cytoskeletal defects and uncover novel mutant phenotypes.

At 0.1 µM concentration, the actin polymerization inhibitor LatB caused a more severe increase in root diameter and reduction in the longitudinal root growth rate in young seedlings of both mutant lines compared with the wt; the difference developed gradually within the first 48 h on LatB (Fig. 2). Higher concentrations severely affected both genotypes, and the difference between the mutant and wt was no longer significant (Supplementary Fig. S1A, B available at *JXB* online).

While the microtubule-depolymerizing drug Oryz also caused root thickening and reduced root growth, its effect was similar in both *fh1* and wt seedlings. (Supplementary Fig. S1C, D at *JXB* online). However, simultaneous addition of 0.33 µM LatB (i.e. a concentration that equally affected mutant and wt roots) increased the sensitivity of *fh1* mutants to a low concentration of Oryz compared with the wt (Supplementary Fig. S1E).

Next, the inhibitor concentrations at which root diameter showed half the maximal increase ($D_{50}$) and at which roots showed a 50% reduction in growth rate ($L_{50}$) were estimated from dose–response curves of mutant and wt seedlings. Radial root expansion was always more sensitive to inhibitors than longitudinal growth. For LatB, both $D_{50}$ and $L_{50}$ were significantly lower in the *fh1* mutants than in the wt (Table 1).

Treatment with cytoskeleton-stabilizing drugs (jasplakinolide for actin or taxol for microtubules) resulted in reduced root growth and increased diameter in both *fh1-1* mutant and wt seedlings. Both genotypes responded similarly, although longitudinal growth of mutant roots was significantly less affected by taxol (Supplementary Fig. S2 at *JXB* online).

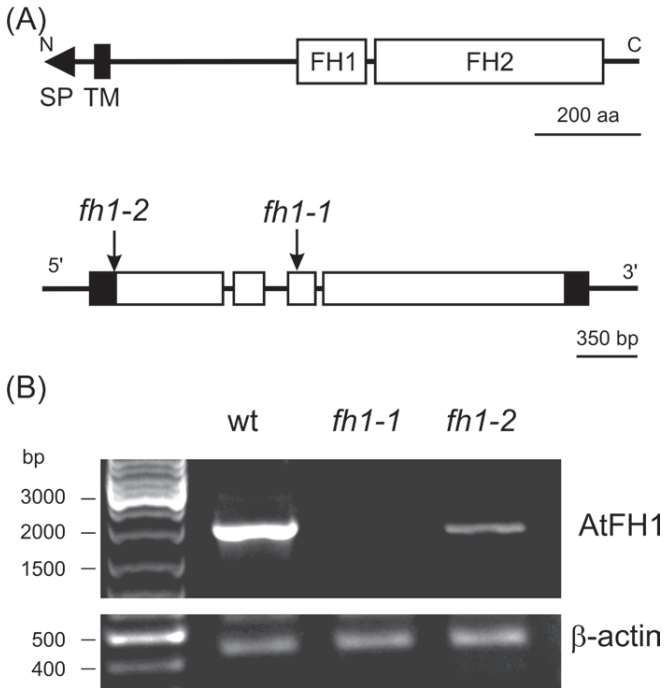


**Fig. 1.** The *AtFH1* (At5g25500) locus and mutants. (A) AtFH1 protein domain structure (above); map of the *AtFH1* gene and location of T-DNA insertions (below: open boxes, coding exons; filled boxes, non-coding exons; lines, introns and non-transcribed sequences). (B) *AtFH1* transcripts in wt and homozygous mutant seedlings determined by semi-quantitative RT–PCR.

### *Cytoskeletal inhibitors affect cell expansion and root hair development in mutants*

Reduced longitudinal root growth can be due to impaired cell division or elongation, or both. To evaluate the contribution of cell elongation, the length of mature trichoblasts and atrichoblasts in inhibitor-treated roots was measured. LatB-grown *fh1-1* and *fh1-2* roots had shorter, wider cells, suggesting that the phenotype is at least partly due to more isodiametric cell growth (Fig. 3A, B; Supplementary Table S1 at *JXB* online).

Mutant rhizodermis cells, especially trichoblasts, were often mis-shapen, exhibiting bulbous structures at root hair bases and/or branched root hairs (Fig. 3C). A significantly higher density of both total and abnormal root hairs was found in mutant, but not wt, seedlings grown on 0.1 µM LatB compared with drug-free control, apparently due to shorter trichoblasts. At 0.33 µM LatB, the total number of root hairs was reduced in both genotypes; mutants had more abnormal root hairs than the wt. A further increase in the LatB concentration completely inhibited root hair development. While *fh1* mutants showed, on average, longer root hairs than the wt on control media or 0.1 µM LatB or Oryz, their root hairs were shorter on 0.33 µM LatB, suggesting increased sensitivity of tip growth to higher LatB doses. However, since root hair length varied substantially, the biological significance of this observation is questionable (Fig. 3D; Supplementary Table S1 at *JXB* online).

### *Actin and microtubule distribution in* fh1 *mutants*

In the above experiments, both *fh1* alleles behaved similarly, though *fh1-1* had more pronounced phenotypes, in

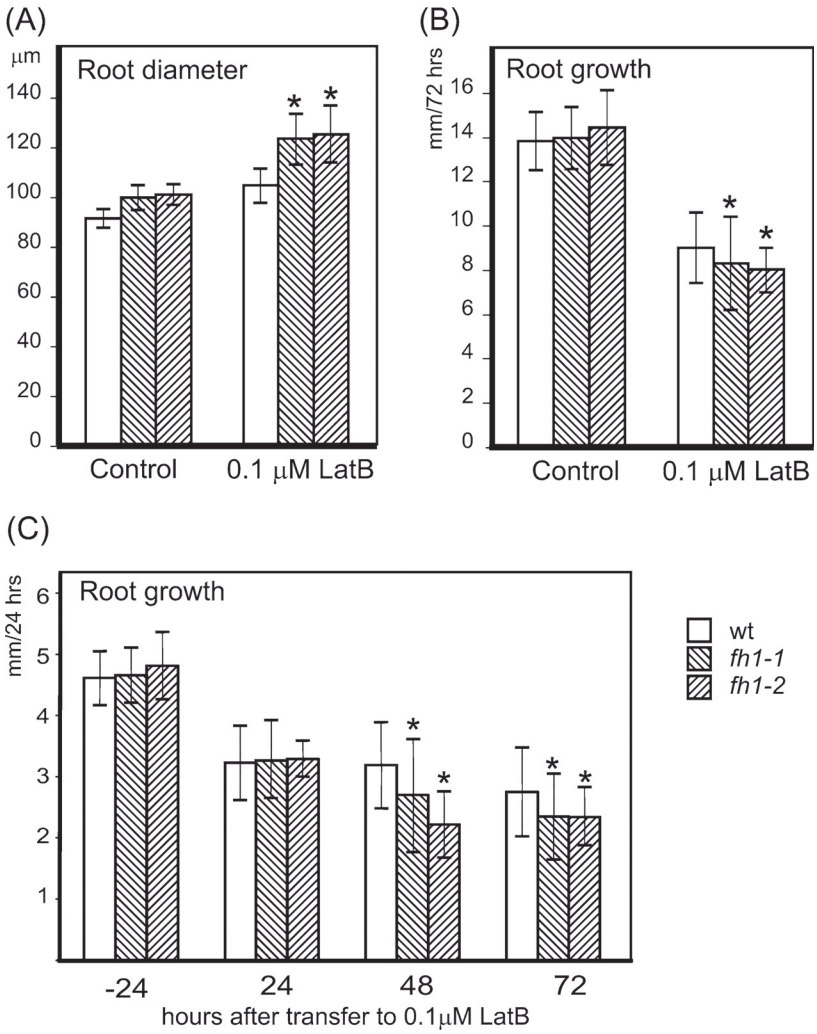


**Fig. 2.** Mutants lacking *AtFH1* exhibit thicker, slower growing roots than the wt when treated with 0.1 μM LatB. (A) Root diameter and (B) incremental root growth during 72 h after transfer to LatB. Significant differences between any of the mutants and the wt in root diameter (*t*-test $P < 0.0001$) or root growth (*t*-test $P < 0.05$) are marked by asterisks. (C) Gradual decrease in root growth rates after 24, 48, and 72 h on LatB. Significant differences between mutant and wt seedlings (*t*-test $P < 0.0001$) are marked by asterisks; data from the last 24 h before transfer are shown for control.

agreement with the residual gene expression in *fh1-2*. *fh1-1* was thus chosen for introduction of *in vivo* fluorescent protein-tagged cytoskeletal markers (GFP–FABD for actin and GFP–MAP4 for microtubules) by crossing. Sister segregants carrying wt AtFH1 were used as controls.

**Table 1.** Effective doses of LatB and Oryz in mutants and the wild type.

| Treatment | $D_{50}$ | | $L_{50}$ | |
|---|---|---|---|---|
| | *fh1-1* | Wt | *fh1-1* | Wt |
| Lat B | 10.1** | 28.3 | 131.6** | 163.7 |
| Oryz | 96* | 114.4 | 233.1 | 224.3 |

$D_{50}$, inhibitor concentration causing response half way between zero and the maximal observed diameter increase; $L_{50}$, inhibitor concentration causing response half way between zero and the maximal observed growth reduction.
*Significant difference from the wt at $P < 0.05$; **significant difference from the wt at $P < 0.001$.

The effects of the markers themselves on root growth in both *fh1-1* and the wt were examined. GFP–MAP4 caused root thickening and reduction of root growth, and induced left-handed root twisting, as described previously (Granger and Cyr, 2001; Hashimoto, 2002); these effects were less pronounced in *fh1-1*mutants than in the wt. GFP–FABD did not show any significant effects in either *fh1-1* or wt seedlings (Supplementary Fig. S3 at *JXB* online).

Given that this study was looking at root development, the focus here was on *in vivo* observations in rhizodermal cells. Thicker and more frequent actin bundles were usually observed in *fh1* mutants than in wt seedlings. Low doses of LatB did not disrupt filaments but rather increased actin bundling, more obviously in mutants than in wt plants. LatB-treated wt plants thus somewhat resembled *fh1* mutants grown under control

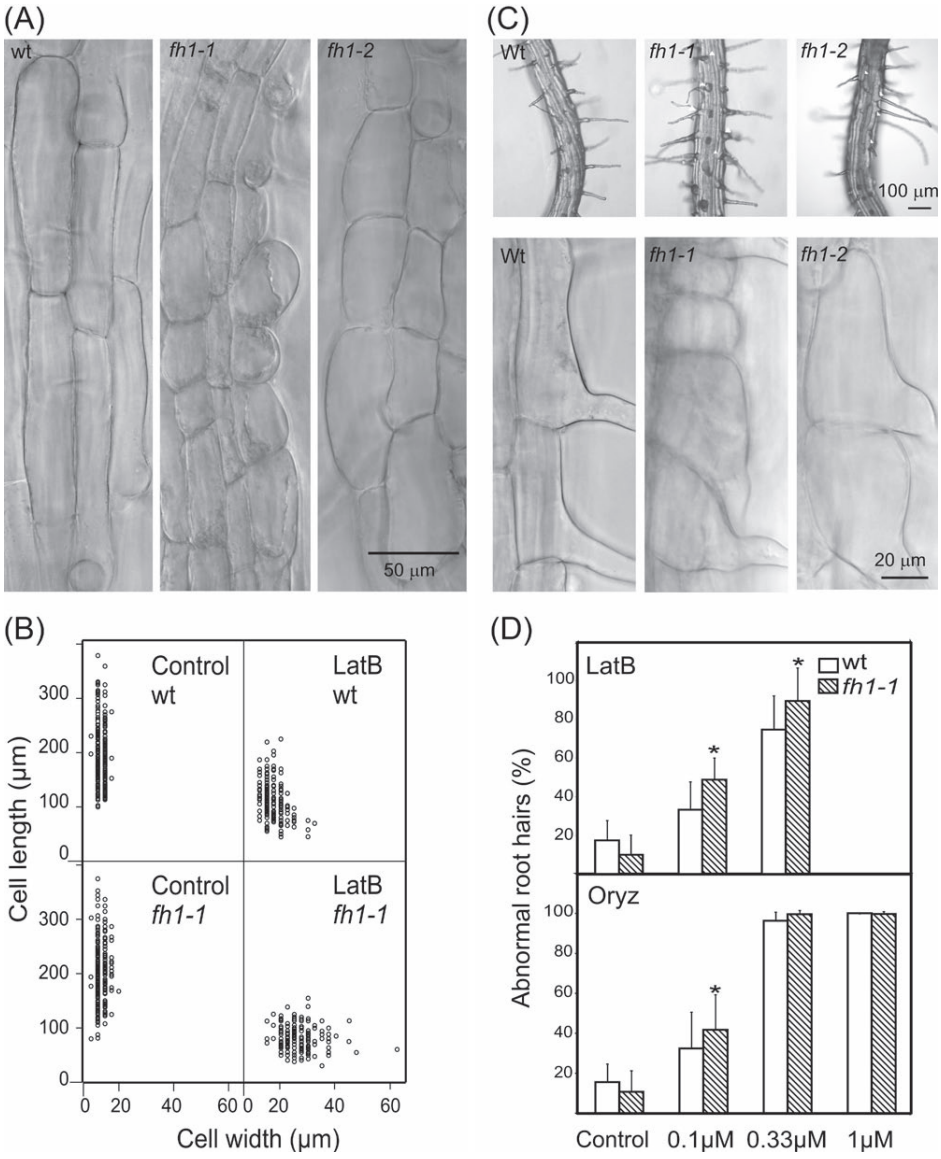


**Fig. 3.** Effects of LatB on rhizodermis and root hair development in *fh1* mutant and wt seedlings. (A) Typical appearance of elongation zone rhizodermis in wt and mutants exposed to LatB. (B) Relationship between mature rhizodermis cell length and width in *fh1-1* mutant and wt seedlings in control conditions and on 0.1 μM LatB (each sample contains equal numbers of trichoblasts and atrichoblasts); compare Supplementary Table S1 at *JXB* online for *fh1-2*. (C) Abnormal root hairs found in mutant but not wt plants grown on 0.1 μM LatB. (D) Percentage of abnormal root hairs in *fh1-1* and wt plants grown in LatB- and Oryz-supplemented media. Significant differences (*t*-test $P < 0.001$) are marked by an asterisk.

conditions (Fig. 4A). Quantification of the microfilament patterns in the rhizodermis of seedlings growing on control media by estimating the skewness of fluorescence intensity distribution (correlated with the level of microfilament bundling) and pixel occupancy (giving insight into the overall density of actin cytoskeleton) showed that mutants have fewer but thicker microfilaments, consistent with increased actin bundling (Fig. 4B). The differences are even more obvious in profiles of individual bundle fluorescence intensity (Fig. 4C), confirming that *fh1* mutants have fewer weakly labelled thin bundles or single filaments, and more bright thick bundles than wt plants.

Surprisingly, differences in microtubule organization between the wt and mutants were more pronounced than those in microfilaments. Even on control media, and more obviously in LatB-treated plants, mutants had fewer microtubules, shorter and less organized compared with the wt (Fig. 4D). Quantitative measurements of microtubule density revealed a significant reduction in LatB-treated *fh1* mutants compared with the wt (Fig. 4E).

### *Effect of* fh1 *mutation on cytoskeletal dynamics monitored by VAEM*

To compare individual microfilament and microtubule dynamics in rhizodermis cells of wt and *fh1* mutant plants carrying GFP–FABD and GFP–MAP4, the VAEM technique was

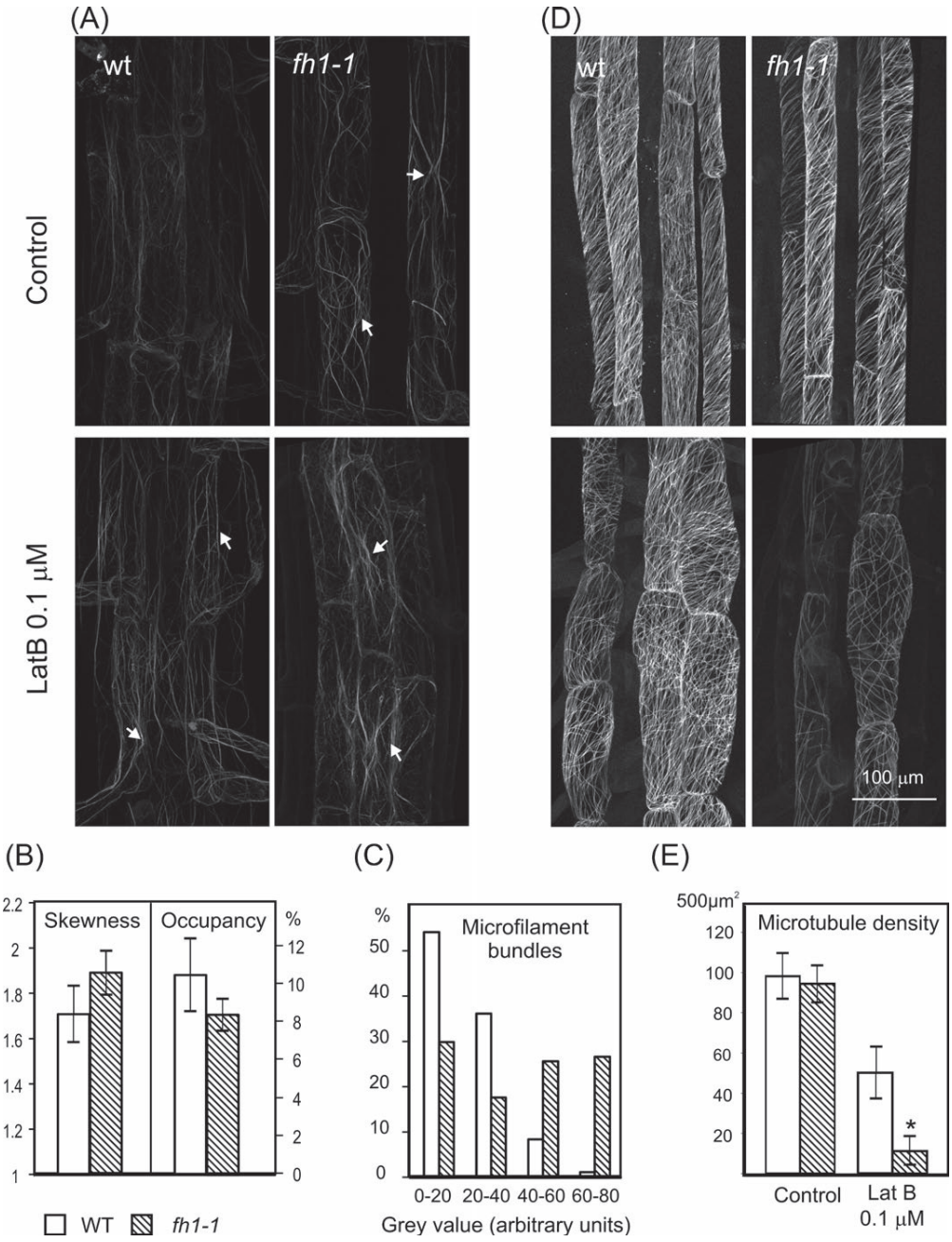


**Fig. 4.** Typical cytoskeleton organization in the rhizodermis of *fh1-1* mutant and wt seedlings. (A) Actin labelled by GFP–FABD; arrows, actin filament bundles. (B) Actin filament bundling (skewness) and density (occupancy) under control conditions. (C) Frequency distribution of actin fluorescence peaks in four fluorescence intensity classes under control conditions. (D) Microtubules labelled by GFP–MAP4. (E) Microtubule density. Significant differences (*t*-test $P < 0.001$) are marked by an asterisk.

employed. Since preliminary experiments indicated that the three developmental zones of the root tip differ in cytoskeletal dynamics, the beginning of the differentiation zone was investigated, where both cytoskeletal systems behaved consistently very dynamically.

Differences in actin dynamics were observed between *fh1* mutants and the wt (Fig. 5; Supplementary Video S1, S2 at *JXB* online). Mutant microfilament bundles were more abundant and less dynamic (in particular, they remained longer at pause) than those of wt seedlings, except a few rapidly moving bundles. This might reflect differences either in bundle size or in the degree of actin cross-linking.

Differences between mutant and wt plants were also observed in microtubule dynamics (Fig. 6; Supplementary Video S3, S4 at *JXB* online). On the control medium, mutant microtubules exhibited increased dynamic instability compared with wt seedlings. LatB increased microtubule dynamics in both genotypes (Fig. 6A, B).

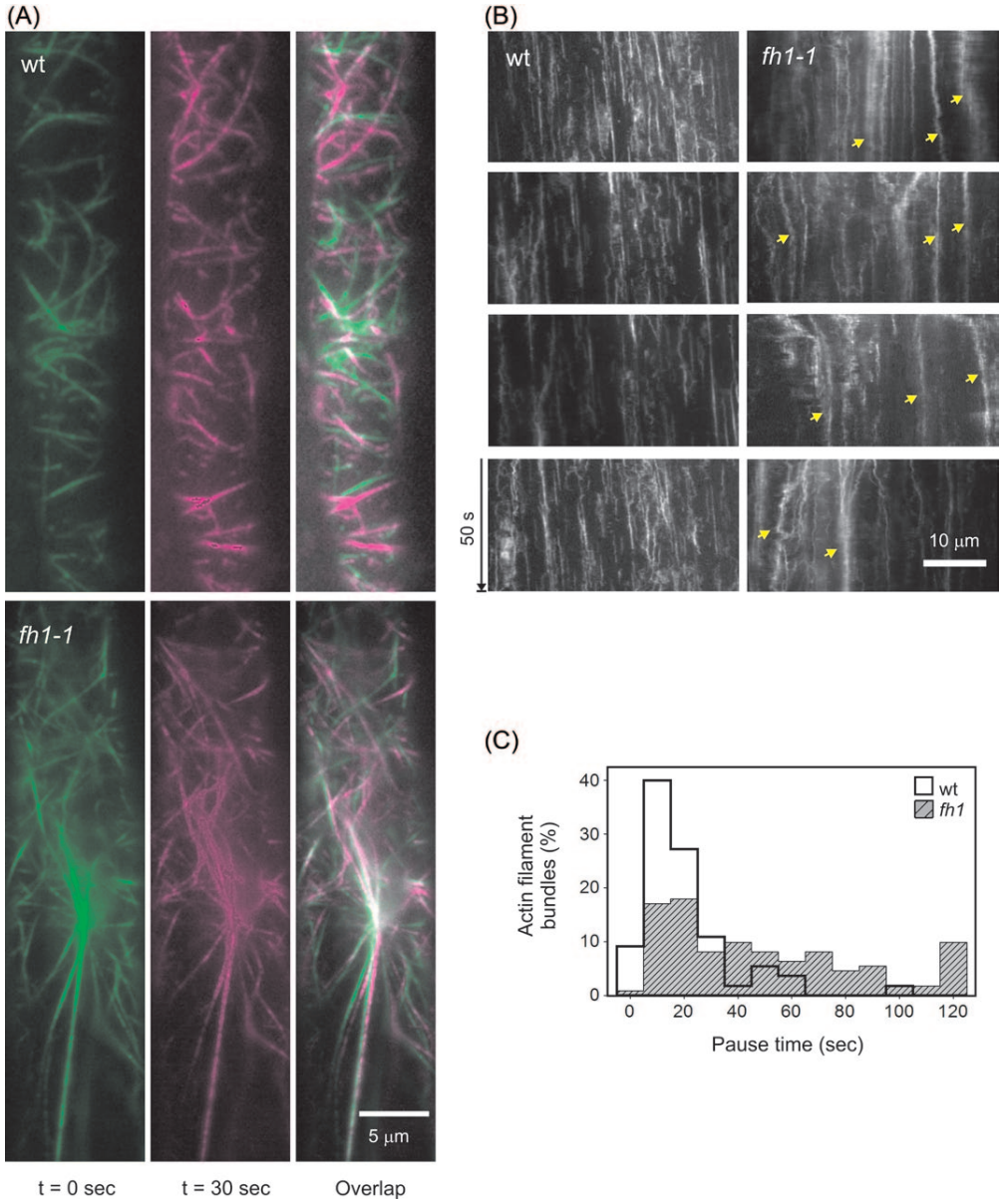


**Fig. 5.** GFP–FABD-tagged microfilament distribution and dynamics in the rhizodermis of *fh1-1* and wt seedlings on standard medium. (A) VAEM images from two time points and their overlap showing growing or moving filaments in magenta, shrinking in green, and pausing and growing/shrinking in light green and light magenta, respectively. (B) Kymograph showing the static thick actin bundles in the mutant (arrows). (C) Distribution of actin bundle pause duration in mutant and wt.

To quantify microtubule turnover, the distribution of microtubule phases was determined in images taken during the time span of 2 min. Mutants had fewer shrinking or pausing microtubules but more microtubules undergoing stochastic transition (i.e. alternatively shrinking and growing) than the wt (Fig. 6C). LatB reduced the fraction of growing microtubules in both genotypes, and increased the fraction of growing/shrinking microtubules even in the wt (again, LatB-treated wt plants resembled *fh1* mutants grown under control conditions). Oryz in both genotypes increased the percentage of pausing microtubules and reduced the growing, shrinking, and growing/shirinking fractions. The distribution of microtubule growth and shrinkage rates differed somewhat between *fh1* and wt roots (Supplementary Fig. S4 at *JXB* online). Despite comparable average growth rates, a higher proportion of microtubules in *fh1* cells grew more slowly than average; this difference persisted upon LatB treatment, while Oryz reduced the growth rate in both the *fh1* mutant and the wt.

### *Effects of the formin inhibitor SMIFH2 mimic the* fh1 *mutation*

To verify that the observed mutant phenotypes are due to disrupted formin function, the effects of a recently described inhibitor of formin-mediated actin assembly, SMIFH2 (Rizvi

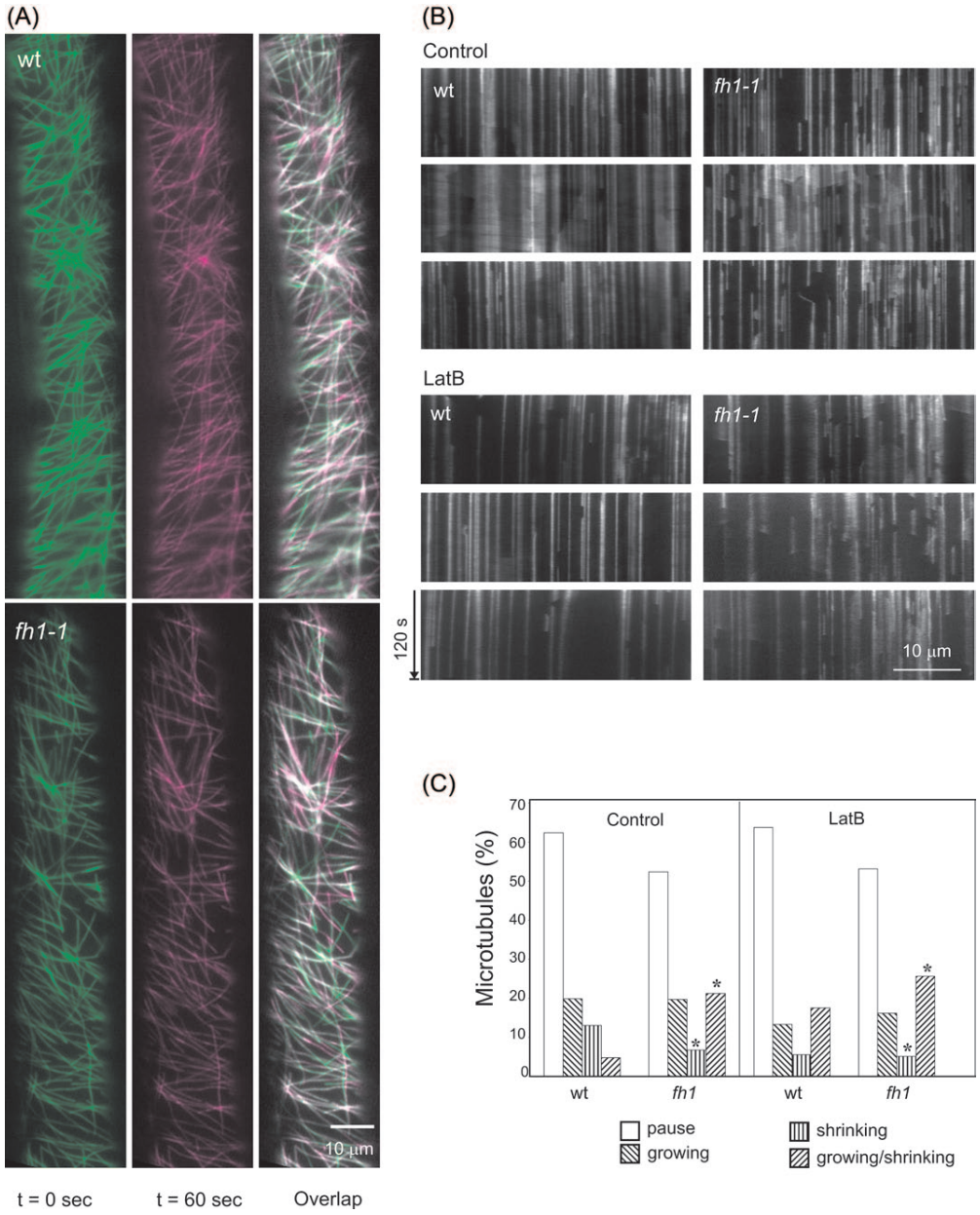


**Fig. 6.** GFP–MAP4-tagged microtubule distribution and dynamics in *fh1-1* mutant and wt rhizodermis. (A) VAEM images from two time points and their overlap showing growing microtubules in magenta, shrinking in green, pausing in light green, and growing/shrinking in light magenta. (B) Kymographs of microtubule dynamics under control conditions and on 0.1 µM LatB-supplemented medium. (C) Distribution of microtubule phases on control and 0.1 µM LatB-containing media. An asterisk indicates a significant difference between mutants and the wt (*t*-test $P < 0.0001$).

*et al.*, 2009), were examined in wt seedlings. In the standard experimental set-up, significant reduction of root growth was observed at or above a concentration of 20 µM in both the wt and *fh1* mutants (Fig. 7A). The effect of SMIFH2 was stronger when seedlings were exposed to the drug in the dark (possibly due to light sensitivity of the drug), and *fh1-1* mutant roots were significantly more affected than those of the wt (Supplementary Fig. S5 at *JXB* online). SMIFH2-treated wt seedlings expressing GFP–FABD and GFP–MAP4 exhibited increased microfilament bundling and reduced microtubule density, especially after additional LatB treatment, again reminiscent of *fh1* mutants (Fig. 7B).

## Discussion

The first description is presented of a mutant phenotype in *A. thaliana* lacking the most expressed housekeeping class I formin, AtFH1. It is shown that AtFH1 affects actin and microtubule dynamics, processes central for cell expansion and development.

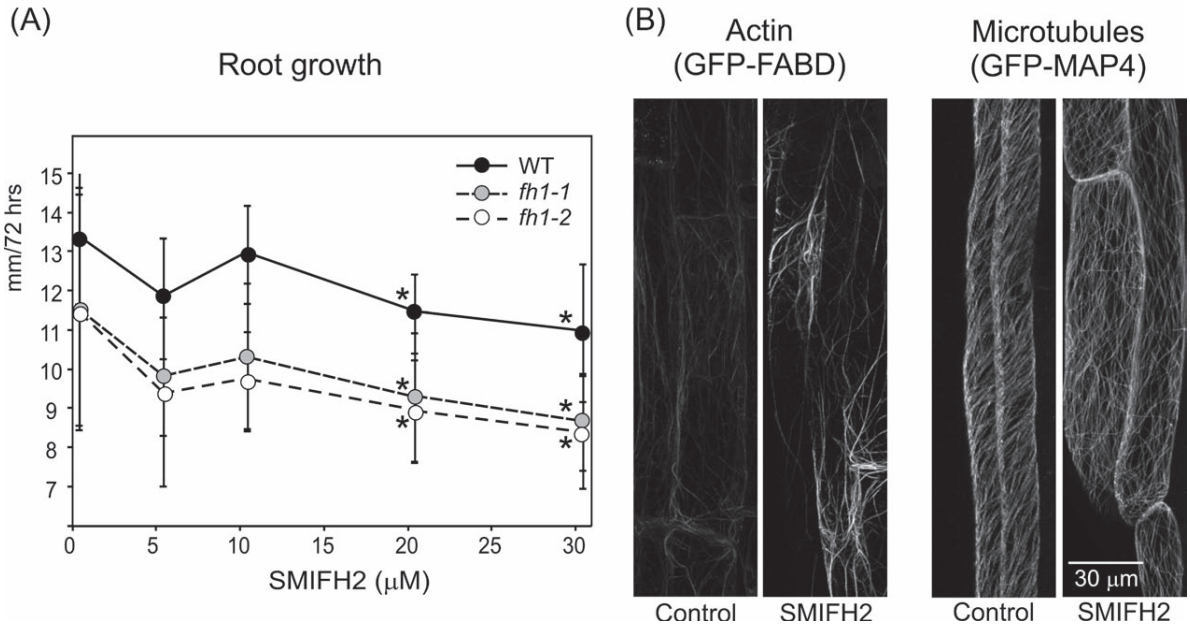


**Fig. 7.** Effects of SMIFH2 on longitudinal root growth and cytoskeletal organization. (A) Concentration-dependent growth inhibition; asterisks denote significant differences from non-treated seedlings of the same genotype (*t*-test $P < 0.0001$). (B) Rhizodermal microfilament and microtubule organization under control conditions and on 20 μM SMIFH2-supplemented medium.

### *Using cytoskeletal inhibitors to uncover mutant phenotypes*

Angiosperm FH2 proteins form a large family of paralogues: *A. thaliana* has 21 formin-encoding genes, 11 of them in class I. Ten of these (including AtFH1) share the characteristic clade-specific domain structure (Deeks *et al.,* 2002; Grunt *et al.,* 2008). Loss of a single formin gene thus rarely causes obvious phenotypic effects due to 'functional redundancy'. Only subtle, if any, phenotypes have so far been documented for loss-of-function class I formin mutants. Such phenotypes are usually tissue specific, reflecting the pattern of gene expression. Loss of AtFH5 caused delayed endosperm cytokinesis (Ingouff *et al.,* 2005), and pollen tube defects were elicited by RNA interference (RNAi) targeting the pollen formins AtFH3 in *Arabidopsis* or NtFH5 in tobacco (Ye *et al.,* 2009; Cheung *et al.,* 2010). Additional phenotypes were produced by overexpression, sometimes ectopic or heterologous, of wt or mutant proteins, such as AtFH1 (Cheung and Wu, 2004) or AtFH8 (Deeks *et al.,* 2005; Yi *et al.,* 2005).

Asymptomatic or mildly symptomatic doses of inhibitors of specific cellular functions may result in a 'synthetic phenotype' in mutants where the inhibitor's target(s) are already weakened. In mutants of *Arabidopsis* formins AtFH8 (Xue *et al.,* 2011) and AtFH12 (Cvrčková *et al.,* 2012), LatB induced alterations in roots and/or root hairs. In the present report, the response of T-DNA mutants with insertions in AtFH1 to cytoskeletal inhibitors targeting either actin (LatB) or microtubules (Oryz) was examined, since no readily noticeable differences between *fh1* mutants and the wt were observed under control conditions.

Low doses of LatB, inhibiting primary root growth and causing radial swelling in young seedlings, and enhancing the phenotype of some cytoskeletal mutations (Collings *et al.,* 2006), affected the *fh1* mutants more than the wt. However, the whole organ phenotype was subtle compared with effects on the level of individual cells or cytoskeletal structures, providing yet another example of organ- and tissue-level compensation of cell-level defects (see Breuninger and Lenhard, 2010). The shorter, thicker roots of LatB-treated mutants consisted of shorter and wider cells, suggesting altered cell expansion rather than cell division, consistent with previous observations (Baluška *et al.,* 2001). LatB can also disrupt intracellular membrane trafficking (Zhang *et al.,* 2010), crucial for polar auxin transport. Since auxin, in turn, affects actin, it is difficult to separate direct and auxin-mediated effects on root growth (Rahman *et al.,* 2007).

LatB-treated *fh1* mutants also exhibited malformed root hairs. Unlike pollen tubes ectopically overexpressing AtFH1, which have bulbous tips (Cheung and Wu, 2004), in the experiments presented here, mainly root hair bases were affected, resembling the phenotype of actin (*act2*) mutants (Gilliland *et al.,* 2002; Nishimura *et al.,* 2003) and suggesting defective focusing of exocytosis during the bulge stage.

Disruption of microtubules affected *fh1* mutants and the wt similarly, consistent with AtFH1 functioning mainly through actin. However, mutants exhibit increased sensitivity to Oryz in the presence of LatB, suggesting that AtFH1 may participate in a cross-talk between microfilaments and microtubules, and that its loss might, under some circumstances, destabilize microtubules. Consistently, mutants are partially resistant towards the root growth inhibition, radial root swelling, and root twisting induced by the GFP–MAP4 marker and taxol, which can stabilize and bundle microtubules (Granger and Cyr, 2001; Hashimoto, 2002).

### *Formin inhibition mimics the mutant phenotype*

The small molecule SMIFH2, a 2-thio-oxodihydropyrimidine-4,6-dione derivative, is an inhibitor of FH2 domain-mediated actin assembly, active *in vitro* against several formins, and eliciting actin-related phenotypes in yeast and mammalian cells (Rizvi *et al.*, 2009). Its *in vitro* characterized targets represent sufficiently distant formin clades (see Grunt *et al.*, 2008) to suggest that SMIFH2 should inhibit most or all formins.

In the present study, SMIFH2 reduced root growth, increased microfilament bundling, and decreased cortical microtubule density; that is, it mimicked some phenotypes observed in *fh1* mutants (especially after LatB treatment). Consistent with SMIFH2 also targeting the remaining formins, *fh1* mutants were still responding to the inhibitor. The stronger mutant allele, *atfh1-1*, was even somewhat more sensitive towards root growth inhibition in the dark, reminiscent of increased sensitivity of some cytoskeletal mutants to inhibitors (see above). While non-specific effects of SMIFH2 cannot be ruled out, as its reported inactive analogue (Rizvi *et al.*, 2009) is not commercially available, the present observations support the notion that the mutant phenotypes are indeed due to perturbation of formin function.

### *Changes in actin and microtubule distribution and dynamics in* fh1 *mutants*

Plant actin and microtubule networks undergo constant remodelling (Staiger *et al.*, 2009; Blanchoin *et al.*, 2010). They are mutually interdependent, and sometimes co-aligned; microtubule-disrupting drugs may affect actin organization, and vice versa (Collings *et al.*, 2006; Smertenko *et al.*, 2010; Sampathkumar *et al.*, 2011). The actin–microtubule 'cross-talk' may be mediated by bifunctional proteins or protein complexes (see Petrášek and Schwarzerová, 2009).

The thicker, more compact actin bundles in the *fh1* mutants are reminiscent of some *Arabidopsis* mutants with an altered balance between fine actin filaments and bundles, such as *adf4* (Henty *et al.*, 2011) or *aip1* (Ketelaar *et al.*, 2004). AtFH1 might stabilize microfilaments by bundling (Michelot *et al.*, 2005, 2006), enhanced polymerization, or capping, as reported for its relative AtFH8 (Yi *et al.*, 2005). Low doses of LatB also disrupt fine actin filaments, resulting in increased actin bundling and reduced stochastic dynamics (Staiger *et al.*, 2009). It is thus not surprising that LatB enhanced the effects of the *fh1* mutation and mimicked its phenotype in wt plants. Consistent with AtFH1 participating in actin–microtubule cross-talk, LatB also aggravated or phenocopied the presumably microtubule-related cell expansion phenotypes.

To gain insight into cytoskeletal dynamics in wt and mutant plants, VAEM, a fluorescence microscopy technique allowing time-lapse imaging of a thin cortical layer of the cytoplasm, recently also adopted in plants (Smertenko *et al.*, 2010; Sparkes *et al.*, 2011; Vizcay-Barrena *et al.*, 2011; Wan *et al.*, 2011), was used. Increased bundling and decreased dynamics of the cortical actin in *fh1* mutants were observed, suggesting altered actin-bundling, capping, or severing activities. Indeed, some formins can sever actin (Harris *et al.*, 2004; Yi *et al.*, 2005), thereby contributing to overall actin mobility, and AtFH1 may also have this ability. AtFH1 also anchors actin filaments across the plasmalemma into the cell wall (Martiniere *et al.*, 2011), which may effectively constrain bundling.

As suggested already by the root growth phenotypes discussed above, *fh1* mutants exhibited increased microtubule dynamics (important for cell elongation; Shaw *et al.*, 2003), although the plus-end growth rates were remarkably decreased. There are multiple documented cases of formins participating in actin–microtubule cross-talk or binding to microtubules (Bartolini and Gundersen, 2010; Chesarone *et al.*, 2010).

Particular microtubule-binding motifs may be restricted to narrow formin lineages (Deeks *et al.*, 2010; Li *et al.*, 2010; Yang *et al.*, 2011; Zhang *et al.*, 2011). Formins might also bind microtubules indirectly via heterodimerization with tubulin-binding paralogues, though heterodimerization is so far documented only among closely related mammalian Diaphanous formins (Copeland *et al.*, 2007). The microtubule-related effects may also be mediated by other microtubule-associated proteins; co-expression of AtFH1 with the At3g16060 kinesin (see data from http://string-db.org; Szklarczyk *et al.*, 2011) is interesting in this respect. However, since AtFH1 is excluded from the areas of cell cortex occupied by microtubules (Martiniere *et al.*, 2011), the effects on microtubule dynamics may be secondary to those on microfilaments.

In summary, phenotypic effects of loss of function of AtFH1, which altered root cell expansion, root hair morphogenesis, and cytoskeletal dynamics especially under conditions perturbing the actin cytoskeleton, were documented. Consistent effects were also elicited by the formin inhibitor SMIFH2. These results suggest the participation of AtFH1 in actin–microtubule cross-talk *in vivo* by an as yet unclear mechanism.

## Supplementary data

Supplementary data are available at *JXB* online.

Table S1. Trichoblast, atrichoblast, and root hair characteristics in inhibitor-treated wt and mutant seedlings.

Figure S1. Dose–response curves of wt and *fh1-1* root growth parameters for varying concentrations of cytoskeletal inhibitors.

Figure S2. Effects of taxol and jasplakinolide on wt and *fh1-1* root growth.

Figure S3. Effects of GFP–MAP4 and GFP–FABD on wt and *fh1-1* root growth.

Figure S4. Distribution of microtubule growth and shrinkage rates in *fh1-1* mutant and wt seedlings.

Figure S5. Effects of SMIFH2 on wt and *fh1* root growth under dark conditions.

Video S1. Actin dynamics in wt rhizodermis under control conditions.

Video S2. Actin dynamics in *fh-1* rhizodermis under control conditions.

Video S3. Microtubule dynamics in wt rhizodermis under control conditions.

Video S4. Microtubule dynamics in *fh1-1* rhizodermis under control conditions.

## Acknowledgements

This work was supported by the MSM 0021620858, GACR P305/10/0433, and SVV 265203 projects. We thank Aleš Soukup, Ondřej Šebesta, and Ondřej Horvath for help with microscopy and image analysis, Marta Čadyová for technical support, and two anonymous reviewers for helpful comments.

## References

**Abe T, Hashimoto T.** 2005. Altered microtubule dynamics by expresion of modified alfa-tubulin protein causes right-handed helical growth in transgenic Arabidopsis plants. *The Plant Journal* **43,** 191–204.

**Abramoff MD, Magelhaes PJ, Ram SJ.** 2004. Image processing with ImageJ. *Biophotonics International* **11,** 36–42.

**Alonso J, Stepanova A, Leisse T, *et al.*** 2003. Genome-wide insertional mutagenesis of Arabidopsis thaliana. *Science* **301,** 653–657.

**Baluška F, Jasik J, Edelmann H, Salajova T, Volkmann D.** 2001. Latrunculin B-induced plant dwarfism: plant cell elongation is F-actin-dependent. *Developmental Biology* **231,** 113–124.

**Bannigan A, Baskin T.** 2005. Directional cell expansion—turning toward actin. *Current Opinion in Plant Biology* **8,** 619–624.

**Banno H, Chua N.** 2000. Characterization of the Arabidopsis formin-like protein AFH1 and its interacting protein. *Plant and Cell Physiology* **41,** 617–626.

**Bartolini F, Gundersen G.** 2010. Formins and microtubules. *Biochimica et Biophysica Acta* **1803,** 164–173.

**Blanchoin L, Boujemaa-Paterski R, Henty J, Khurana P, Staiger C.** 2010. Actin dynamics in plant cells: a team effort from multiple proteins orchestrates this very fast-paced game. *Current Opinion in Plant Biology* **13,** 714–723.

**Blanchoin L, Staiger C.** 2010. Plant formins: diverse isoforms and unique molecular mechanism. *Biochimica et Biophysica Acta* **1803,** 201–206.

**Breuninger H, Lenhard M.** 2010. Control of tissue and organ growth in plants. *Current Topics in Developmental Biology* **91,** 185–220.

**Chesarone M, DuPage A, Goode B.** 2010. Unleashing formins to remodel the actin and microtubule cytoskeletons. *Nature Reviews. Molecular Cell Biology* **11,** 62–74.

**Cheung A, Niroomand S, Zou Y, Wu H.** 2010. A transmembrane formin nucleates subapical actin assembly and controls tip-focused growth in pollen tubes. *Proceedings of the National Academy of Sciences, USA* **107,** 16390–16395.

**Cheung A, Wu H.** 2004. Overexpression of an Arabidopsis formin stimulates supernumerary actin cable formation from pollen tube cell membrane. *The Plant Cell* **16,** 257–269.

**Cole R, Synek L, Žárský V, Fowler J.** 2005. SEC8, a subunit of the putative Arabidopsis exocyst complex, facilitates pollen germination and competitive pollen tube growth. *Plant Physiology* **138,** 2005–2018.

**Collings D, Lill A, Himmelspach R, Wasteneys G.** 2006. Hypersensitivity to cytoskeletal antagonists demonstrates microtubule–microfilament cross-talk in the control of root elongation in Arabidopsis thaliana. *New Phytologist* **170,** 275–290.

**Copeland S, Green B, Burchat S, Papalia G, Banner D, Copeland J.** 2007. The diaphanous inhibitory domain/diaphanous autoregulatory domain interaction is able to mediate heterodimerization between mDia1 and mDia2. *Journal of Biological Chemistry* **282,** 30120–30130.

**Cvrčková F.** 2000. Are plant formins integral membrane proteins? *Genome Biology* **1**, RESEARCH001.

**Cvrčková F, Grunt M, Žárský V.** 2012. Expression of GFP–mTalin reveals an actin-related role for the arabidopsis class II formin AtFH12. *Biologia Plantarum* **3,** 431–440.

**Deeks M, Cvrčková F, Machesky L, Mikitová V, Žárský V, Davies B, Hussey P.** 2005. Arabidopsis group Ie formins localize to specific cell membrane domains, interact with actin-binding proteins and cause defects in cell expansion upon aberrant expression. *New Phytologist* **168,** 529–540.

**Deeks M, Fendrych M, Smertenko A, Bell K, Oparka K, Cvrčková F, Žárský V, Hussey P.** 2010. The plant formin AtFH4 interacts with both actin and microtubules, and contains a newly identified microtubule-binding domain. *Journal of Cell Science* **123,** 1209–1215.

**Deeks M, Hussey P, Davies B.** 2002. Formins: intermediates in signal-transduction cascades that affect cytoskeletal reorganization. *Trends in Plant Science* **7,** 492–498.

**Dvořáková L, Cvrčková F, Fischer L.** 2007. Analysis of the hybrid proline-rich protein families from seven plant species suggests rapid diversification of their sequences and expression patterns. *BMC Genomics* **8,** 412.

**Emons A, Hofte H, Mulder B.** 2007. Microtubules and cellulose microfibrils: how intimate is their relationship? *Trends in Plant Science* **12,** 279–281.

**Gilliland L, Kandasamy M, Pawloski L, Meagher R.** 2002. Both vegetative and reproductive actin isovariants complement the stunted root hair phenotype of the Arabidopsis act2-1 mutation. *Plant Physiology* **130,** 2199–2209.

**Gilliland L, Pawloski L, Kandasamy M, Meagher R.** 2003. Arabidopsis actin gene ACT7 plays an essential role in germination and root growth. *The Plant Journal* **33,** 319–328.

**Granger CL, Cyr RJ.** 2001. Spatiotemporal relationships between growth and microtubule orientation as revealed in living root cells of Arabidopsis thaliana transformed with green-fluorescent-protein gene construct GFP–MBD. *Protoplasma* **216,** 201–214.

**Grunt M, Žárský V, Cvrčková F.** 2008. Roots of angiosperm formins: the evolutionary history of plant FH2 domain-containing protein. *BMC Evolutionary Biology* **8,** 115.

**Harris E, Li F, Higgs H.** 2004. The mouse formin, FRL, slows actin filament barbed end elongation, competes with capping protein,

accelerates polymerization from monomers, and severs filaments. *Journal of Biological Chemistry* **279,** 20076–20087.

**Hashimoto T.** 2002. Molecular genetic analysis of left-right handedness in plants. *Philosophical Transactions of the Royal Society B: Biological Sciences* **357,** 799–808.

**Henty J, Bledsoe S, Khurana P, Meagher R, Day B, Blanchoin L, Staiger C.** 2011. Arabidopsis actin depolymerizing factor 4 modulates the stochastic dynamic behavior of actin filaments in the cortical array of epidermal cells. *The Plant Cell* **23,** 3711–3726.

**Higaki T, Kutsuna N, Sano T, Kondo N, Hasezawa S.** 2010. Quantification and cluster analysis of actin cytoskeletal structures in plant cells: role of actin bundling in stomatal movement during diurnal cycles in Arabidopsis guard cells. *The Plant Journal* **61,** 156–165.

**Ingouff M, Fitz J, Guerin C, Robert H, Sorensen M, Van Damme D, Geelen D, Blanchoin L, Berger F.** 2005. Plant formin AtFH5 is an evolutionarily conserved actin nucleator involved in cytokinesis. *Nature Cell Biology* **7,** 374–380.

**Ketelaar T, Allwood E, Anthony R, Voigt B, Menzel D, Hussey P.** 2004. The actin-interacting protein AIP is essential for actin organization and plant development. *Current Biology* **14,** 145–149.

**Knezevic S, Streibig J, Ritz C.** 2007. Utilizing R software package for dose–response studies: the concept and data analysis. *Weed Technology* **21,** 840–848.

**Li Y, Shen Y, Cai C, Zhong C, Zhu L, Yuan M, Ren H.** 2010. The type II Arabidopsis formin 14 interacts with microtubules and microfilaments to regulate cell division. *The Plant Cell* **22,** 2710–2726.

**Marc J, Granger C, Brincat J, Fisher D, Kao T, McCubbin A, Cyr R.** 1998. A GFP–MAP4 reporter gene for visualizing cortical microtubule rearrangements in living epidermal cells. *The Plant Cell* **10,** 1927–1939.

**Martiniere A, Gayral P, Hawes C, Runions J.** 2011. Building bridges: formin 1 of Arabidopsis forms a connection between the cell wall and the actin cytoskeleton. *The Plant Journal* **66,** 354–365.

**Michelot A, Derivery E, Paterski-Boujemma R, Guerin C, Huang S, Parcy F, Staiger C, Blanchoin L.** 2006. A novel mechanism for the formation of actin-filament bundles by a nonprocessive formin. *Current Biology* **16,** 1924–1930.

**Michelot A, Guerin C, Huang S, Ingouff M, Richard S, Rodiuc N, Staiger C, Blanchoin L.** 2005. The formin homology 1 domain modulates the actin nucleation and bundling activity of Arabidopsis Formin 1. *The Plant Cell* **17,** 2296–2313.

**Nishimura T, Yokota E, Wada T, Shimmen T, Okada K.** 2003. An Arabidopsis ACT2 dominant-negative mutation, which disturbs F-actin polimerization, reveals its distinctive function in root development. *Plant and Cell Physiology* **44,** 1131–1140.

**Peremyslov V, Prokhnevsky A, Dolja V.** 2010. class XI myosins are required for development, cell expansion and F-actin organization in Arabidopsis. *The Plant Cell* **22,** 1883–1897.

**Petrášek J, Schwarzerová K.** 2009. Actin and microtubule cytoskeleton interactions. *Current Opinion in Plant Biology* **12,** 728–734.

**Rahman A, Bannigan A, Sulaman W, Pechter P, Blancaflor E, Baskin T.** 2007. Auxin, actin and growth of the Arabidopsis thaliana primary root. *The Plant Journal* **50,** 514–528.

**Rizvi S, Neidt E, Cui J, Feiger Z, Skau C, Gardel M, Kozmin S, Kovar D.** 2009. Identification and characterization of a small molecule inhibitor of formin-mediated actin assembly. *Chemistry and Biology* **16,** 1158–1168.

**Sampathkumar A, Lindeboom J, Debolt S, Gutierrez R, Ehrhardt D, Ketelaar T, Persson S.** 2011. Live cell imaging reveals structural associations between the actin and microtubule cytoskeleton in Arabidopsis. *The Plant Cell* **23,** 2302–2313.

**Shaw S, Kamyar R, Ehrhardt D.** 2003. Sustained microtubule treadmilling in Arabidopsis cortical arrays. *Science* **300,** 1715–1718.

**Smertenko A, Deeks M, Hussey P.** 2010. Strategies of actin reorganisation in plant cells. *Journal of Cell Science* **123,** 3019–3028.

**Smith LG, Oppenheimer DG.** 2005. Spatial control of cell expansion by the plant cytoskeleton. *Annual Review of Cell and Developmental Biology* **21,** 271–295.

**Sparkes I, Graumann K, Martiniere A, Schoberer J, Wang P, Osterrieder A.** 2011. Bleach it, switch it, bounce it, pull it: using laser to reveal plant cell dynamics. *Journal of Experimental Botany* **62,** 1–7.

**Staiger C, Sheahan M, Khurana P, Wang X, McCurdy D, Blanchoin L.** 2009. Actin filament dynamics are dominated by rapid growth and severing activity in the Arabidopsis cortical array. *Journal of Cell Biology* **182,** 269–280.

**Szklarczyk D, Franceschini A, Kuhn M, *et al.*** 2011. The STRING database in 2011: functional interaction networks of proteins, globally integrated and scored. *Nucleic Acids Research* **39,** D561–D568.

**Thitamadee S, Tuchihara K, Hashimoto T.** 2002. Microtubule basis for left-handed helical growth in Arabidopsis. *Nature* **417,** 193–196.

**van der Honing H, Kieft H, Emons A, Ketelaar T.** 2012. Arabidopsis VILLIN2 and VILLIN3 are required for the generation of thick actin filament bundles and for directional organ growth. *Plant Physiology* **58,** 1426–1438.

**Vizcay-Barrena G, Webb S, Martin-Fernandez M, Wilson Z.** 2011. Subcellular and single-molecule imaging of plant fluorescent proteins using total internal reflection fluorescent microscopy (TIRFM). *Journal of Experimental Botany* **62,** 5419–5428.

**Wan Y, Ash W, Fan L, Hao H, Kim M, Lin J.** 2011. Variable-angle total internal reflection fluorescence microscopy of intact cells of Arabidopsis thaliana. *Plant Methods* **7,** 27.

**Wang J, Xue X, Ren H.** 2012. New insights into the role of plant formins: regulating the organization of the actin and microtubule cytoskeleton. *Protoplasma* **249** Suppl. 2, S101–S107.

**Xue X, Guo C, Du F, Lu Q, Zhang C, Ren H.** 2011. AtFH8 is involved in root development under effect of low-dose latrunculin B in dividing cells. *Molecular Plant* **4,** 264–278.

**Yang W, Ren S, Zhang X, *et al.*** 2011. BENT UPPERMOST INTERNODE1 encodes the class II Formin FH5 crucial for actin organization and rice development. *The Plant Cell* **23,** 661–680.

**Ye J, Zheng Y, Yan A, Chen N, Wang Z, Huang S, Yang Z.** 2009. Arabidopsis Formin3 directs the formation of actin cables and polarized growth in pollen tubes. *The Plant Cell* **21,** 3868–3884.

**Yi K, Guo C, Chen D, Zhao B, Yang B, Ren H.** 2005. Cloning and functional characterization of a formin-like protein (AtFH8) from Arabidopsis. *Plant Physiology* **138,** 1071–1082.

**Zhang Y, He J, McCormick S.** 2010. Interdependence of endomembrane trafficking and actin dynamics during polarized growth of arabidopsis pollen tubes. *Plant Physiology* **152,** 2200–2210.

**Zhang Z, Zhang Y, Tan H, Wan Y, Li G, Liang W, Yuan Z, Hu J, Ren H, Zhang D.** 2011. RICE MORPHOLOGY DETERMINANT encodes the type II formin FH5 and regulates rice morphogenesis. *The Plant Cell* **23,** 681–700.

**Zimmermann P, Hirsch-Hoffmann M, Hennig L, Gruissem W.** 2004. GENEVESTIGATOR. Arabidopsis microarray database and analysis toolbox. *Plant Physiology* **136,** 2621–2632.

### 3.2. Paper 2.

**Rosero A, Grunt M, Schiebertova P, Zarsky V, Cvrckova F. 2013. AtFH1 and AtFH2 formins affect pavement cell morphogenesis and vascular patterning in Arabidopsis by modulating cytoskeleton and membrane dynamics.** ***Submitted paper.***

Formin mutants had cotyledon pavement cells which exhibited more pronounced lobes compared to the wild type, and alterations in vascular tissue patterning were found. The double *fh1/fh1 fh2/fh2* homozygote was not found, suggesting that at least one functional formin gene is required for proper gametophyte development. *fh1* mutant phenotype analogous to that previously observed in roots, and further aggravated by a (heterozygous) *fh2* mutation. Defects in membrane trafficking were observed in formin mutants and confirmed by SMIFH2 inhibitor which slowed down the movement of CLC-GFP dots. Experiments using cytoskeletal, endocytosis and formin inhibitors showed consistent resuĺts as formin mutants.

**My contribution:** Evaluation of pavement cell shape and vascular tissue in formin mutants; *fh1*, *fh2* and *fh1/fh1 FH2/fh2*. Detailed observations by optical, confocal and VAEM microscopy. Analysis of cytoskeleton organization and dynamics using reported methods. Writing the draft of the manuscript.

# Arabidopsis FH1 and FH2 formins affect pavement cell shape and vascular patterning by modulating cytoskeleton and membrane dynamics

Amparo Rosero[1], Michal Grunt[1], Petra Schiebertová[1], Viktor Žárský[1,2], Fatima Cvrčková[1]*

[1]Department of Experimental Plant Biology, Faculty of Sciences, Charles University, Viničná 5, CZ 128 44 Praha 2, Czech Republic.
[2]Institute of Experimental Botany, Academy of Sciences of the Czech Republic, Rozvojová 135, CZ 160 00 Prague 6, Czech Republic.

**Running title:** Formins in pavement cell morphogenesis

*Corresponding Author; e-mail: fatima@natur.cuni.cz

Number of characters in the manuscript (include spaces): 63215
Number of 1-column figures: 3
Number of 2-column figures: 6
Number of 1-column tables: 0
Number of 2-column tables: 0
Estimated number of printed pages: 13.5

The author(s) responsible for distribution of materials integral to the findings presented in this article in accordance with the policy described in the Instructions for Authors (www.plantcell.org) is Fatima Cvrčková (fatima@natur.cuni.cz).

**Abstract**

Plant cell morphogenesis depends upon concerted rearrangements of microtubules and actin microfilaments. We previously reported that FH1 (AtFH1, At3g25500), the main housekeeping Arabidopsis Class I membrane-targeted formin, contributes to actin dynamics and microtubule stability in rhizodermis cells. Here we examine the effects of mutations in *FH1* and its closest relative, *FH2* (At2g43800) on cell morphogenesis and above-ground organ development in seedlings. In single homozygous *fh1* or *fh2* mutants, as well as in plants carrying a single *FH2* functional copy in *fh1* mutant background, cotyledon pavement cells exhibited more pronounced lobes than in wild type, and alterations in vascular tissue patterning and connectivity were found. We failed to obtain double *fh1 fh2* homozygotes, suggesting that at least one of these two paralogous formin genes is required for proper development of both gametophytes. Using confocal and VAEM microscopy we observed increased actin bundling and enhanced microtubular dynamics in mutant cotyledons, i.e. phenotypes analogous to those previously observed in roots, as well as defects in membrane trafficking, especially endocytosis. Consistent results were obtained also upon treatments with cytoskeletal, endocytosis and formin inhibitors. Formins, especially FH1 and FH2, thus participate in co-ordination of cytoskeletal dynamics and membrane turnover, with effects on subsequent tissue-level processes.

## Introduction

Plant cell shapes are determined by the interplay of microtubule and microfilament organization and dynamics, affecting membrane trafficking, and resulting in coordinated expansion and recycling of plasma membrane, as well as in cell wall expansion (reviewed in Hussey et al., 2006; Smith and Oppenheimer, 2005; Mathur, 2004; Zarsky et al., 2009).

Microfilaments contribute to the determination of growth sites and are essential for the movement of Golgi-derived vesicles (Baluska et al., 2000, see Zarsky et al., 2009), endosomes movement and morphology (Voigt et al., 2005; Guimil and Dunand, 2007) and configuration and/or distribution of cell wall components (Chen et al., 2007). Microtubules significantly participate in the organization of cell wall cellulose microfibrils assembly (Sugimoto et al., 2003; Bringmann et al., 2012). Their depolymerization or stabilization in apically growing cells causes a loss of growth directionality, formation of multiple growth points and even isotropic expansion (Bibikova et al., 1999; Mathur, 2004). Thus, actin filaments, microtubules and their co-ordination are important for all plant cell morphogenetic processes, as well as for tissue and organ level processes depending upon them e.g. due to a contribution of plasmalemma auxin carriers turnover such as the PIN proteins (see Yang, 2008).

Epidermal pavement cell mophogenesis, producing the characteristic interlocking puzzle-like cell shapes, involves lobe initiation (anisotropic growth) followed by lateral isotropic expansion (Zhang et al., 2011; Fu et al., 2005). Interdigitating growth of neighboring cells appears to be controlled by cortical microtubule bands located in the neck regions of the cell, while lobe formation depends on patches of microfilaments (Fu et al., 2005; Fu et al., 2009; Xu et al., 2010). The Rho of plants (ROP) GTPases and their RIC family interactors control cytoskeleton arrangement and membrane trafficking (see Smith and Oppenheimer, 2005; Hussey et al., 2006; Yalovsky et al., 2008). Microtubule bands in neck regions are induced by the RIC1/ROP6 pathway which antagonizes the RIC4/ROP2 pathway, promoting microfilament assembly in the lobes. ROP2 is activated by auxin; it also inhibits PIN1 endocytosis via promoting accumulation of cortical actin filaments, resulting thus in local positive-feedback promoting growth in lobes (Xu

et al., 2010; Nagawa et al., 2012). Thus, epidermal pavement cells have recently emerged as an important model for studying co-ordinated interplay of cytoskeleton and membrane dynamics.

Formins, a major family of evolutionarily ancient actin nucleators, have been recognized as key molecular regulators of cytoskeletal assembly and organization also in plants (see Blanchoin and Staiger, 2010) and some of them were shown to interact with microtubules (Deeks et al., 2010; Li et al., 2010; see Wang et al., 2012). Based on FH2 domain phylogeny, angiosperm formins can be divided into two clades (Class I and Class II), which also exhibit characteristic domain organization; Class I formins are often transmembrane proteins (Deeks et al., 2002; Cvrcková et al., 2004).

The Class I formin FH1 (AtFH1, At3g25500) is the main housekeeping formin in *Arabidopsis thaliana*. It contains a putative signal peptide, a transmembrane domain (Banno and Chua, 2000) and a proline-rich extracellular domain similar to cell-wall extensins which may enable FH1-mediated anchoring of the actin cytoskeleton across the plasma membrane into the cell wall and was shown to restrict lateral mobility of the formin in the membrane (Martiniere et al., 2011; Martiniere et al., 2012). FH1 can nucleate and bundle actin (Michelot et al., 2005; Michelot et al., 2006). Its ectopic overexpression in pollen results in an abundance of membrane-associated actin cables and causes pollen tube growth depolarization (Cheung and Wu, 2004). The effects of its mutation or general formin inhibition reveal that it affects also microtubule dynamics in vegetative tissues, in particular seedling rhizodermis, possibly via microtubules-actin filaments crosstalk (Rosero et al., 2013a).

Here we report the characterization of T-DNA insertion mutants affecting FH1 and its closest relative FH2 (At2g43800), in particular their effects on cotyledon pavement cell shape determination, but also on other morphogenetic and developmental processes, including auxin-dependent cotyledons vascular development.

## Results

### *FH1 and FH2 are essential for development of both gametophytes*

To examine the function of *FH1* (At3g25500) and its closest paralog *FH2* (At2g43800), homozygous *fh1-1* and *fh2* mutants were crossed, F1 progeny from the crosses was allowed to self-fertilize, and the genotype of F2 progeny was determined by PCR. No double homozygous *fh1/fh1fh2/fh2* plants were found and just two *fh1* homozygotes carrying heterozygous *fh2* (*fh1/fh1FH2/fh2*) was recovered among 43 F2 plants (Supplemental Table 1 online). Empty seed positions were found in mature siliques of double heterozygous plants (*FH1/fh1FH2/fh2*), suggesting early seed abortion (Figure 1A). Reduced fertility was also observed in *fh1/fh1FH2/fh2* plants; however, the line could still be maintained. One half of pollen grains from double heterozygote and *fh1/fh1FH2/fh2* mature anthers were visibly small and shriveled. DAPI staining revealed unusual appearance, number, and position of nuclei in those defective pollen grains, suggestive of a mitotic defect (Figure 1B).

Seed abortion and pollen lethality were observed also when *fh1-2* was crossed with plants expressing GFP-mTalin, an actin marker known to perturb the actin cytoskeleton and enhance the phenotype of some mutants (Ketelaar et al., 2004b; Cvrcková et al., 2012) but not with a less intrusive actin marker – GFP-FABD and no homozygous *fh1-2* plants homozygous for GFP-mTalin were found (Supplemental Tables 2 and 3 online), suggesting that pollen development is extremely sensitive to the decreased FH1 level. Ultrastructure visualization by TEM revealed detachment of the plasma membrane from the cell wall, amorphous lipid bodies or collapsed pollen grains in double heterozygote and *fh1/fh1FH2/fh2* pollen (Figure 1C). Additionally, the tapetum cells appeared to detach from adjacent endothecial cells and amorphous lipid bodies were found in both tapetum and endothecial cells in double heterozygotes (Figure 1D). Both double heterozygote and *fh1/fh1FH2/fh2* plants, but not single (homozygous) *fh1* or *fh2* mutants, showed a significant fraction of aborted seeds and defective pollen grains (Figure 1E, F). These observations are suggestive of both male and female gametophytic defects, which were confirmed also in reciprocal crosses (Supplemental Table 1 online) and which are consistent with an essential function

of FH2 in development of both gametophytes under condition of reduced FH1 expression, but not at wild type FH1 level.

***Formin mutations affect cotyledon pavement cell shape***

We have not observed any gross phenotypic alterations in single formin mutant seedlings, as well as in *fh1/fh1FH2/fh2* plantlets (albeit close observation revealed alterations in cotyledon positioning – see Figure 2A and below). We thus focused on detailed observation of above-ground organ epidermis, as we previously found that *fh1* mutations affect rhizodermal cell morphogenesis (Rosero et al., 2013a). Indeed, we found considerable alterations in interdigitating pavement cell shape in mutant plants (Figure 2B-D). Five days old *fh1* seedlings had longer pavement cell lobes than wild type (wt), and appeared to lack a single or main axis which follows the leaf long axis in wt seedlings (Zhang et al., 2011), suggesting partial loss of cell growth anisotropy (Figure 2B).

Cell area and circularity (which provides a measure of lobing as less lobed cells have higher circularity) were measured from older (10 DAG) seedlings. Both *fh1-1* and *fh1/fh1FH2/fh2* seedlings showed bigger and more lobed (less circular) cells than wt. Although the difference in cell size was not seen in the *fh1-2* mutant, which produces reduced amount of nearly full length transcript (Rosero et al., 2013a), cell circularity was still significantly lower than in wt. In *fh2* mutants, the only significant differences were found in cell area (mutants had bigger cells than wt). Changes in cell circularity analogous to those seen in mutants and *fh1/fh1FH2/fh2* seedlings, were obtained also upon treatment with the formin inhibitor SMIFH2 (Rizvi et al., 2009; Rosero et al., 2013a), although the cell size did not change significantly, supporting the notion that the increased lobing was due to reduced formin function (Figure 2C, D).

***Cytoskeletal structure and dynamics in pavement cells of formin mutants***

Fluorescent protein-tagged cytoskeletal markers (GFP-FABD for actin and GFP-MAP4 for microtubules) were then introduced by crossing into the *fh1-1* (reported by Rosero et al., 2013a), *fh2* and *fh1/fh1FH2/fh2* genetic backgrounds.

We first evaluated the effect of the markers themselves on cell shape. In 5 DAG wt seedlings, GFP-MAP4 produced significant increase of cell size and reduction in cell lobing, and an even stronger effect in the same direction was observed in *fh2* mutants. In contrast, *fh1* and *fh1/fh1FH2/fh2* plants had larger cells but cell lobing was not affected. GFP-FABD induced significant increase in cell size in wt and single mutant seedlings, accompanied by significant increase of cell lobing in wt and *fh2* mutants. However, marker expression was reduced in some cells of *fh1* plants and completely silenced in *fh1/fh1FH2/fh2* plants, preventing thus evaluation of its effects on cell shape (Supplemental Figure 1 online).

Similar to our previous observations in rhizodermis cells (Rosero et al., 2013a); differences in microtubule organization between wt and *fh1-1* mutants were found in the cotyledon epidermis. Mutants exhibited generally less microtubule-associated fluorescence; varying levels of GFP-MAP4 expression and in some cases marker silencing were observed, while wt plants showed steady fluorescence levels. No obvious alterations in microtubule organization were observed in *fh2* mutants, but *fh1/fh1FH2/fh2* plants exhibited decreased and variable GFP-MAP4 expression similar to *fh1,* and also enhanced accumulation of microtubules in the neck zone (Figure 3A, B), consistent with their increased lobing.

Mutant *fh1* seedlings showed thicker actin bundles and fewer weakly labeled thin bundles or single filaments than wt seedlings, again reminiscent of the situation in roots (Rosero et al., 2013a). Quantification of the microfilament patterns by estimating microfilament bundling (skewness of fluorescence distribution) and network density (occupancy) showed that mutants have fewer single filaments but thicker microfilament bundles. The *fh2* seedlings showed an intermediate phenotype between *fh1* and wt. Variation was extremely high in *fh1* occupancy estimation due to patchy marker expression, and *fh1/fh1FH2/fh2* mutants could not be evaluated at all because of complete silencing of GFP-FABD expression (Figure 3C, D).

VAEM observations of individual cortical microtubule bundles, surprisingly possible under the thick cotyledon cuticle and cell wall, revealed increased dynamic instability of *fh1* and *fh1/fh1FH2/fh2* mutant microtubules but decreased

microtubule dynamics compared to wt, as well as to *fh2* seedlings whose microtubules may have been even somewhat less dynamic, as estimated from distribution of microtubule phases. The *fh1* and *fh1/fh1FH2/fh2* mutants had fewer pausing microtubules but more microtubules undergoing stochastic transition (i.e. alternatively shrinking and growing) than wt, while *fh2* had more microtubules at pause phase and less at shrinking phase compared to wt (Figure 4A, B, C).

In VAEM recordings from GFP-FABD tagged plants, *fh1* mutants had fewer single microfilaments and their filament bundles were less dynamic than those of wt seedlings (in line with our previous observations in the rhizodermis), while *fh2* did not show obvious differences from the wt with exception of filament bundles spending longer time at pause (Figure 4D, E, F).

***Effects of cytoskeletal inhibitors on pavement cell morphogenesis***

Next, we evaluated the effect of actin and/or microtubule perturbations by low doses of latrunculin B (LatB, an F-actin-depolymerizing drug), oryzalin (Oryz, a microtubule-depolymerizing drug) or both inhibitors on interdigitating cell development and cytoskeletal structure in wt and *fh1-1* seedlings (either non-transgenic or expressing fluorescent protein-tagged cytoskeletal markers). Qualitative observations in wt seedlings expressing both FABD-GFP and mCherry-TUA5 (Sampathkumar et al., 2011), revealed, consistent with previous reports (Staiger et al., 2009), that low dose LatB treatment results in an apparent shift towards thicker actin filament bundles due to thin filament disruption, as well as a decrease in microtubule fluorescence, possibly due to microtubule destabilization. Oryzalin also appeared to destabilize not only microtubules but also actin filaments (Figure 5A).

In marker-free plants, low concentration of either LatB or Oryz increased cell area and reduced lobing in wt, while in *fh1-1* seedlings LatB reduced lobing and Oryz increased cell area. Simultaneous application of LatB and Oryz did not affect cell area but reduced cell lobbing in both wt and *fh1-1* seedlings (Supplemental Figure 2 online). In GFP-MAP4-labeled wild type or *fh1-1* plants, treatment with LatB did not affect cell lobing, while Oryz increased significantly lobe length in the wt,

mimicking thus the effect of the *fh1* mutation. Together LatB and Oryz reduced lobe length and cell area but the number of lobes in both *fh1* mutant and wt was increased (Figure 5B, C; Supplemental Figure 2 online). Quantification of microtubule distribution showed significantly lower density in *fh1* mutant than in wt even in seedlings grown in control media, while LatB caused further reduction of microtubule density in *fh1* plants but not in wt, and Oryz treatment (alone or in combination with LatB) reduced microtubule density (as expected) in both *fh1* and wt plants comparably (Figure 5D).

***Formins contribute to membrane trafficking***

We next examined the effects of formin impairment on membrane turnover by analyzing pavement cell development under control conditions and after treatment with specific inhibitors of membrane traffic – tyrphostin A23 (TyrA23, an inhibitor of clathrin coat dependent endocytosis) and brefeldin A (BFA, inhibiting the secretory pathway). While BFA did not exhibit significant effects, TyrA23 stimulated cell lobing with stronger effect in *fh1-1* than wt seedlings (Figure 6A, B). Disruption of formin function in wild type seedlings by SMIFH2 reduced significantly the motility of GFP-tagged clathrin light chain (CLC-GFP) dots as followed by VAEM (Figure 6C, D), supporting thus the notion of participation of formins in membrane recycling.

Pavement cell ultrastructure visualized by TEM showed invaginations in the plasma membrane which may be associated with defects in the cell membrane recycling, and thickened cell walls in *fh1/fh1FH2/fh2* seedlings (Figure 6E, F).

***Whole-organ phenotypes caused by formin impairment suggest involvement in auxin signalling***

Since pavement cell morphogenesis involves auxin signaling (Xu et al., 2010), the effects of formin mutations on pavement cell lobing combined with the above described membrane trafficking phenotypes hint at the intriguing possibility of formins participating in auxin-related regulatory processes. We thus examined formin mutants for possible organ-scale developmental phenotypes.

We found that some formin-impaired mutants had reduced cotyledon-to petiole angle compared to the wt (Figure 2A, Figure 7). Moreover, formin mutations affected cotyledon shape and vascular tissue development (Figure 8A). Mutant *fh1* and, even more pronouncedly, also *fh1/fh1FH2/fh2* seedlings had larger and more rounded cotyledons than wt. Vascular complexity and connectivity was evaluated by scoring frequencies of distinct venation patterns; formin mutants showed higher fraction of cotyledons displaying defective vascular complexity and connectivity patterns than wt (Figure 8B).

To probe the role of cytoskeleton in vascular tissue development, we treated wt seedlings with LatB, Oryz and SMIFH2 inhibitors. SMIFH2 treatment mimics to some extent the formin mutations, however LatB and Oryz also exhibited significant effects in vascular connectivity (Figure 8A, 8B). Examination of the expression pattern of the auxin reporter DR5-GFP showed lower hydatode auxin maxima in *fh1* and *fh1/fh1FH2/fh2* seedlings compared to wt (Supplemental Figure 3 online), consistent with involvement of auxin signalling.

**Discussion**

In this paper, we report results of a detailed analysis of the consequences of formin function impairment on cytoskeletons organization and dynamics in above-ground organs of young Arabidopsis seedlings, as well as on downstream cellular processes including membrane turnover, with subsequent morphogenetic implications.

Numerous recent reports have documented the participation of Arabidopsis formins in the organization and dynamics of actin (Michelot et al., 2006; Michelot et al., 2005; Cheung and Wu, 2004; Yi et al., 2005) and microtubules (Deeks et al., 2010; Li et al., 2010; Rosero et al., 2013a). However, phenotypic consequences of mutational loss of a single formin gene are often subtle due to functional overlap among the numerous formin paralogs (reviewed in (Cvrckova, 2012). We have employed mutants in a pair of closely related Class I formins – the major housekeeping formin FH1, which is highly expressed in most plant tissues according to publicly available microarray data (Zimmermann et al., 2004), and its closest relative FH2 – as well as a pharmacological approach to

examine the effects of formin deficiency in Arabidopsis. Both FH1 and FH2 are typical Class I formins containing a transmembrane domain (Banno and Chua, 2000) and a proline-rich extracellular domain. FH1 was previously shown to be located in the plasmalemma, preferentially in areas devoid of cortical microtubules (Banno and Chua, 2000; Martiniere et al., 2011), to bundle actin (Cheung and Wu, 2004; Michelot et al., 2005; Michelot et al., 2006) and to anchor the actin cytoskeleton across the plasma membrane into the cell wall (Martiniere et al., 2011). We have previously reported its participation in both actin and microtubule dynamics in rhizodermis cells (Rosero et al., 2013a).

***Gametophytic function of FH1 and FH2***

We failed to obtain double homozygous *fh1fh2* mutants, and both defective pollen grains and aborted seeds in siliques of self-pollinated double heterozygotes or *fh1/fh1FH2/fh2* plants were observed. Thus, *FH2* appear to be essential for normal gametophytes development under subnormal expression levels of *FH1* (including its absence), or a certain minimum expression of *FH1* and/or *FH2* seem to be required for normal male and most probably also female gametophytic development. The observed pollen grain defects included nuclear abnormalities reminiscent of pollen mitosis defects in microtubule-affecting mutants, such as e.g. γ-tubulin mutants (Pastuglia et al., 2006). Remarkably, mutants in a microtubule-binding Class II formin, *FH14*, exhibit defects already at meiosis, i.e. at an earlier developmental stage (Li et al., 2010). Seed abortion and pollen lethality was observed also in crosses of *fh1* with plants tagged by GFP-mTalin, an actin marker known to perturb actin cytoskeleton dynamics (Ketelaar et al., 2004b) that also exhibits synthetic lethality with a mutation in another formin gene, *FH12* (Cvrcková et al., 2012). Ultrastructural aberrations were observed in the defective pollen grains, as well as in tapetum and endothecial cells of the formin-impaired plants, including detachement of the plasma membrane from the cell wall and presence of amorphous lipid bodies. While we could not find any reports on the effects of cytoskeletal mutants or inhibitors on mature pollen ultrastructure, and thus the possibility that this phenotype is due to actin and/or microtubule disruption alone cannot be entirely excluded, observed membrane

alterations are suggestive of possible downstream effects on intracellular dynamics including the endomembrane system. A similar phenotype has been reported in plants expressing RNAi against phospholipase $A_2$ (Kim et al., 2011), whose metazoan homologs participate in the control of cytoskeletal rearrangements and membrane dynamics, including membrane recycling, albeit the mechanism remains subject to discussion (Moes et al., 2010; Bechler et al., 2011; Liu et al., 2012; Cai et al., 2012). In Arabidopsis, pharmacological inhibition of phospholipase $A_2$ disrupts microtubule organization Gardiner et al., 2008).

***Formins participate in epidermal pavement cell morphogenesis through modulating cytoskeletal organization and dynamics***

When attempting to use the cytoskeletal markers in pavement cells, we found extreme variation in both GFP-FABD and GFP-MAP4 expression levels in *fh1* and *fh1/fh1FH2/fh2* plants, with complete silencing of GFP-FABD in the *fh1/fh1FH2/fh2* background. This genotype thus had to be excluded from subsequent cytoskeletal phenotype analysis. As proposed previously for the GFP-mTalin actin marker in *fh12* mutants (Cvrcková et al., 2012), silencing may be a mechanism to avoid marker toxicity.

Consistent with our previous observations in roots (Rosero et al., 2013a), decreased density of actin filaments together with increased actin bundling, as well as reduction of actin dynamics, were found in pavement cells of both *fh1* and *fh2* mutants. *FH1* was previously proposed to participate in actin nucleation and elongation (Michelot et al., 2005; Michelot et al., 2006) and in anchoring of actin filaments across the plasmalemma into the cell wall (Martiniere et al., 2011). *FH2* is closely related and thus likely to have similar functions. Decreased availability of these proteins might disrupt the association between actin and cell wall, by reducing new filament polymerization from cell membrane and by rendering some fine cortical actin filaments free to move and bundle (perhaps with participation of other members of the formin family), with the net effect being a shift in the balance between fine, presumably cortically anchored filaments and massive, more stable bundles (Figure 9). Consequently also microtubule distribution may

be affected, possibly by removing the restrictions on their distribution or movement imposed by cell wall-anchored formin-actin complexes (Martiniere et al., 2011).

The interdigitating cell shape of epidermal pavement cells results from coordinated anisotropic and lateral isotropic expansion, itself a product of orchestrated cytoskeletal rearrangements and membrane trafficking (see Introduction; reviewed in Kotzer and Wasteneys, 2006, Mathur, 2006). At early steps of lobed epidermal cell development, elongated polygons are generated by cell elongation taking place preferentially along the leaf axis (Zhang et al., 2011). Polarity of this initial elongation, apparent in the preferential direction of mature lobes, appears to be reduced while overall cell lobing is increased in the cotyledons of *fh1* mutant seedlings; alternatively, the frequently observed cells with multiple axes may result from increased lobing complexity, i.e. development of secondary lobes upon existing ones. Loss of *FH2* leads to increased cell size, and these phenotypes are additive in *fh1/fh1FH2/fh2* seedlings. An increase in cell lobing was found also in plants treated with the formin inhibitor SMIFH2, confirming that this phenotype is due to formin perturbation.

The currently accepted model of interdigitating growth highlights the role of microtubule bands in neck formation, lobe expansion depends on patches of microfilaments (Fu et al., 2005; Fu et al., 2009; Xu et al., 2010). While this may, at the first glance, suggest that more lobed cells ought to have more developed microtubule bands due to increased microtubule stability, formation of the neck bands in fact requires reorganization of branched microtubules (Lin et al., 2013) and may thus depend on microtubule mobility. Cell expansion, in general, also depends upon microtubule turnover (Shaw et al., 2003; Wang et al., 2007) which affects cellulose microfibrils arrangement (Sugimoto et al., 2003; Panteris and Galatis, 2005; Bringmann et al., 2012). Indeed, we observed less dense and more dynamic microtubules in pavement cells of GFP-MAP4 tagged *fh1* and *fh1/fh1FH2/fh2* seedlings than in wt. In *fh2* mutants, only reduced microtubule dynamics but no obvious changes in microtubule organization were found,

Microtubule stabilization generally decreases growth anisotropy (Bibikova et al., 1999; Mathur, 2004), and in pavement cells of wt plants, stabilization of

microtubules by the GFP-MAP4 marker indeed reduced cell lobing (and increased cell size, confirming that the phenotype is not due to impaired cell expansion *per se*). Thus, formin mutations appear to destabilize microtubules, or counter the stabilizing effect of GFP-MAP4, similar to the previously described *fh1* phenotype in rhizodermis (Rosero et al., 2013a), and one of the consequences is more pronounced pavement cell lobing.

Cytoskelelal inhibitors LatB (at concentrations disrupting thin actin filaments, with subsequent microubule destabilization, and preserving bundles) and Oryz (destabilizing microtubules and secondarily also actin) affected, in our hands, cytoskeletal organization in a manner consistent with previous reports (Collings et al., 2006; Sampathkumar et al., 2011; Smertenko et al., 2010). They also at low concentration increased cell area and reduced lobing in untransformed plants, i.e. exhibited different effects on cell lobing than the formin mutations, suggesting that formins exert a more specific effect than just modulation of overall cytoskeletal dynamics. The reduction of microtubule density in *fh1* pavement cells expressing GFP-MAP4 was aggravated by LatB, while tagged microtubules in wt plants were less affected. Nevertheless, LatB did not counter the effect of GFP-MAP4 on cell shape in wt plants, while Oryz (alone or in combination with LatB) reduced the difference between wt and *fh1* mutant due to significant reduction of microtubule density. The combination of Oryz and LatB also increased significantly the number of cell lobes. In summary, these pharmacological studies support the notion that the effects of formin mutations on pavement cell lobing are at least in part due to alterations in microtubule dynamics that themselves may be secondary to changes in the actin architecture and dynamics.

***Formins contribute to membrane trafficking***

The altered ultrastructure of formin mutant pollen suggested disruption of membrane trafficking, probably secondary to modifications of cytoskeletal organization and dynamics. Endocytic membrane turnover is central to any form of plant cell growth (Žárský et al., 2009), and it is thus not surprising that it has a central role in the interdigitating cell development. Indeed, TyrA23, an inhibitor of clathrin-dependent endocytosis, increased cell lobing i.e. it mimicked the

formin mutation, and its effect was stronger in *fh1* plants. Conversely, the formin inhibitor SMIFH2 impaired movement of clathrin-containing compartments in wt plants expressing GFP-tagged clathrin light chain (CLC-GFP). SMIFH2 slowed down the movement of CLC-GFP dots comparable with the LatB effect on endosomal movements (Voigt et al., 2005), confirming thus the important role of cytoskeleton in cell membrane recycling.

In mammalian and yeast cells, actin participation in endocytosis is well described (see Kaksonen et al., 2006; Mooren et al., 2012). F-actin dynamics contributes to clathrin-coated vesicle formation (Yarar et al., 2005), and actin nucleators such as Arp2/3 have been found at sites of endocytosis (Ferguson et al., 2009). Motility of endosomes can be modulated by stabilizing their association with the actin cytoskeleton involving a human Diaphanous-related formin, hDia2C (Gasman et al., 2003). Equatorial endocytosis was inhibited in fission yeast cells lacking the formin For3, which exhibit defects in both actin and microtubule organization (Gachet and Hyams, 2005). The budding yeast Bni1 formin mediates actin cable nucleation and elongation, and is required for Rho1-mediated endocytosis (Prosser et al., 2011). Thus, participation of plant formins in membrane turnover would be in line with observations from other model systems.

The ultrastructure of *fh1/fh1FH2/fh2* pavement cells showed plasma membrane invaginations and thickened cell walls similar to the phenotype of dynamin mutants *drp1*(Carter et al., 2004) and *adl1A-2* (Kang et al., 2003), which may be due to the inhibited membrane recycling. This process is important to control cell expansion and maintain the membrane homeostasis (Baluska et al., 2000; Voigt et al., 2005; Guimil and Dunand, 2007; Chen et al., 2007; see Žárský et al., 2009). Taken together, our observations suggest that *FH1* and *FH2* are participating in endocytosis, by analogy with other systems via modulating actin filament arrangement and turnover, and in plants probably specifically also due the role of microfilament assembly anchorage to plasmalemma and cell wall (Martiniere et al., 2011).

***Effects of formin impairment on tissue and organ development***

The planar morphogenesis of pavement cells is regulated by the interplay of ROP-GTPases, cytoskeleton and auxin transport (Xu et al., 2010; see Pietra and Grebe, 2010). Our observations suggest that formins participate in membrane turnover, affecting, among other processes, also distribution of PIN auxin carriers. Indeed, pavement cell lobe development was proposed to involve the accumulation of the cortical F-actin in the lobing region which induces PIN1 polarization by localized inhibition of PIN1 endocytocis (Nagawa et al., 2012). Auxin signalling may be therefore contributing to the observed pavement cell phenotypes (Figure 9).

We have thus looked for possible effects of *fh1* and *fh2* mutations on vascular tissue patterning, a process known to be auxin – and PIN-dependent (Sachs, 1981), see also (Scarpella et al., 2010). While examining vascular patterns in cotyledons, we noticed that *fh1* and *fh1/fh1FH2/fh2* plants had bigger and more rounded cotyledons than wt, possibly due to alterations in cell expansion. However, specific alterations of vascular patterns were also observed in the formin mutants, and these defects in vascular connectivity were also in part phenocopied by SMIFH2, while vascular pattern alterations reminded of those seen in LatB and Oryz treatments; the differences between formin mutant and SMIFH2-induced phenotypes may be attributed to the inhibitor interfering with the function of other formins as well. Moreover, auxin maxima visualized by DR5-GFP expression were altered in formin mutants, consistent with possible defects in PIN polarity due to alterations in membrane recycling, which is an important part of the polarization process (Geldner et al., 2001; Dhonukshe et al., 2008).

In summary, we have shown here that plant Class I formins *FH1* and *FH2* participate not only in the control of actin and subsequently also microtubule dynamics and architecture, but that they also affect membrane turnover, with downstream effects on the level of cell and tissue development that might be at least in part due to modulation of auxin carrier turnover.

## Methods

### *Plants*

Two T-DNA insertional mutants (*fh1-1:* SALK-032981 and *fh1-2:* SALK-009693) in the *FH1* gene (At3g25500) and one (*fh2:*GK-066D02) in the *FH2* gene (At2g43800) were obtained through NASC (Alonso et al., 2003; Kleinboelting et al., 2012). The *fh1-1* mutant line was previously shown to produce no detectable transcript, while *fh1-2* showed a low level of mRNA truncated at the 5´UTR and possibly capable of encoding full-length protein (Rosero et al., 2013a). The *FH1* and *FH2* allelic status was determined by PCR using the primers described in Rosero et al., 2013a for *FH1* and the primers *fh2*-LP (5´CAATTGGTCCAACCAAACAAC3´) with *fh2*-RP (5´TTCTGTTTCTTAGAGCCGTCG3´) for *FH2*. For mutant alleles, the RP primers were combined with the SALK primer LBb1.3 (5´ATTTTGCCGATTTCGGAAC3´) or Go8409 (5´ATATTGACCATCATACTCATTGC) for the T-DNA insertion. Crossing between *fh1-1* and *fh2* mutants, and with reporter lines GFP-MAP4 (for microtubules) and GFP-FABD (for microfilaments) (Marc et al., 1998; Ketelaar et al., 2004a) was performed as described (Cole et al., 2005); for construction of *fh1* lines with cytoskeletal markers (see Rosero et al., 2013a). Formin wild type seedlings expressing both FABD-GFP and mCherry-TUA5 (Sampathkumar et al., 2011) or tagged clathrin light chain CLC-GFP (Ito et al., 2012) were used in some experiments.

### *Growth conditions and inhibitor treatments*

Seed germination was synchronized by several days at 4°C, followed by growth on vertical MS or inhibitor-containing plates for 5, 10 or 15 days at 22°C with a 16h-light/8h-dark cycle. Inhibitor stock solutions were prepared in dimethylsulfoxide (DMSO), stored at −20°C (Lat B, Oryz, BFA and TyrA23) or 4°C (SMIFH2) and added to liquid agar to desired concentrations, DMSO concentration was adjusted to 0.2% (v/v). All inhibitors were purchased from Sigma. In all experiments 2 to 3 replicates of around 20 plants were used per data point.

***Pollen and silique analysis***

Histochemical analysis of pollen was done according to Howden et al., 1998. Pollen from 4-5 fully open flowers was stained with DAPI (0.5μg/ml) for 5 min and then viewed by light and UV epi-ilumination using light microscope (BX-51, Olympus) at 20 or 40x magnification. Fertilized and aborted seeds were counted from mature siliques that were carefully opened and observed under binocular microscope. For each data point shown at least 400 seeds from at least 20 siliques were counted.

***Pavement cell morphometric analysis***

Pavement cell shape parameters were determined according to Zhang et al., 2008 from 10 DAG cotyledons stained with 1μM FM4-64 for 1 hour in the dark. Three images were taken from nonoverlapping regions in the apical third of the cotyledons using confocal laser-scanning microscope (LCS 510; Leica) with a 20x/1.2 water-immersion objective and 515 nm excitation. 8-10 cells per sample within a field were selected for evaluation; to avoid bias, cells that made contact with a diagonal line were chosen in each measured field. Measurements were performed using the ImageJ software (http://rsbweb.nih.gov; Abramoff et al., 2004) using its built-in functions for calculating circularity.

***Analysis of vascular tissue development***

Cotyledons from 15 DAG seedlings were dissected and cleared using ethanol 90% for 24 hours, washed and observed under light microscope (BX-51, Olympus) at 4x magnification. Venation complexity and connectivity were characterized according to Cnops et al., 2006. Between 60 and 115 cotyledons were analyzed per data point (except LatB, where 32 plants were scored).

***Confocal microscopy and image analysis***

GFP-tagged cytoskeleton was observed in cotyledons of 5 DAG seedlings using a confocal laser-scanning microscope (LCS 510; Leica) with a 63x/1.2 water-immersion objective and 488-nm argon laser (25 mW) excitation as described previously Rosero et al., 2013a with minor modifications (see Rosero et al., 2013b

*in press*). Images were acquired as xyz-series with a 0.7-1 $\mu$m interval or as xyt-series with the minimum interval for the given settings. Microfilament bundling and density was quantified according to Higaki et al., 2010. Skewness of fluorescence intensity distribution and occupancy were determined from 20-30 single cells as reported before Rosero et al., 2013a. Microtubule density was determined as the number of microtubules in an area of 400 $\mu m^2$ from confocal images in 5 cells from several plants. For measuring clathrin compartment dynamics, time-lapse images spanning two minutes were analyzed with the aid of the MTrackJ plugin incorporated in the Fiji ImageJ distribution (Meijering et al., 2012).

***VAEM Microscopy***

To evaluate cytoskeletal dynamics, we used the Leica AF6000 LX fluorescence platform with integrated TIRF module, the HCX PL APO 100x/1.46 oil inmersion objective, 400 nm peak excitation and 210 ms exposure time. Plants were mounted in water on chambered slides; images were captured with a Leica DFC350FXR2 digital camera in 0.5 seconds intervals in the course of 2 minutes and analyzed with Leica Application Suite (LAS) and ImageJ software as described before Rosero et al., 2013a. Kymographs were generated using Multiple Kymograph ImageJ plug-in from time-lapse image series collected from well-focused diagonal line of 400$\mu m^2$ (Sampathkumar *et al.,* 2011). The distribution of microtubule growth and shrinkage rates was estimated from at least 150 microtubule ends from at least 20 cells of at least 8 plants in each genotype or treatment.

***Electron microscopy***

For transmission electron microscopy (TEM), 5-8 anthers or 9-10 cotyledons per sample were fixed for 24 h in 2,5% glutaraldehyde in 0,1 M cacodylate buffer (pH 7,2) and postfixed in 2% $OsO_4$ in the same buffer. Fixed specimens were dehydrated through an ascending ethanol and acetone series and embedded in Araldite - Poly/Bed® 812 resin mixture. Thin sections were cut on a Reichert-Jung Ultracut E ultramicrotome and stained using uranyl acetate and lead citrate.

Sections were examined and photographed using JEOL JEM-1011 electron microscope with Megaview III camera and analySIS 3.2 software (Soft Imaging System®).

**Supplemental data**

**Supplemental Figure 1.** Effects of GFP-MAP4 and GFP-FABD expression on pavement cell shape in wt and formin mutants.

**Supplemental Figure 2.** Effects of LatB and Oryz on pavement cell shape in wt and *fh1* mutant plants.

**Supplemental Figure 3.** Auxin maxima visualised using the DR5-GFP reporter in wt and formin mutants (10 DAG).

**Supplemental Table 1.** Segregation ratios in crosses involving *fh1-1 and fh2* mutants.

**Supplemental Table 2.** Segregation ratios of *fh1-1* in genetic backgrounds expressing stable mTalin-GFP and GFP-FABD markers.

**Supplemental Table 3.** Seed abortion and pollen lethality in *FH1/fh1* plants expressing stable mTalin-GFP and GFP-FABD markers.

**Acknowledgements**

This work was supported by the MSM 0021620858, GACR P305/10/0433 and SVV 265203 projects. We thank Ondřej Šebesta and Ondřej Horvath for help with microscopy and image analysis, Marta Čadyová for technical support and Julian Weisburd for help with some experiments during his internship.

**Author contributions**

F.C., V.Z. and A.R. designed the research. A.R. and P.S. performed research experiments. A.R., M.G., P.S. and F.C. analyzed data, A.R. drafted the manuscript and F.C. and V.Z.participated in writing the article.

**Figure legends**

**Figure 1.** Reduced fertility and pollen lethality in crosses of *fh1-1* and *fh2* mutants. (A) Aborted seeds in an *FH1/fh1-1FH2/fh2* (double heterozygote) plant. (B) Bright field and DAPI stained micrographs of mature pollen of wild type (wt), double heterozygote and *fh1/fh1FH2/fh2* lines. (C) Ultrastructure (TEM) of pollen from wt, double heterozygote and *fh1/fh1FH2/fh2* plants. (D) Ultrastructure (TEM) of tapetum cells from wt and double heterozygote lines; anomalous structures marked by arrows. (E) Frequency of seed abortion in formin mutants. (F) Fraction of abnormal pollen in formin mutants.

**Figure 2.** Seedling appearance and cotyledon pavement cells in wt, formin mutants and plantlets treated with the formin inhibitor SMIFH2 (30μM). (A) Seedlings at 10 days after germination (DAG). (B) Completely expanded pavement cells from 10 DAG plants. (C) Pavement cells from 5 DAG plants - appearance (expansion axis marked) and lobe length (D) Pavement cell area and circularity from 10 DAG cotyledons. Significant differences from wt (T-test $P < 0.001$) marked by an asterisk.

**Figure 3.** Microtubule and actin filament organization in pavement cells of wt and formin mutant seedlings at 5 DAG. (A) Microtubules labeled by GFP-MAP4. Microtubule accumulation in the neck region is marked by an arrow. (B) Varying levels of GFP-MAP4 intensity in cells (arbitrary classes corresponding to high, weak or no fluorescence determined visually). (C) Actin filaments labeled by GFP-FABD. (D) Actin filament bundling (skewness) and density (occupancy).

**Figure 4.** Microtubule (GFP-MAP4) and actin filament (GFP-FABD) dynamics in pavement cells of wt and formin mutant seedlings at 4 DAG. (A, D) Overlay of VAEM images from two time points showing growing microtubules (A) or microfilaments (D) in magenta, shrinking in green, pausing in light green and alternating in light magenta. (B, E) Kymographs of microtubule (B) or microfilament (E) dynamics. Events of microtubule appearance/disappearance

across the scanned line are marked by asterisks in (B), arrows in (E) denote stable thick actin bundles. (C) Distribution of microtubule phases, quantified from time-lapse images taken across the time span of 2 min. (F) Actin filament bundles lifetimes; asterisk – significant differences between mutants and wt (T-test $P < 0.005$).

**Figure 5.** Cell shape and cytoskeleton organization in pavement cells of 5 DAG wt and *fh1-1* mutants grown in the presence of inhibitors. (A) Actin and microtubules in wt plants labeled simultaneously by GFP-FABD (green) and mCherry-TUA5 (magenta) grown in LatB (0.2μM) and Oryz (0.2μM)-supplemented media. (B) Cell shape and microtubules in plants labeled by GFP-MAP4 and grown in LatB (0.1μM), Oryz (0.1μM) and LatB+Oryz supplemented media. (C) Lobe length from cells of plants labeled by GFP-MAP4. (D) Microtubule density. Significant differences (T-test $P < 0.001$) marked by an asterisk.

**Figure 6.** Effects of membrane trafficking inhibition in formin-impaired seedlings. (A) Cell shape changes induced by BFA (15μM) and TyrA23 (0.1μM) in wt and *fh1-1* mutant (10 DAG). (B) Circularity of pavement cells from 10 DAG wt and *fh1-1* plants treated by BFA and TyrA23. (C) Dynamics of clathrin-containing compartments in pavement cells of 10 DAG seedlings grown on control medium and/or in the presence of SMIFH2 (20μM). Green channel – location of CLC-GFP dots in time zero, magenta – location at the time shown (D) Velocity of CLC-GFP dots on control and SMIFH2 (20μM)-containg medium, from data from the experiment shown in (C). (E) TEM images of cell-cell boundary between two cotyledon pavement cells in wt and *fh1/fh1FH2/fh2* seedlings (5 DAG) showing plasmalemma invaginations. (F) Surface of pavement cells from wt and *fh1/fh1FH2/fh2* seedlings (5 DAG). Significant differences from relevant controls (T-test $P < 0.05$) are marked by asterisks in all graphs.

**Figure 7.** Cotyledon positioning in wt and formin mutants. (A) Seedlings at 5 DAG. (B) Cotyledon to petiole angles (in at least 30 seedlings per data point).

Significant differences from wt marked by asterisks (* T-test P < 0.01, **T-test P < 0.0001).

**Figure 8.** Cotyledon shape and venation pattern in seedlings grown on inhibitor-supplemented media. (A) Shape and venation pattern in cleared cotyledons from wt controls, formin mutants and wt grown on SMIFH2 (30μM), LatB (0.2μM) and Oryz (0.2μM) supplemented media (15 DAG). (B) Venation complexity and connectivity pattern definition and distribution.

**Figure 9**. Model summarizing the role of FH1 and FH2 in pavement cell morphogenesis. Both formins facilitate formation of fine, dynamic actin arrays nucleated from the membrane and anchoredto the cell wall, i.e. they shift the balance away from cytoplasmic actin filaments that are free to bundle, possibly by action of other formins. FH1 (and presumably also FH2) – anchored actin filaments also restrict the lateral mobility and dynamics of cortical microtubules, "corralling" them into actin-free zones (Martiniere et al. 2011, 2012). Decreased FH1 activity frees these microtubules, facilitating thus formation of bundles at pavement cell "necks". FH1 and FH2 also, probably by a cytoskeleton-dependent mechanism, promote endocytosis, which reduces the abundance of PIN auxin transporters at lobe tips, which facilitate lobe outgrowth (Xu et al.2010). Endocytosis is also important for PIN recycling as a pre-requisite of auxin-dependent organ polarity signaling, and its disruption in the mutants may contribute to the loss of alignment between pavement cell and organ axis.

**References**

**Abramoff, M., Magalhaes, P., and Ram, S.** (2004). Image processing with ImageJ. Biophotonics International **11:** 36-42.

**Alonso, J., Stepanova, A., Leisse, T., Kim, C., Chen, H., Shinn, P., Stevenson, D., Zimmerman, J., Barajas, P., Cheuk, R., Gadrinab, C., Heller, C., Jeske, A., Koesema, E., Meyers, C., Parker, H., Karnes, M., Mulholland, C., Ndubaku, R., Schmidt, I., Guzman, P., Aguilar-Henonin, L., Schmid, M., Weigel, D., Carter, D.E., Marchand, T., Risseeuw, E., Brogden, D.,**

**Zeko, A., Crosby, W.L., Berry, C.C., and Ecker, J.R.** (2003). Genome-wide insertional mutagenesis of *Arabidopsis thaliana*. Science **301**: 653-657.

**Baluška, F., Salaj, J., Mathur, J., Braun, M., Jasper, F., Šamaj, J., Chua, N., Barlow, P., and Volkmann, D.** (2000). Root hair formation: F-actin-dependent tip growth is initiated by local assembly of profilin-supported F-actin meshworks accumulated within expansin-enriched bulges. Dev. Biol. **227**: 618-632.

**Banno, H., and Chua, N.** (2000). Characterization of the arabidopsis formin-like protein AFH1 and its interacting protein. Plant Cell Phys. **41**: 617-626.

**Bechler, M., Doody, A., Ha, D., Judson, B., Chen, I., and Brown, W.** (2011). The phospholipase A2 enzyme complex PAFAH lb mediates endosomal membrane tubule formation and trafficking. Mol. Biol. Cell. **22**: 2348-2359.

**Bibikova, T., Blancaflor, E., and Gilroy, S.** (1999). Microtubules regulate tip growth and orientation in root hairs of *Arabidopsis thaliana*. Plant J. **17**: 657-665.

**Blanchoin, L., and Staiger, C.** (2010). Plant formins: diverse isoforms and unique molecular mechanism. Curr. Opin. Plant Biol. **1803**: 201-206.

**Bringmann, M., Li, E., Sampathkumar, A., Kocabek, T., Hauser, M., and Persson, S.** (2012). POM-POM2/CELLULOSE SYNTHASE INTERACTING1 is essential for the functional association of cellulose synthase and microtubules in Arabidopsis. Plant Cell **24**: 163-177.

**Cai, B., Caplan, S., and Naslavsky, N.** (2012). cPLA2α and EHD1 interact and regulate the vesiculation of cholesterol-rich, GPI-anchored, protein-containing endosomes. Mol. Biol. Cell **23**: 1874-1888.

**Carter, C., Bednarek, S., and Raikhel, N.** (2004). Membrane trafficking in plants: new discoveries and approaches. Curr. Opin. Plant Biol. **7**: 701-707.

**Chen, T., Teng, N., Wu, X., Wang, Y., Tang, W., Samaj, J., Baluška, F., and Lin, J.** (2007). Disruption of actin filaments by Latrunculin B affects cell wall construction in *Picea meyeri* pollen tube by disturbing vesicle trafficking. Plant Cell Physiol. **48**: 19-30.

**Cheung, A., and Wu, H.** (2004). Overexpression of an arabidopsis formin stimulates supernumerary actin cable formation from pollen tube cell membrane. Plant Cell **16**: 527-269.

**Cnops, G., Neyt, P., Raes, J., Petrarulo, M., Nelissen, H., Malenica, N., Luschnig, C., Tietz, O., Ditengou, F., Palme, K., Azmi, A., Prinsen, E., and Van Lijsebettens, M.** (2006). The TORNADO1 and TORNADO2 genes function in several patterning processes during early leaf development in *Arabidopsis thaliana*. Plant Cell **18**: 852-866.

**Cole, R., Synek, L., Žárský, V., and Fowler, J.** (2005). SEC8, a subunit of the putative arabidopsis exocyst complex, facilitates pollen germination and competitive pollen tube growth. Plant Physiol. **138**: 2005-2018.

**Collings, D., Lill, A., Himmelspach, R., and Wasteneys, G.** (2006). Hypersensitivity to cytoskeletal antagonists demonstrates microtubule-microfilament cross-talk in the control of root elongation in *Arabidopsis thaliana*. New Phytologist **170**: 275-290.

**Cvrčková, F., Grunt, M., and Žárský, V.** (2012). Expression of GFP-mTalin reveals an actin-related role for the arabidopsis class II formin AtFH12. Biologia Plantarum **3**: 431-440.

**Cvrčková, F., Novotný, M., Pícková, D., and Žárský, V.** (2004). Formin homology 2 domains occur in multiple contexts in angiosperms. BMC Genomics **5**: doi:10.1186/1471-216.

**Cvrčková, F.** (2012). Formins: emerging players in the dynamic plant cell cortex. Scientifica ID: 712605: doi: 10.6064/2012/712605.

**Deeks, M., Fendrych, M., Smertenko, A., Bell, K., Oparka, K., Cvrčková, F., Žárský, V., and Hussey, P.** (2010). The plant formin AtFH4 interacts with both actin and microtubules, and contains a newly identified microtubule-binding domain. J. Cell Sci. **123**: 1209-1215.

**Deeks, M., Hussey, P., and Davies, B.** (2002). Formins: intermediates in signal-transduction cascades that affect cytoskeletal reorganization. Trends Plant Sci. **7**: 492-498.

**Dhonukshe, P., Grigoriev, I., Fischer, R., Tominaga, M., Robinson, D., Hašek, J., Paciorek, T., Petrášek, J., Seifertová, D., Tejos, R., Meisel, L.,**

**Zažímalová, E., Gadella,T., Stierhof, Y., Ueda, T., Oiwaf, K., Akhmanova, A., Brock, R., and Spang, A.** (2008). Auxin transport inhibitors impair vesicle motility and actin cytoskeleton dynamics in diverse eukaryotes. PNAS **105**: 4489-4494.

**Ferguson, S., Raimondi, A., Paradise, S., Shen, H., Mesaki, K., Ferguson, A., Destaing, O., Ko, G., Takasaki, J., Cremona, O., Toole, E., and De Camilli, P.** (2009). Coordinated actions of actin and BAR proteins upstream of dynamin at endocytic Clathrin-coated pits. Developmental Cell **17**: 811-822.

**Fu, Y., Xu, T., Wen, M., and Yang, Z.** (2009). A ROP GTPase signaling pathway controls cortical microtubule ordering and cell expansion in Arabidopsis. Current Biology **19**: 1827-1832.

**Fu,Y., Gu, Y., Zheng, Z., Wasteneys, G., and Yang, Z.** (2005). Arabidopsis interdigitating cell growth requires two antagonistic pathways with opposing action on cell morphogenesis. Cell **120**: 687-700.

**Gachet, Y., and Hyams, J.** (2005). Endocytosis in fission yeast is spatially associated with the actin cytoskeleton during polarised cell growth and cytokinesis. J. Cell Sci. **118**: 4231-4242.

**Gardiner, J., Andreeva, Z., Barton, D., Ritchie, A., Overall, R., and Marc, J.** (2008). The phospholipase A2 inhibitor, aristolochic acid, disrupts cortical microtubule arrays and root growth in Arabidopsis. Plant Biology **10**: 725-731.

**Gasman, S., Kalaidzidis, Y., and Zerial, M.** (2003). RhoD regulates endosome dynamics through Diaphanous-related Formin and Src tyrosine kinase. Nature Cell Biology **5**: 195-204.

**Geldner, N., Friml, J., Stierhof, Y., Jurgens, G., and Palme, K.** (2001). Auxin transport inhibitors block PIN1 cycling and vesicle trafficking. Nature **413**: 425-428.

**Guimil, S., and Dunand, C.** (2007). Cell growth and differentiation in Arabidopsis epidermal cells. J. Exp Botany **58**: 3829-3840.

**Higaki, T., Kutsuna, N., Sano, T., Kondo, N., and Hasezawa, S.** (2010). Quantification and cluster analysis of actin cytoskeletal structures in plant

cells: role of actin bundling in stomatal movement during diurnal cycles in Arabidopsis guard cells. Plant J. **61**: 156-165.

**Howden, R., Park, S., Moore, J., Orme, J., Grossniklaus, U., and Twell, D.** (1998). Selection of T-DNA-tagged male and female gametophytic mutants by segregation distortion in Arabidopsis. Genetics **149**: 621-631.

**Hussey, P., Ketelaar, T., and Deeks, M.** (2006). Control of the actin cytoskeleton in plant cell growth. Annu. Rev. Plant Biol. **57**: 109-125.

**Ito, E., Fujimoto, M., Ebine, K., Uemura, T., Ueda, T., and Nakano, A.** (2012). Dynamic behavoir of clathrin in *Arabidopsis thaliana* unveiled by live imaging. Plant Journal **69**: 204-216.

**Kaksonen, M., Toret, C., and Brubin, D.** (2006). Harnessing actin dynamics for clathrin-mediated endocytosis. Nature Reviews-Molecular Cell Biology. **7**: 404-414.

**Kang, B., Busse, J., and Bednarek, S.** (2003). Members of the Arabidopsis Dynamin-Like Gene Family, ADL1, are essential for plant cytokinesis and polarized cell growth. Plant Cell **15**: 899-913.

**Ketelaar, T., Allwood, E., Anthony, R., Voigt, B., Menzel, D., and Hussey, P.** (2004a). The actin-interacting protein AIP is essential for actin organization and plant development. Current Biology **14**: 145-149.

**Ketelaar, T., Anthony, R., and Hussey, P.** (2004b). Green fluorescent protein-mTalin causes defects in actin organization and cell expansion in Arabidopsis and inhibits actin depolymerizing factor's actin depolymerizing activity *in vitro*. Plant Physiol. **36**: 3990-3998.

**Kim, H., Ok, S., Bahn, S., Jang, J., Oh, S., Park, S., Twell, D., Ryu, S., and Shin, J.** (2011). Endoplasmic reticulum– and Golgi-localized phospholipase A2 plays critical roles in Arabidopsis pollen development and germination. Plant Cell **3**: 94-110.

**Kleinboelting, N., Huep, G., Kloetgen, A., Viehoever, P., and Weisshaar, B.** (2012). GABI-Kat SimpleSearch: new features of the *Arabidopsis thaliana* T-DNA mutant database. Nucleic Acids Res. **40**: 1211-1215.

**Kotzer, A., and Wasteneys, G.** (2006). Mechanism behind the puzzle: microtubule-microfilament cross-talk in pavement cell formation. Canadian J. Bot. **84**: 594-603.

**Li, Y., Shen, Y., Cai, C., Zhong, C., Zhu, L., Yuan, M., and Ren, H.** (2010). The type II Arabidopsis Formin 14 interacts with microtubules and microfilaments to regulate cell division. Plant Cell **22**: 2710-2726.

**Lin, D., Cao, L., Zhou, Z., Zhu, L., Ehrhardt, D., Yang, Z., and Fu, Y.** (2013). Rho GTPase signaling activates microtubule severing to promote microtubule ordering in Arabidopsis. Current Biology **23**: 290-297.

**Liu, D., Zhao, W., Fang, W., and Chen, Y.** (2012). cPLA2α-mediated actin rearrangements downstream of the Akt signaling is required for *Cronobacter sakazakii* invasion into brain endothelial cells. Biochem. Biophys. Res. Commun. **417**: 925-930.

**Marc, J., Granger, C., Brincat, J., Fisher, D., Kao, T., McCubbin, A., and Cyr, R.** (1998). A GFP-MAP4 reporter gen for visualizing cortical microtubule rearrangements in living epidermal cells. Plant Cell **10**: 1927-1939.

**Martiniere, A., Gayral, P., Hawes, C., and Runions, J.** (2011). Building bridges: formin 1 of Arabidopsis forms a connection between the cell wall and the actin cytoskeleton. Plant J. **66**: 354-365.

**Martiniere, A., Lavagi, I., Nageswaran, G., Rolfe, D., Maneta, L., Luu, D., Botchway, S., Webb, S., Mongrand, S., Maruel, C., Martin, M., Kleine-Vehn, J., Friml, J., and Runions, J.** (2012). Cell wall contrains lateral diffussion of plant plasma-membrane proteins. PNAS **109**: 12805-12810.

**Mathur, J.** (2004). Cell shape development in plants. Trends Plant Sci. **9**: 583-590.

**Mathur, J.** (2006). Local interactions shape plant cells. Curr. Opin. Cell Biol. **18**: 40-46.

**Meijering, E., Dzyubachyk, O., and Smal, I.** (2012). Methods for cell and particle tracking. Methods in Enzymology **504**: 183-200.

**Michelot, A., Derivery, E., Paterski-Boujemma, R., Guerin, C., Huang, S., Parcy, F., Staiger, C., and Blanchoin, L.** (2006). A novel mechanism for

the formation of actin-filament bundles by a nonprocessive formin. Current Biology **16**: 1924-1930.

**Michelot, A., Guerin, C., Huang, S., Ingouff, M., Richard, S., Rodiuc, N., Staiger, C., and Blanchoin, L.** (2005). The formin homology 1 domain modulates the actin nucleation and bundling activity of Arabidopsis Formin 1. Plant Cell **17**: 2296-2313.

**Moes, M., Boonstra, J., and Regan-Klapisz, E.** (2010). Novel role of cPLA(2)alpha in membrane and actin dynamics. Cell Mol. Life Sci. **67**: 1547-1557.

**Mooren, O., Galletta, B., and Cooper, J.** (2012). Roles of actin assembly in endocytosis. Ann. Rev. Biochem. **81**: 661-686.

**Nagawa, S., Xu, T., Lin, D., Dhonukshe, P., Zang, X., Friml, J., Scheres, B., Fu, Y., and Yang, Z.** (2012). ROP GTPase-dependent actin microfilaments promote PIN1 polarization by localized inhibition of clathrin-dependent endocytosis. PLOS Biology **10**: e1001299, doi:10.1371/journal.pbio.1001299.

**Panteris, E., and Galatis, B.** (2005). The morphogenesis of lobed plant cells in the mesophyll and epidermis: organization and distinct roles of cortical microtubules and actin filaments. New Phytologist **167**: 721-732.

**Pastuglia, M., Azimzadeh, J., Goussot, M., Camilleri, C., Belcram, K., Evrard, J., Schmit, A., Guerche, P., and Bouchez, D.** (2006). γ-Tubulin is essential for microtubule organization and development in Arabidopsis. Plant Cell **18**: 1412-1425.

**Pietra, S., and Grebe, M.** (2010). Auxin paves the way for planar morphogenesis. Cell **43**: 29-31.

**Prosser, D., Drivas, T., Maldonado, L., and Wendland, B.** (2011). Existence of a novel clathrin-independent endocytic pathway in yeast that depends on Rho1 and formin. J. Cell Sci. **195**: 657-671.

**Rizvi, S., Neidt, E., Cui, J., Feiger, Z., Skau, C., Gardel, M., Kozmin, S., and Kovar, D.** (2009). Identification and characterization of a small molecule inhibitor of formin-mediated actin assembly. Chemistry and Biology **16**: 1158-1168.

**Rosero, A., Žárský, V., and Cvrčková, F.** (2013a). AtFH1 formin mutation affects actin filament and microtubule dynamics in *Arabidopsis thaliana*. J. Exp. Botany **64**: 585-597.

**Rosero, A., Žárský, V., and Cvrčková, F.** (2013b). Visualizing and quantifying the in vivo structure and dynamics of the Arabidopsis cortical cytoskeleton using CLSM and VAEM. In: Plant cell morphogenesis: Methods and protocols, V. Žárský and F. Cvrčková (eds.), Springer – Humana Press, *in press*.

**Sachs, T.** (1981). The control of the patterned differentiation of vascular tissues. Advances in Botanical Research **9**: 151-262.

**Sampathkumar, A., Lindeboom, J., Debolt, S., Gutierrez, R., Ehrhardt, D., Ketelaar, T., and Persson, S.** (2011). Live cell imaging reveals structural associations between the actin and microtubule cytoskeleton in Arabidopsis. Plant Cell **23**: 2302-2313.

**Scarpella, E., Barkoulas, M., and Tsiantis, M.** (2010). Control of leaf and vein development by auxin. Cold Spring Harb. Perspect. Biol. **2**: a001511

**Shaw, S., Kamyar, R., and Ehrhardt, D.** (2003). Sustained microtubule treadmilling in Arabidopsis cortical arrays. Science **300**: 1715-1718.

**Smertenko, A., Deeks, M., and Hussey, P.** (2010). Strategies of actin reorganisation in plant cells. J. Cell Sci. **123**: 3019-3028.

**Smith, L., and Oppenheimer, D.** (2005). Spatial control of cell expansion by the plant cytoskeleton. Ann. Rev. Cell Dev. Biol. **21**: 271-295.

**Staiger, C., Sheahan, M., Khurana, P., Wang, X., McCurdy, D., and Blanchoin, L.** (2009). Actin filament dynamics are dominated by rapid growth and severing activity in the Arabidopsis cortical array. J. Cell Biol. **182**: 269-280.

**Sugimoto, K., Himmelspach, R., Williamson, R., and Wasteneys, G.** (2003). Mutation or drug-dependent microtubule disruption causes radial swelling without altering parallel cellulose microfibril deposition in Arabidopsis root cells. Plant Cell **5**: 1414-1429.

**Voigt, B., Timmers, A., Šamaj, J., Hlavačka, A., Ueda, T., Preuss, M., Nielsen, E., Mathur, J., Emans, N., Stenmark, H., Nakano, A., Baluška,**

**F., and Menzel, D.** (2005). Actin-based motility of endosomes is linked to the polar tip growth of root hairs. Eur. J. Cell Biol. **84**: 609-621.

**Wang, J., Xue, X., and Ren, H.** (2012). New insights into the role of plant formins: regulating the organization of the actin and microtubule cytoskeleton. Protoplasma **249 Suppl 2**:S101-S107.

**Wang, X., Zhu, L., Liu, B., Wang, C., Jin, L., Zhao, Q., and Yuan, M.** (2007). Arabidopsis MICROTUBULE-ASSOCIATED PROTEIN18 functions in directional cell growth by destabilizing cortical microtubules. Plant Cell **9**: 877-889.

**Xu, T., Wen, M., Nagawa, S., Fu, Y., Chen, J., Wu, M., Perrot-Rechenmann, C., Friml, J., Jones, A., and Yang, Z.** (2010). Cell surface- and Rho GTPase- based auxin signaling controls cellular interdigitation in Arabidopsis. Cell **143**: 99-110.

**Yalovsky, S., Bloch, D., Sorek, N., and Kost, B.** (2008). Regulation of membrane trafficking, cytoskeleton dynamics, and cell polarity by ROP/RAC GTPases. Plant Physiol. **147**: 1527-1543.

**Yang, Z.** (2008). Cell polarity in Arabidopsis. Ann. Rev. Cell Dev. Biol. **24**: 551-575.

**Yarar, D., Waterman-Storer, C., and Shmid, S.** (2005). A dynamic actin cytoskeleton functions at multiple stages of clathrin-mediated endocytosis. Mol. Biol. Cell **16**: 964-975.

**Yi, K., Guo, C., Chen, D., Zhao, B., Yang, B., and Ren, H.** (2005). Cloning and functional characterization of a Formin-Like Protein (AtFH8) from Arabidopsis. Plant Physiol. **138**: 1071-1082.

**Žárský, V., Cvrčková, F., Potocký, M., and Hála, M.** (2009). Exocytosis and cell polarity in plants – exocyst and recycling domains. New Phytologist **183**: 255-272.

**Zhang, C., Halsey, L., and Szymanski, D.** (2011). The development and geometry of shape change in *Arabidopsis thaliana* cotyledon pavement cells. BMC Plant Biology **11**: doi 10.1186/1471-2229-11-2.

**Zhang, C., Mallery, E., Schlueter, J., Huang, S., Fan, Y., Brankle, S., Staiger, C., and Szymanski, D.** (2008). Arabidopsis SCARs function interchangeably

to meet actin-related protein 2/3 activation thresholds during morphogenesis.. Plant Cell **20**: 995-1011.

**Zimmermann, P., Hirsch-Hoffmann, M., Hennig, L., and Gruissem, W.** (2004). GENEVESTIGATOR. Arabidopsis microarray database and analysis toolbox. Plant Physiology **136**: 2621-2632.

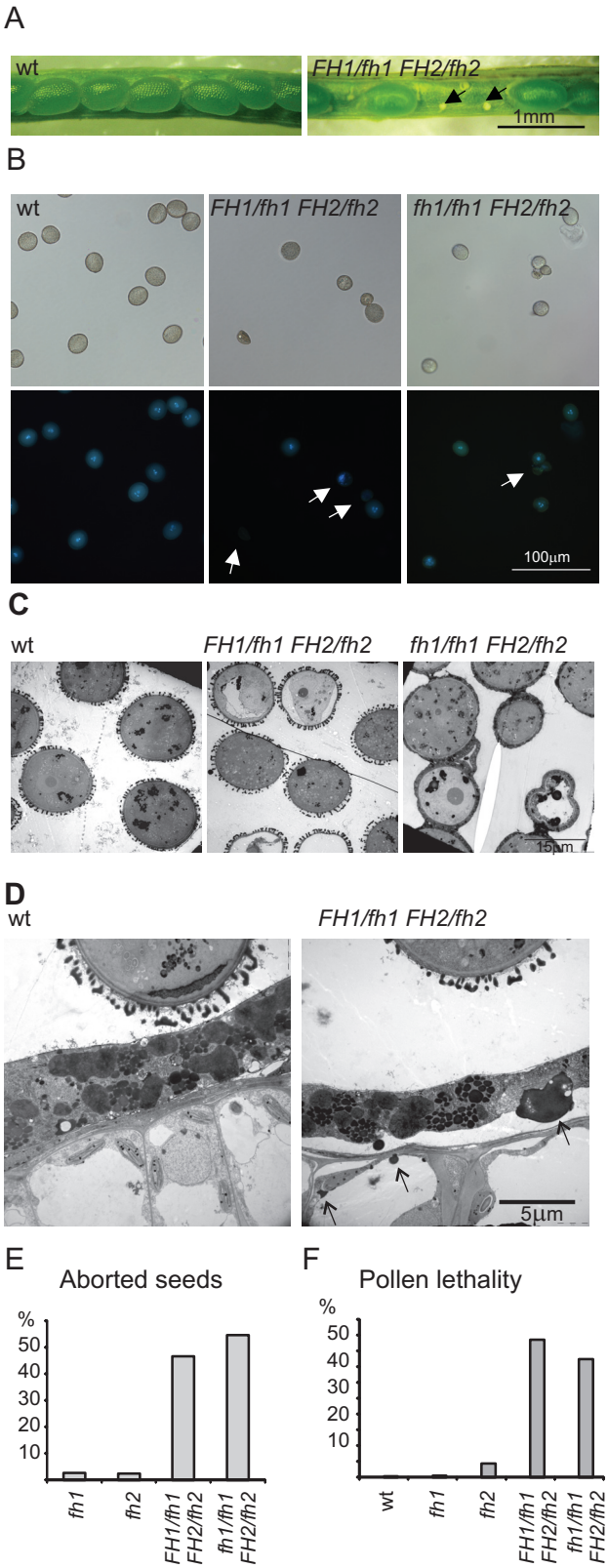


**Figure 1.** Reduced fertility and pollen lethality in crosses of *fh1-1* and *fh2* mutants. (A) Aborted seeds in an *FH1/fh1-1 FH2/fh2* (double heterozygote) plant. (B) Bright field and DAPI stained micrographs of mature pollen of wild type (wt), double heterozygote and *fh1/fh1FH2/fh2* lines. (C) Ultrastructure (TEM) of pollen from wt, double heterozygote and *fh1/fh1FH2/fh2* plants. (D) Ultrastructure (TEM) of tapetum cells from wt and double heterozygote lines; anomalous structures marked by arrows. (E) Frequency of seed abortion in formin mutants. (F) Fraction of abnormal pollen in formin mutants.

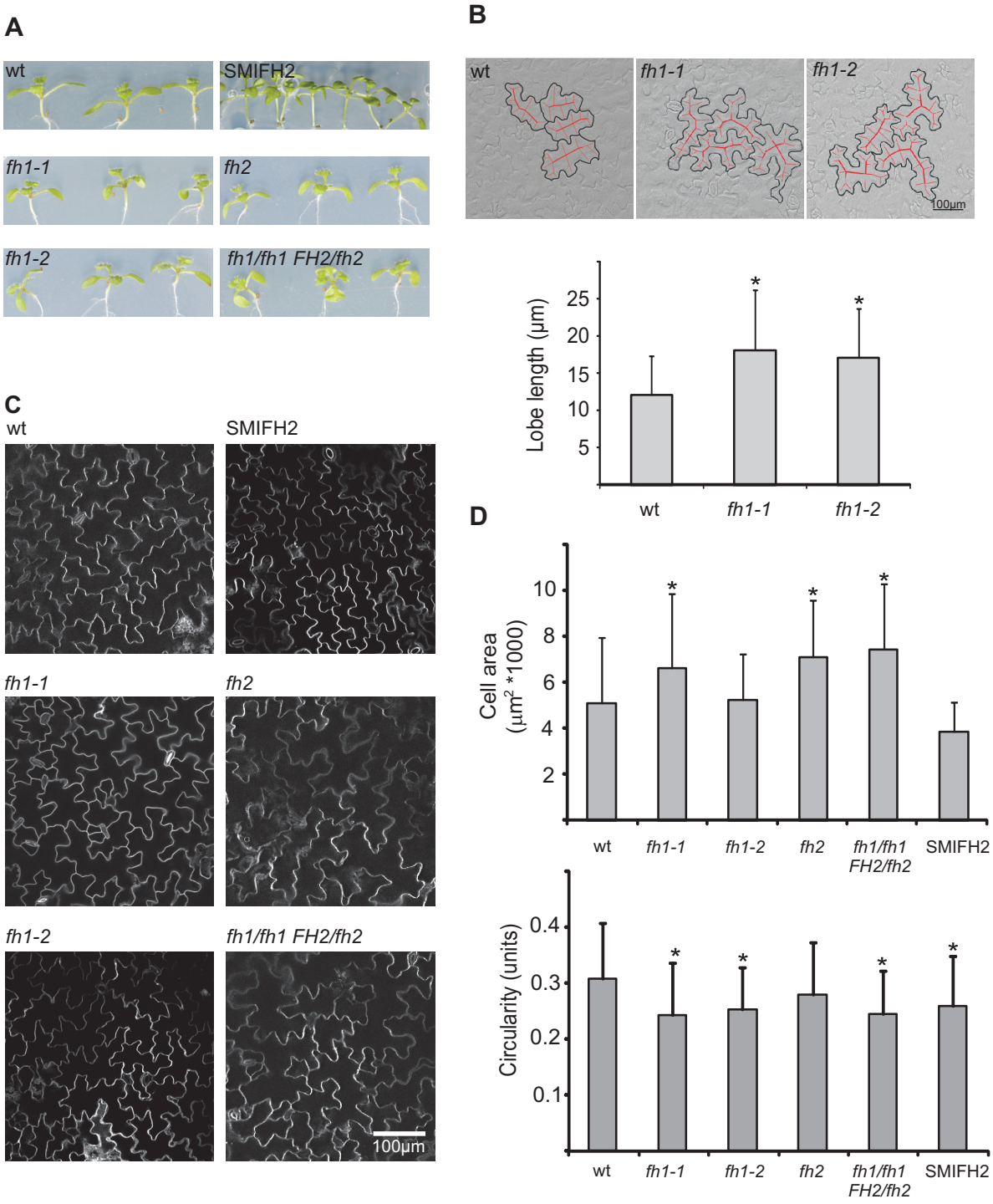


**Figure 2.** Seedling appearance and cotyledon pavement cells in wt, formin mutants and plantlets treated with the formin inhibitor SMIFH2 (30µM). (A) Seedlings at 10 days after germination (DAG). (B) Completely expanded pavement cells from 10 DAG plants. (C) Pavement cells from 5 DAG plants - appearance (expansion axis marked) and lobe length (D) Pavement cell area and circularity from 10 DAG cotyledons.

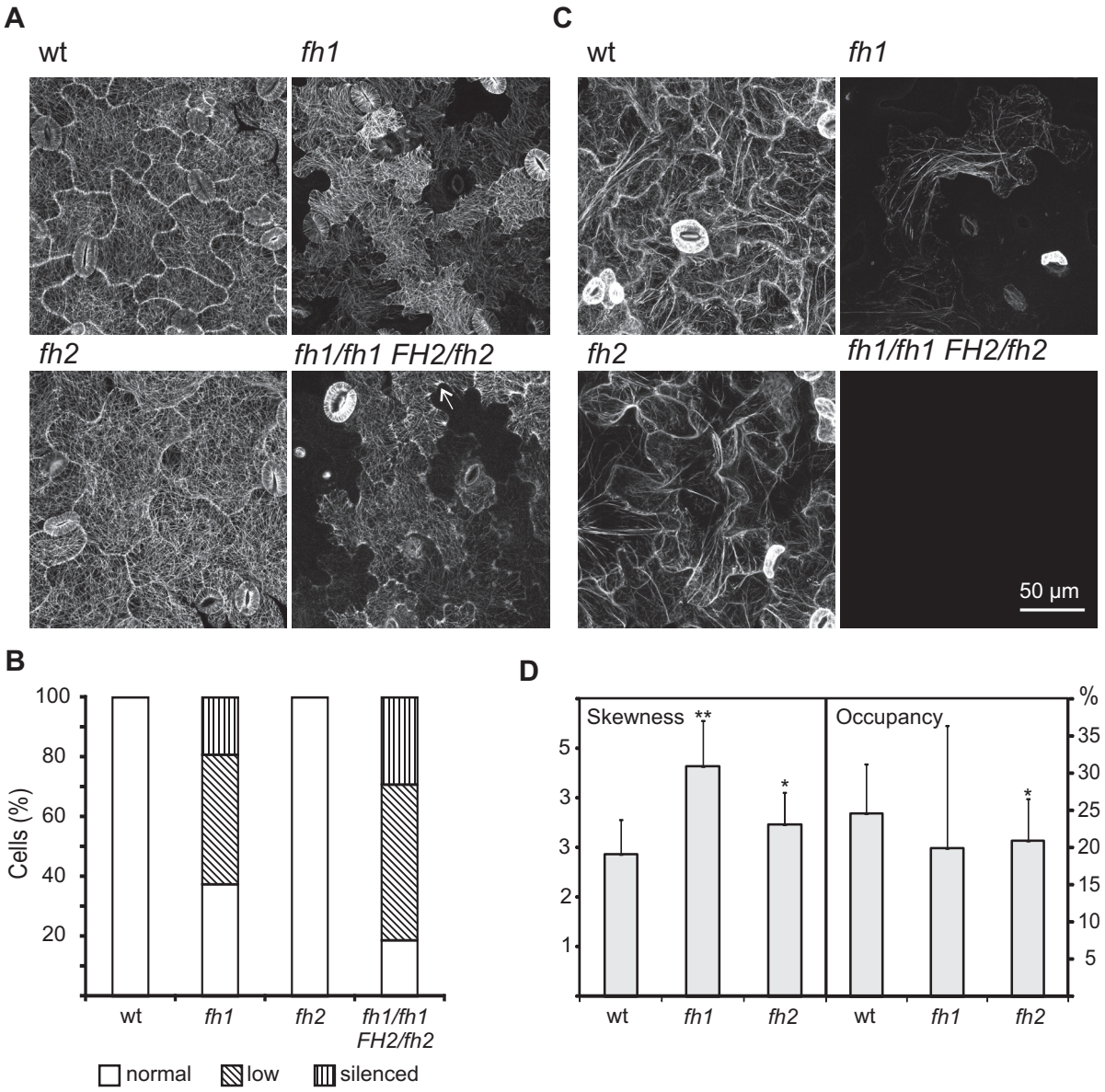


**Figure 3.** Microtubule and actin filament organization in pavement cells of wt and formin mutant seedlings at 5 DAG. (A) Microtubules labeled by GFP-MAP4. Microtubule accumulation in the neck region is marked by an arrow. (B) Varying levels of GFP-MAP4 intensity in cells (arbitrary classes corresponding to high, weak or no fluorescence determined visually). (C) Actin filaments labeled by GFP-FABD. (D) Actin filament bundling (skewness) and density (occupancy).

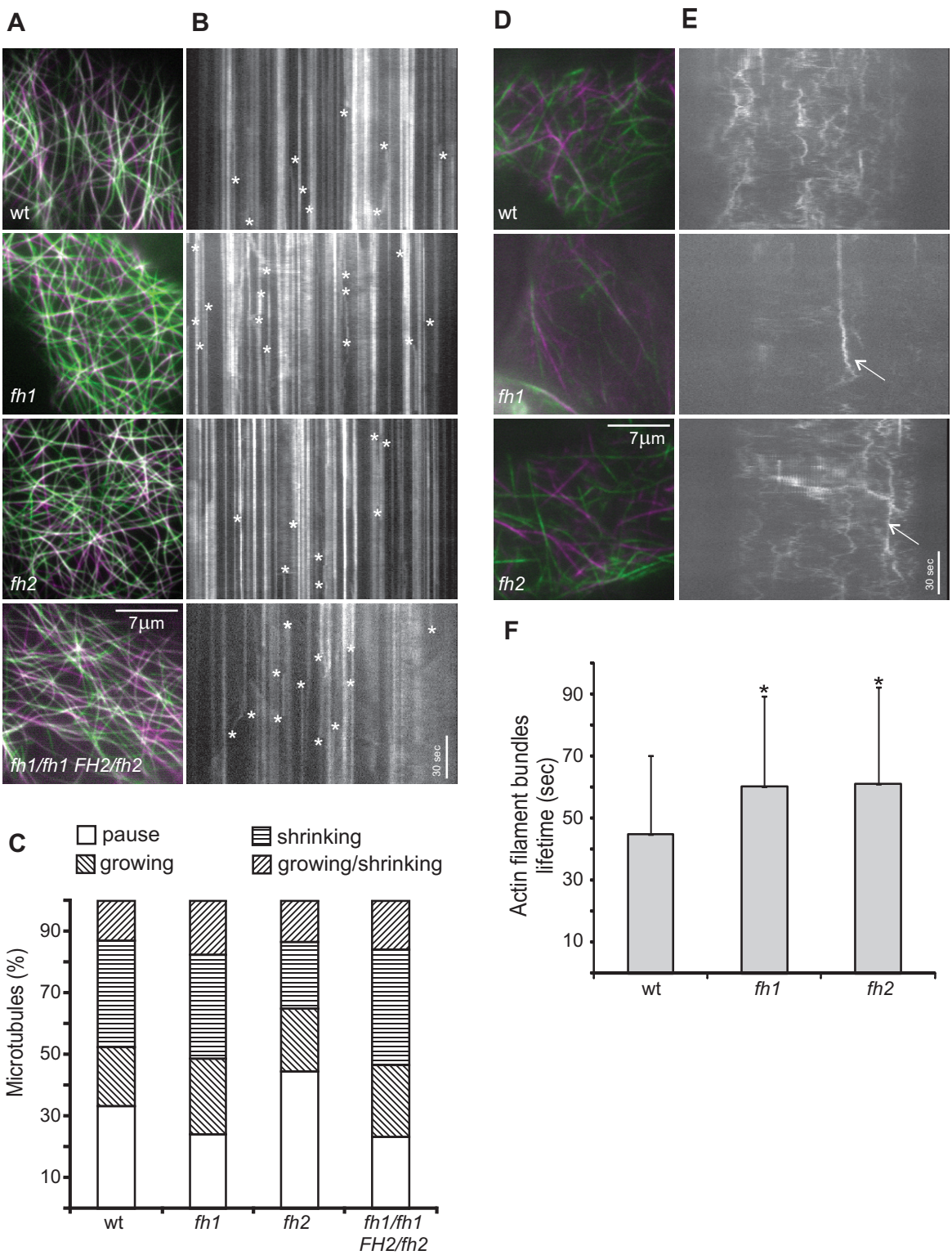


**Figure 4.** Microtubule (GFP-MAP4) and actin filament (GFP-FABD) dynamics in pavement cells of wt and formin mutant seedlings at 4 DAG. (A, D) Overlay of VAEM images from two time points showing growing microtubules (A) or microfilaments (D) in magenta, shrinking in green, pausing in light green and alternating in light magenta. (B, E) Kymographs of microtubule (B) or microfilament (E) dynamics. Events of microtubule appearance/disappearance across the scanned line are marked by asterisks in (B), arrows in (E) denote stable thick actin bundles. (C) Distribution of microtubule phases, quantified from time-lapse images taken across the time span of 2 min. (F) Actin filament bundles lifetimes; asterisk significant differences between mutants and wt (T-test $P < 0.005$).

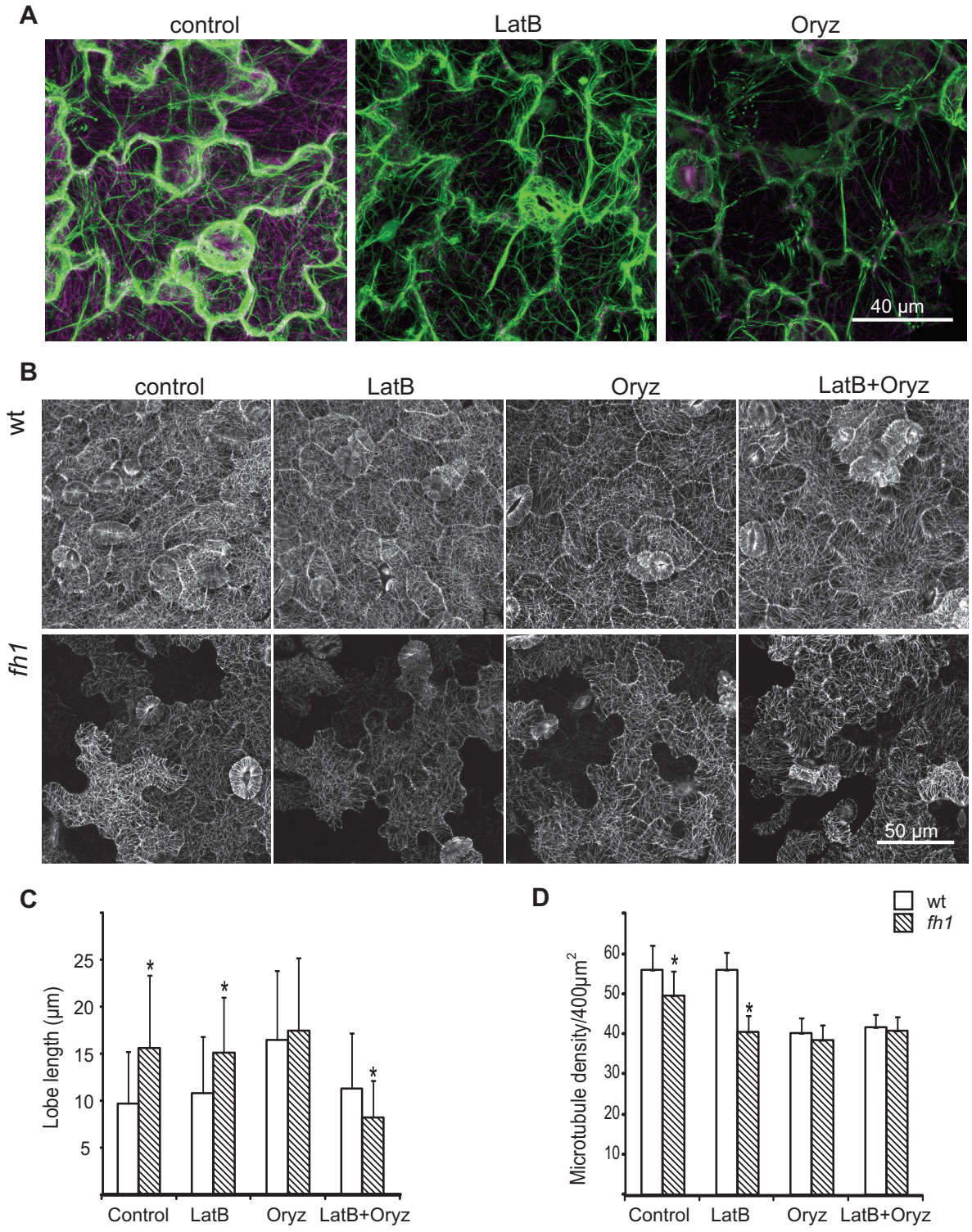


**Figure 5.** Cell shape and cytoskeleton organization in pavement cells of 5DAG wt and *fh1-1* mutants grown in the presence of inhibitors. (A) Actin and microtubules in wt plants labeled simultaneously by GFP-FABD (green) and mCherry-TUA5 (magenta) grown in LatB (0.2µM) and Oryz (0.2µM)-supplemented media. (B) Cell shape and microtubules in plants labeled by GFP-MAP4 and grown in LatB (0.1µM), Oryz (0.1µM) and LatB+Oryz supplemented media. (C) Lobe length from cells of plants labeled by GFP-MAP4. (D) Microtubule density. Significant differences (T-test $P < 0.001$) marked by an asterisk.

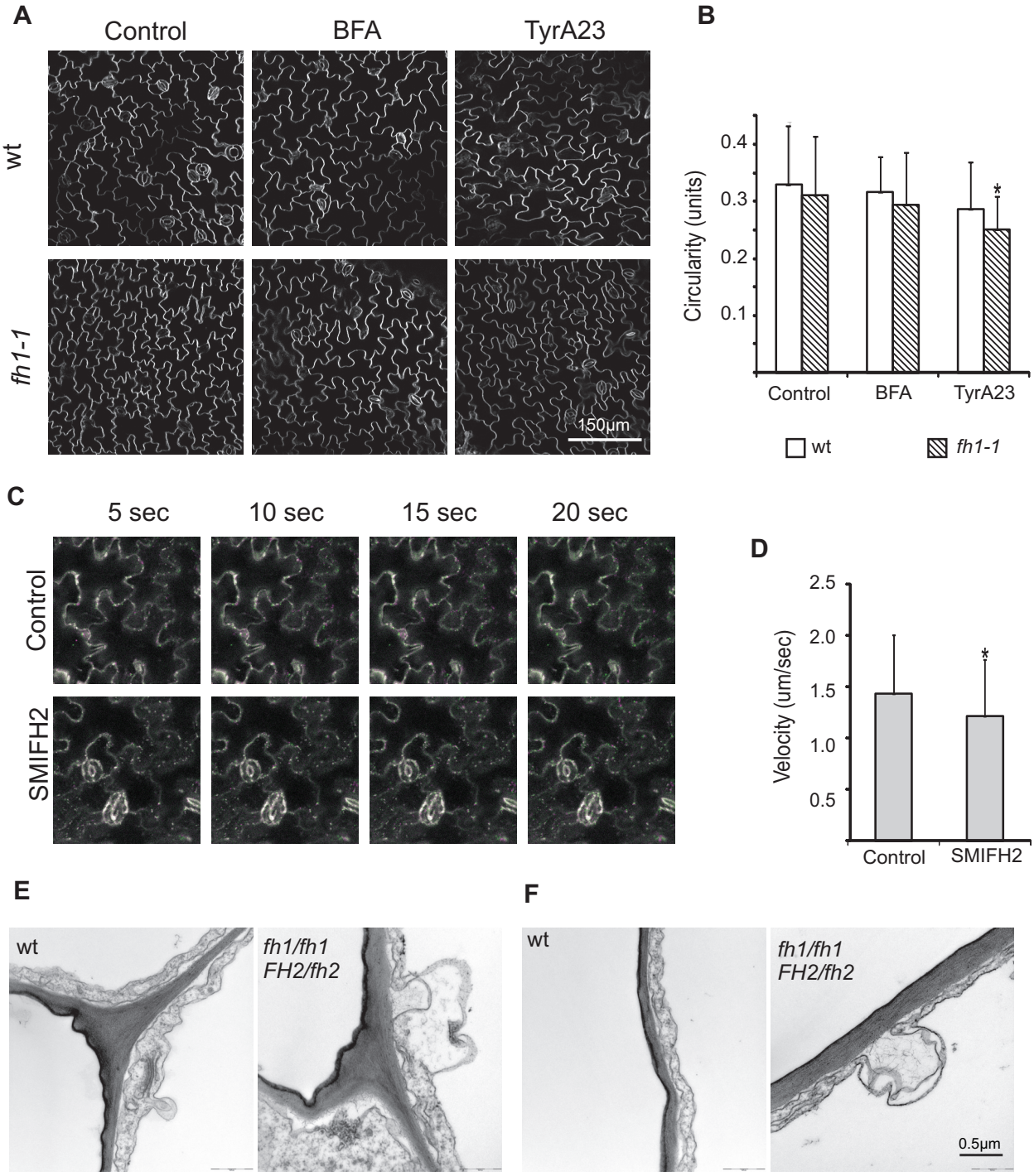


**Figure 6.** Effects of membrane trafficking inhibition in formin-impaired seedlings. (A) Cell shape changes induced by BFA (15µM) and TyrA23 (0.1µM) in wt and *fh1-1* mutant (10 DAG). (B) Circularity of pavement cells from 10 DAG wt and *fh1-1* plants treated by BFA and TyrA23. (C) Dynamics of clathrin-containing compartments in pavement cells of 10 DAG seedlings grown on control medium and/or in the presence of SMIFH2 (20µM). Green channel location of CLC-GFP dots in time zero, magenta - location at the time shown (D) Velocity of CLC-GFP dots on control and SMIFH2 (20µM)-containing medium, from data from the experiment shown in (C). (E) TEM images of cell-cell boundary between two cotyledon pavement cells in wt and *fh1/fh1FH2/fh2* seedlings (5 DAG) showing plasmalemma invaginations. (F) Surface of pavement cells from wt and *fh1/fh1FH2/fh2* seedlings (5 DAG). Significant differences from relevant controls (T-test $P < 0.05$) are marked by asterisks in all graphs.

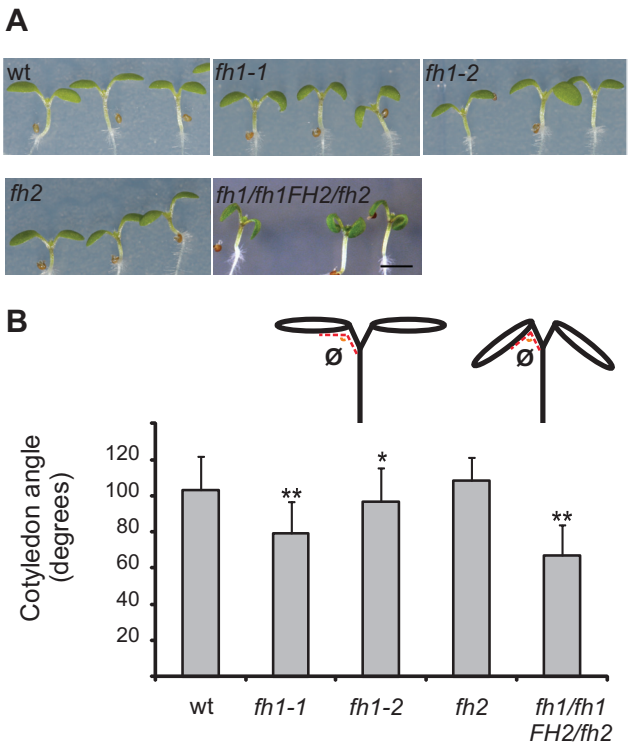


**Figure 7.** Cotyledon positioning in wt and formin mutants. (A) Seedlings at 5 DAG. (B) Cotyledon to petiole angles (in at least 30 seedlings per data point). Significant differences from wild type marked by asterisks (* T-test $P < 0.01$, ** T-test $P < 0.0001$).

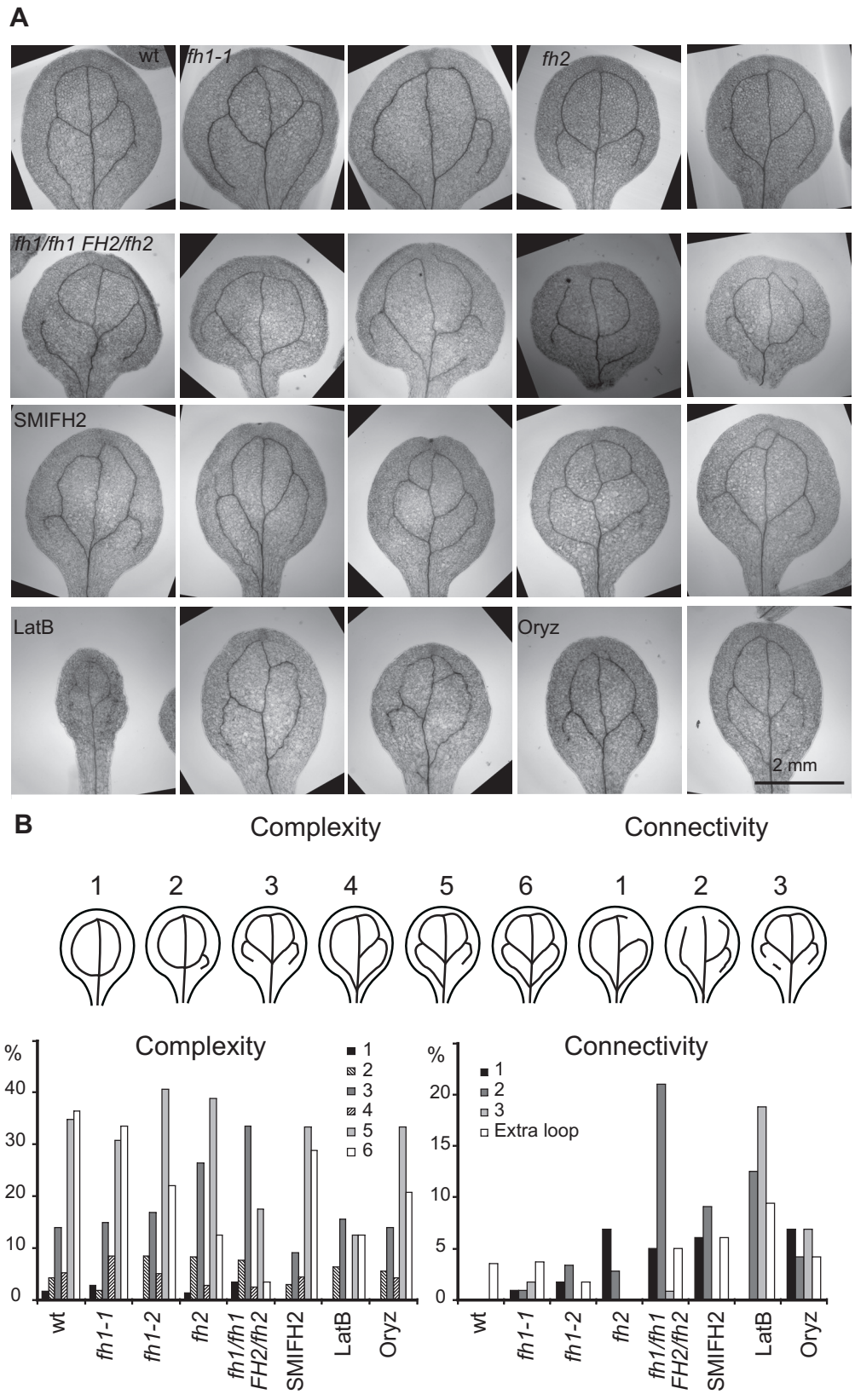


**Figure 8.** Cotyledon shape and venation pattern in seedlings grown on inhibitor-supplemented media. (A) Shape and venation pattern in cleared cotyledons from wt controls, formin mutants and wt grown on SMIFH2 (30μM), LatB (0.2μM) and Oryz (0.2μM) supplemented media (15 DAG). (B) Venation complexity and connectivity pattern definition and distribution.

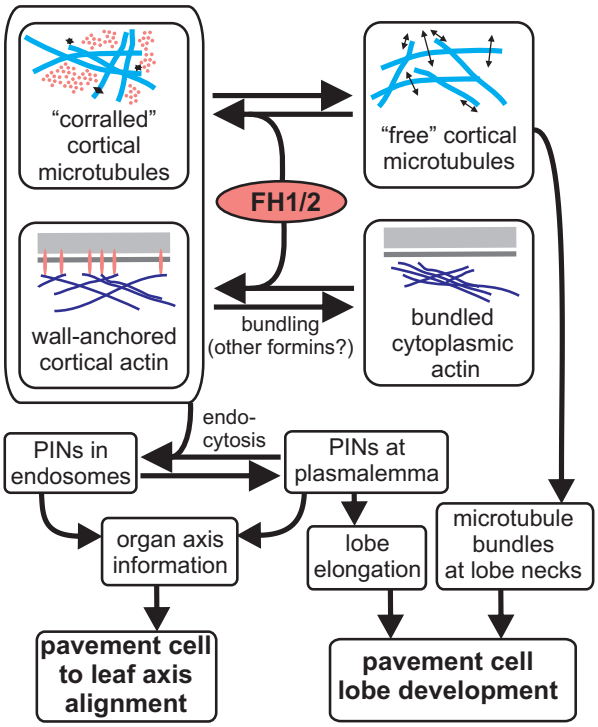


**Figure 9**. Model summarizing the role of FH1 and FH2 in pavement cell morphogenesis. Both formins facilitate formation of fine, dynamic actin arrays nucleated from the membrane and anchoredto the cell wall, i.e. they shift the balance away from cytoplasmic actin filaments that are free to bundle, possibly by action of other formins. FH1 (and presumably also FH2) anchored actin filaments also restrict the lateral mobility and dynamics of cortical microtubules, "corralling" them into actin-free zones (Martiniere et al. 2011, 2012). Decreased FH1 activity frees these microtubules, facilitating thus formation of bundles at pavement cell "necks". FH1 and FH2 also, probably by a cytoskeleton-dependent mechanism, promote endocytosis, which reduces the abundance of PIN auxin transporters at lobe tips, which facilitate lobe outgrowth (Xu et al. 2010). Endocytosis is also important for PIN recycling as a pre-requisite of auxin-dependent organ polarity signaling, and its disruption in the mutants may contribute to the loss of alignment between pavement cell and organ axis.

**Supplemental materials for Rosero et al: Arabidopsis FH1 and FH2 formins affect pavement cell shape and vascular patterning by modulating cytoskeleton and membrane dynamics**

**Supplemental Table 1.** Segregation ratios in crosses involving *fh1-1* and *fh2* mutants.

| Parent genotype or crossing | Segregants | N | Fo | Fe | $X^2_1$ |
|---|---|---|---|---|---|
| *FH1/fh1FH2/fh2* | *FH1/FH1FH2/FH2* | 43 | 0 | 2.7 | 2.70 |
| | *FH1/FH1FH2/fh2* | | 2 | 5.4 | 2.14 |
| | *FH1/fh1FH2/FH2* | | 0 | 5.4 | 5.40* |
| | *FH1/fh1FH2/fh2* | | 22 | 10.8 | 11.61** |
| | *FH1/FH1fh2/fh2* | | 11 | 2.7 | 25.51** |
| | *FH1/fh1fh2/fh2* | | 0 | 5.4 | 5.40* |
| | *fh1/fh1FH2/FH2* | | 6 | 2.7 | 4.03* |
| | *fh1/fh1FH2/fh2* | | 2 | 5.4 | 2.14 |
| | *fh1/fh1fh2/fh2* | | 0 | 2.7 | 2.70 |
| *fh1/fh1FH2/fh2*(♂) x | *fh1/fh1FH2/fh2* | 81 | 15 | 40.5 | 16.05** |
| *fh1/fh1FH2/FH2* (♀) | *fh1/fh1FH2/FH2* | | 66 | 40.5 | 16.05** |
| *fh1/fh1FH2/FH2* (♂) x | *fh1/fh1FH2/fh2* | 67 | 8 | 33.5 | 19.41** |
| *fh1/fh1FH2/fh2* (♀) | *fh1/fh1FH2/FH2* | | 59 | 33.5 | 19.41** |

N – numer of segregants scored, $F_o$ - observed segregant numbers; $F_e$ – expected segregant numbers assuming Mendelian frequencies,. $X^2_1$ is chi-square value. *P<0.05; **P<0.001.

**Supplemental Table 2.** Segregation ratios of *fh1-1* in genetic backgrounds expressing stable mTalin-GFP and GFP-FABD markers.

| Parent genotype | Segregants | N | Fo | Fo | $X^2_1$ |
|---|---|---|---|---|---|
| mTalin-GFP homozygous | *FH1/FH1* | 88 | 35 | 22 | 7.68* |
| *FH1/fh1* | *FH1/fh1* | | 53 | 44 | 1.84 |
| | *fh1/fh1* | | 0 | 22 | 22.00** |
| GFP-FABD homozygous | *FH1/FH1* | 48 | 14 | 12 | 0.33 |
| *FH1/fh1* | *FH1/fh1* | | 21 | 24 | 0.37 |
| | *fh1/fh1* | | 13 | 12 | 0.08 |

N – numer of segregants scored, $F_o$ - observed segregant numbers; $F_e$ – expected segregant numbers assuming Mendelian frequencies. $X^2_1$ is chi-square value. *P<0.05; **P<0.001.

**Supplemental Table 3.** Seed abortion and pollen lethality in *FH1/fh1-1* plants expressing stable mTalin-GFP and GFP-FABD markers.

| | Seed abortion | | | pollen lethality | | |
|---|---|---|---|---|---|---|
| **Genotype** | **N** | **aborted seeds** | **(%)** | **N** | **abnormal pollen** | **(%)** |
| mTalin-GFP | 378 | 184 | 48.7 | 1064 | 285 | 26.78 |
| GFP-FABD | 433 | 0 | 0 | 315 | 8 | 2.54 |

N is number of evaluated pollen grains or seeds.

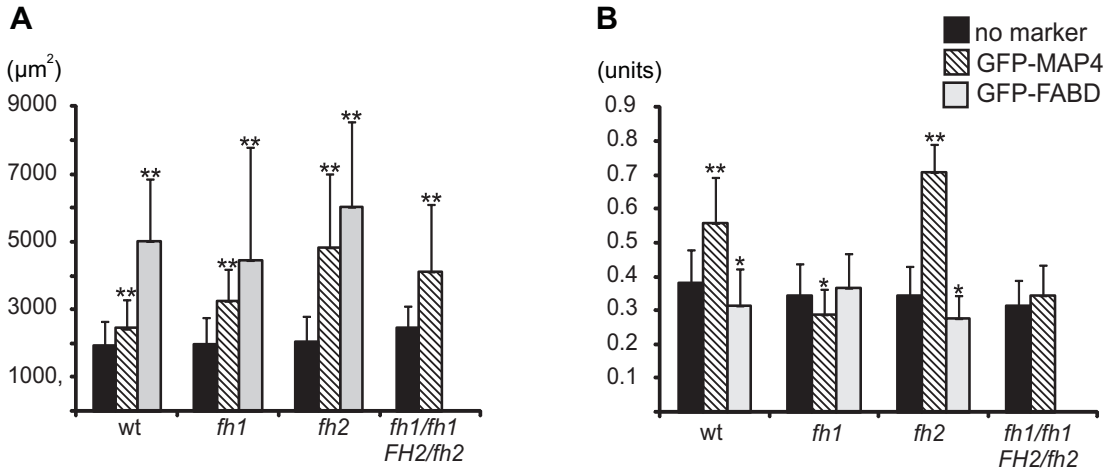


**Supplemental Figure 1.** Effects of GFP-MAP4 and GFP-FABD expression on pavement cell shape in wt and formin mutants. (A) Cell area, (B) Cell circularity. Significant differences from non-transgenic plants are marked by an asterisk (*T-test P <0.05,**T-test P <0.0001). All measurements are from 5DAG seedlings.

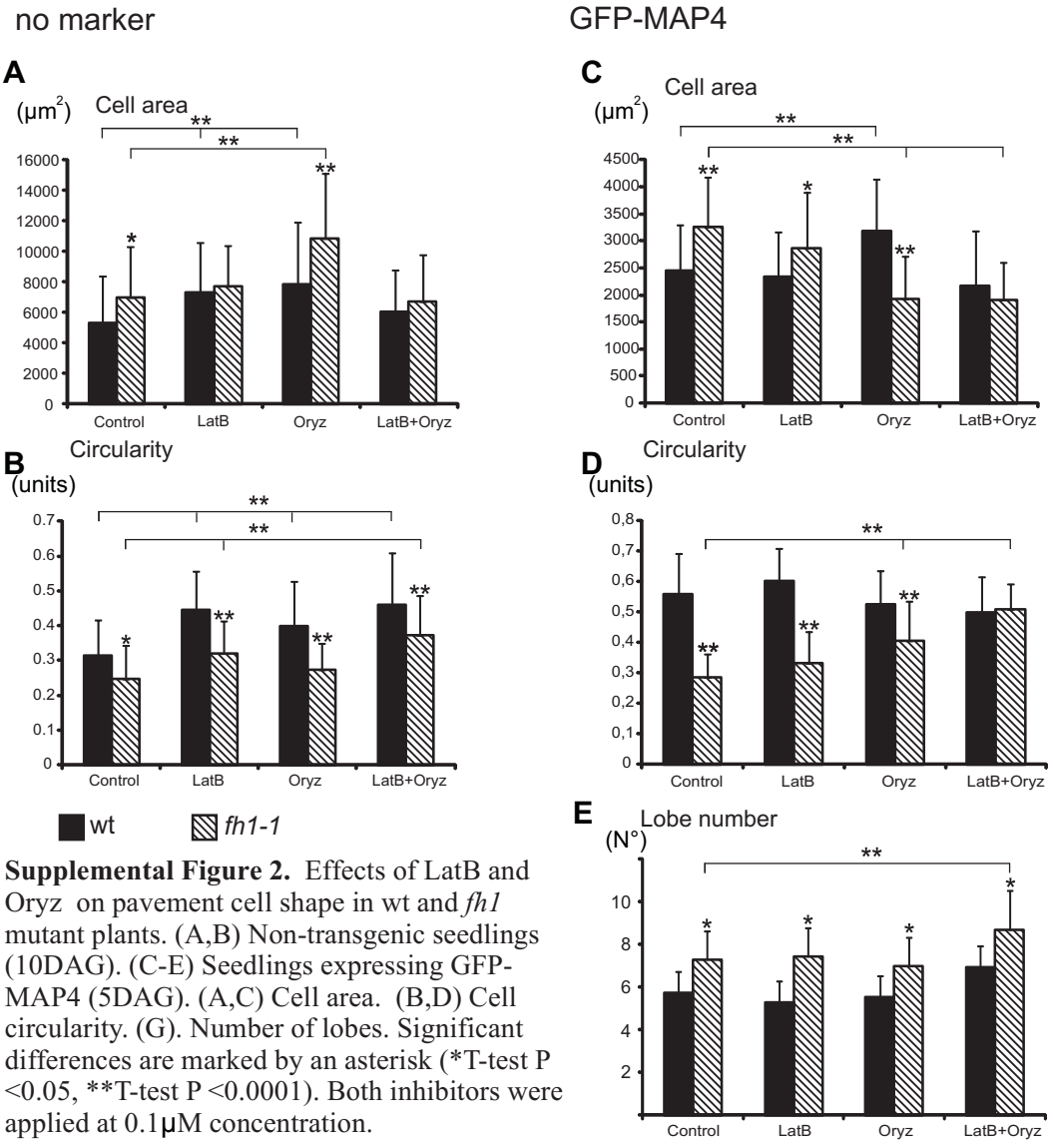


**Supplemental Figure 2.** Effects of LatB and Oryz on pavement cell shape in wt and *fh1* mutant plants. (A,B) Non-transgenic seedlings (10DAG). (C-E) Seedlings expressing GFP-MAP4 (5DAG). (A,C) Cell area. (B,D) Cell circularity. (G). Number of lobes. Significant differences are marked by an asterisk (*T-test P <0.05, **T-test P <0.0001). Both inhibitors were applied at 0.1μM concentration.

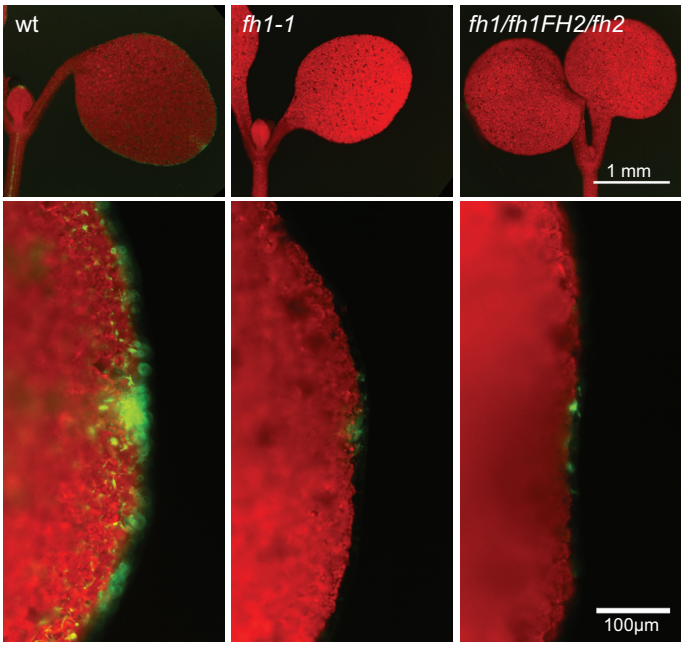


**Supplemental Figure 3.** Auxin maxima visualised using the DR5-GFP reporter in wt and formin mutants (10 DAG).

### 3.3. Paper 3.

**Rosero A, Zarsky V, Cvrckova F. 2013. Visualizing and quantifying the in vivo structure and dynamics of the Arabidopsis cortical cytoskeleton using CLSM and VAEM. In: Plant cell morphogenesis: Methods and protocols, V. Žárský and F. Cvrčková (eds.), Springer – Humana Press, *in press*.**

Detailed description of the methods used to observe and quantify both architecture and dynamics of the cortical cytoskeleton using transgenic plants expressing fluorescent protein markers specifically tagging the two main cytoskeletal systems and advanced microscopy techniques, in particular confocal laser scanning microscopy (CLSM) and variable angle epifluorescence microscopy (VAEM). With the aid of suitable computing techniques, quantitative information can be extracted from microscopic images and video sequences.

**My contribution:** writing parts of the text – detailed description of methods used to evaluate the cortical cytoskeleton in arabidopsis by confocal and VAEM microscopy images, and their analysis using Image J plugins, optimized during my experimental work on papers 1 and 2.

# Chapter 7

## Visualizing and Quantifying the In Vivo Structure and Dynamics of the *Arabidopsis* Cortical Cytoskeleton Using CLSM and VAEM

**Amparo Rosero, Viktor Žárský, and Fatima Cvrčková**


### Abstract

The cortical microtubules, and to some extent also the actin meshwork, play a central role in the shaping of plant cells. Transgenic plants expressing fluorescent protein markers specifically tagging the two main cytoskeletal systems are available, allowing noninvasive in vivo studies. Advanced microscopy techniques, in particular confocal laser scanning microscopy (CLSM) and variable angle epifluorescence microscopy (VAEM), can be nowadays used for imaging the cortical cytoskeleton of living cells with unprecedented spatial and temporal resolution. With the aid of suitable computing techniques, quantitative information can be extracted from microscopic images and video sequences, providing insight into both architecture and dynamics of the cortical cytoskeleton.


**Key words** Actin, Microtubules, Fluorescent proteins, CLSM, VAEM, Image analysis

## 1 Introduction

Cortical microtubules are long known to play a major part in the morphogenesis of plant cells, in particular due to their intimate relationship with the biosynthesis of the cellulosic cell wall microfibrils (*see* ref. 1). However, the actin cytoskeleton, which undergoes constant dynamic remodeling [2], is crucial for processes such as trichome morphogenesis [3], tip growth in root hairs [4], or development of epidermal cell lobes [5] and apparently contributes to the localization of exocytosis, affecting also the positioning of cellulose synthase complexes [1, 6]. Detailed characterization of the spatial structure and temporal behavior of the two main cytoskeletal systems in vivo may thus substantially contribute to our understanding of plant cell shaping.

Such studies depend on several prerequisites. Sufficiently specific and nondisruptive fluorescent cytoskeletal markers must be introduced into the tissues of interest, and suitable high-resolution imaging technology must be available, even if the aim of the study

Viktor Žárský and Fatima Cvrckova (eds.), *Plant Cell Morphogenesis: Methods and Protocols*, Methods in Molecular Biology, vol. 1080, DOI 10.1007/978-1-62703-643-6_7, © Springer Science+Business Media New York 2013

was a "mere" morphological characterization. In addition, if quantitative information is to be extracted from image data, appropriate protocols and software are needed.

A variety of fluorescent protein-based markers has been used to trace cytoskeletal structures in living cells, including those of plants. Plant microtubules have been successfully visualized using both GFP-tubulin fusions [7, 8] and GFP-tagged ortho- or heterologous microtubule-associated proteins (MAPs) such as mammalian MAP4 [9] or several isoforms of *Arabidopsis* MAP65 [10]. In addition to labeling microtubules along their whole length, microtubule ends can be specifically marked by tags based on end-binding proteins such as EB1 preferring minus ends [11] or mammalian CLIP170 for plus ends [12]. For actin visualization, fluorescent protein-tagged mammalian talin [13] or constructs based on the C-terminal actin-binding domain of *Arabidopsis* fimbrin (FABD, refs. 14, 15) can be used. A very promising actin marker is the 17 amino acid actin-binding peptide known as LifeAct, which has been successfully used to target fluorescent proteins to actin filaments also in plant cells [16].

It has to be stressed that any experiments including (over) expression of tagged (i.e., modified) and possibly heterologous proteins have to be interpreted with caution, as (1) only a subset of the relevant cytoskeletal structures may be labeled, as shown, e.g., for the various MAP65 isoforms [10], and (2) the tag itself may affect cytoskeletal structure and dynamics. Both talin and MAP4-based markers cause visible phenotypic alteration on the whole plant level [17], and in particular GFP-tagged talin was shown to interfere with actin dynamics and aggravate the effects of some treatments and mutations affecting the actin cytoskeleton [18, 19].

A suitable high-resolution fluorescence microscopy and microphotography equipment is required to make full advantage of in vivo cytoskeletal labeling. Conventional fluorescence microscopy, although useful, is limited by spatial resolution, interfering background (auto)fluorescence, and usually also by long exposure times. However, advanced microscopy techniques, such as confocal laser scanning microscopy (CLSM), can be used to improve spatial resolution. Very thin samples can be observed with supreme spatial and temporal resolution using the total internal reflection microscopy (TIRFM) technique; however, TIRFM can only reach up to some 200 nm from the cover slip. Nevertheless, TIRFM hardware can also be used in variable angle epifluorescence microscopy (VAEM) mode with a reasonable trade-off between lateral resolution and imaging depth, allowing thus visualization of a thin cortical layer of the cytoplasm through the cell wall [20–25]. However, it is possible that in plant cells, the evanescent wave might be initiated between the cell wall and plasmalemma, the cell wall thus being a part of the optical system, and even true TIRFM may thus work [22].

A variety of computational techniques can be used to analyze high-resolution images of the plant cortical cytoskeleton and quantify their biologically relevant parameters. With a bit of exaggeration, there may be as many, or even more, image analysis methods as there are publications devoted to the topic, which often hampers comparison of data from different laboratories. Here we are presenting the protocols currently used in our laboratory [25], but based to a large extent on previous work published by others [26–29], with the hope to contribute to the standardization of basic approaches. Some of the quantification methods presented here can be used also for evaluation of images obtained from fixed material, e.g., after antibody staining.

## 2 Materials and Equipment

Besides specialized equipment and materials listed below, standard equipment, tools, and consumables for plant in vitro culture will be required.

### 2.1 Plants

The fluorescent markers listed above are likely to be available upon request from the authors who published them (*see* also Chapter 6), either in the form of a plasmid suitable for transformation (which may be useful for introducing the marker into mutants) or in the form of seeds of stable transgenic lines. Transgenic *A. thaliana* lines carrying GFP-tagged tubulin markers, GFP-TUB6 and GFP-TUA6, can be obtained also from the public Arabidopsis stock collections—NASC (http://arabidopsis.info) and ABRC (http://www.arabidopsis.org)—under stock codes N6550 and N6551 (NASC) or CS6550 and CS6551 (ABRC), respectively. Stable transgenic plants carrying the marker of interest can be then used to introduce the markers into different genetic backgrounds (e.g., various mutants) by crossing.

While, in principle, any fluorescent cytoskeletal marker can be used for in vivo imaging, our experience is based mainly on observations in plant lines carrying two marker constructs expressed under the viral 35S promoter—GFP-MAP4 [9] and GFP-FABD [30].

We usually observe roots and cotyledons of young seedlings (5–8 days after germination) grown on vertical MS plates at 22 °C with a 16 h-light/8 h-dark cycle (*see* **Note 1**). Pharmacological treatments may be included during cultivation, and seedlings may be alternatively grown in the dark to achieve etiolation, as etiolated hypocotyls provide another interesting model especially for TIRF observation ([20]; *see* **Note 2**). Appropriate controls (e.g., wild type for mutants, or non-treated plants for pharmacological studies) have to be included at the same time, since all measurements can be interpreted only in comparison with data from simultaneously grown control plants (*see* **Note 3**).

### 2.2 Microscopy and Image Processing

For both CLSM and VAEM, we provide information on instrument configuration we are using, as well as basic settings (in Subheading 3.2) as a guide, albeit modifications and some experimenting will be necessary with different hardware (*see* **Note 4**):

1. CLSM: Leica TCS SP2 confocal laser scanning microscope equipped with a 63×/1.2 water-immersion objective and 488-nm argon laser for excitation.
2. VAEM: Leica AF6000 LX fluorescence platform with integrated TIRF module, HCX PL APO 100×/1.46 oil immersion objective, equipped with the Leica DFC350FXR2 digital camera for recording.
3. Microscopy slides, cover slips (preferentially larger size to accommodate the whole length of a stretched seedling), chambered slides (Nunc Lab-Tek II, 1 well, catalogue number 154453), sterile water, immersion oil, tweezers, sterile toothpick, paper tissues ~~(optional)~~, and nail polish.
4. Personal computer with the Windows operation system (XP or higher) with the microscope manufacturer's image processing software installed (LCS Lite for CLSM, Leica Application Suite AF Lite for VAEM).
5. On the same or another computer (*see* **Note 5**), ImageJ ([31]; http://rsbweb.nih.gov/ij/) or its distribution Fiji (http://fiji.sc) should be installed, with the following plug-ins: the MBF plug-in collection to open file formats provided by the microscope from McMaster Biophotonics Facility ([32]; http://rsbweb.nih.gov/ij/plugins/mbf-collection.html), the KashiwaBioImaging plug-in collection (KBI ImageJ Plugins and the Scala runtime library, available from http://hasezawa.ib.k.u-tokyo.ac.jp/zp/Kbi/ImageJKbiPlugins), the Higaki Laboratory macros hig_skewness.txt and hig_255counts.txt (from http://hasezawa.ib.k.u-tokyo.ac.jp/zp/Kbi/HigStomata), and Multiple Kymograph from European Molecular Biology Laboratory (http://www.embl.de/eamnet/html/kymograph.html; not required if using Fiji as it is already contained within the package). A table calculator (such as Microsoft Excel or Libre Office Calc) will be also required.

## 3 Methods

### 3.1 Preparing Plant Materials for Visualization

1. For CLSM, place a seedling (collected off the agar plate using sterile toothpick) into a drop of water or cultivation medium on a microscope slide and cover with a cover slip, avoiding bubbles as far as possible. Remove excess water at the slide edges with a torn bit of paper tissue (*see* **Notes 6** and 7).

2. For VAEM, cut a piece of agar containing the seedlings (width 1.5 cm, length according to the seedling size). We usually observe ~~two or~~ three 5 days old plants per agar piece. Put a drop of water on the chambered slide and put the piece of agar placing the seedlings in contact with the glass, avoiding bubbles (the piece of agar helps to press the seedling tissues in contact with the slide). Remove excess water by gently touching the edges of agar with paper tissue.

### 3.2 Image Acquisition

Follow the recommended standard procedures for your microscope.

1. In case of CLSM, we record single slices (capturing an area of the cell cortex adjacent to the cover slip) and Z series using the following settings: excitation laser (488-nm argon) intensity 25 mW, detector window using the GFP preset values (*see* **Note 8**), XY field size 1,024 × 1,024 pixels, line averaging of 4–8 times, Z series interval 0.7–1 μm, and color depth of 12 bits.
2. In case of VAEM, we use 400 nm peak excitation for GFP constructs, 150–210 ms exposure time, frames taken in 0.5 s intervals over the course of 2 min, and color depth of 8 bits.

### 3.3 Measuring Cytoskeletal Network Density on CLSM Stacks

1. Obtain serial optical sections (XYZ, i.e., Z-stack) of the cortical cytoplasm of a cell expressing a suitable marker by CLSM. In general, we aim towards imaging about 7–10 plants per sample, with 5–10 cells per plant evaluated (*see* **Note 9**).
2. Open the stack by dragging the microscope-generated *.lei file onto the ImageJ window; use the "open as hyperstack" option in the dialog box. Skeletonize the original serial optical sections (Fig. 1a) using Plug-ins > kbi > Kbi_Filter2d (set filter: lineFilters and parms linemode: thinLine; Fig. 1b). Generate a Z projection (Image > Stacks > Zproject) using the maximum intensity option and save the resulting image as a new 8 bits *.tif file (Image > Type > 8bits; Fig. 1c).
3. Select the area to be analyzed (a whole cell or a well-focused region of the image) manually by ROI selection (Plugins > ROI > Specify ROI). To specify multiple ROIs of the same size and shape within an image, you may duplicate the selected ROI (right mouse click > duplicate).
4. Evaluate the filament density within the ROI by estimation of the GFP signal occupancy, i.e., the fraction of pixels constituting the skeletonized filaments relative to the total pixel number of the ROI. Count pixel number of selected ROI using the macro: hig_255counts.txt (Plugins > hig_255counts). The occupancy value is proportional to the overall filament density in the cell region of interest and was shown to serve as a useful indicator to evaluate, e.g., the changes in the microfilament organization induced by physiological processes, treatments

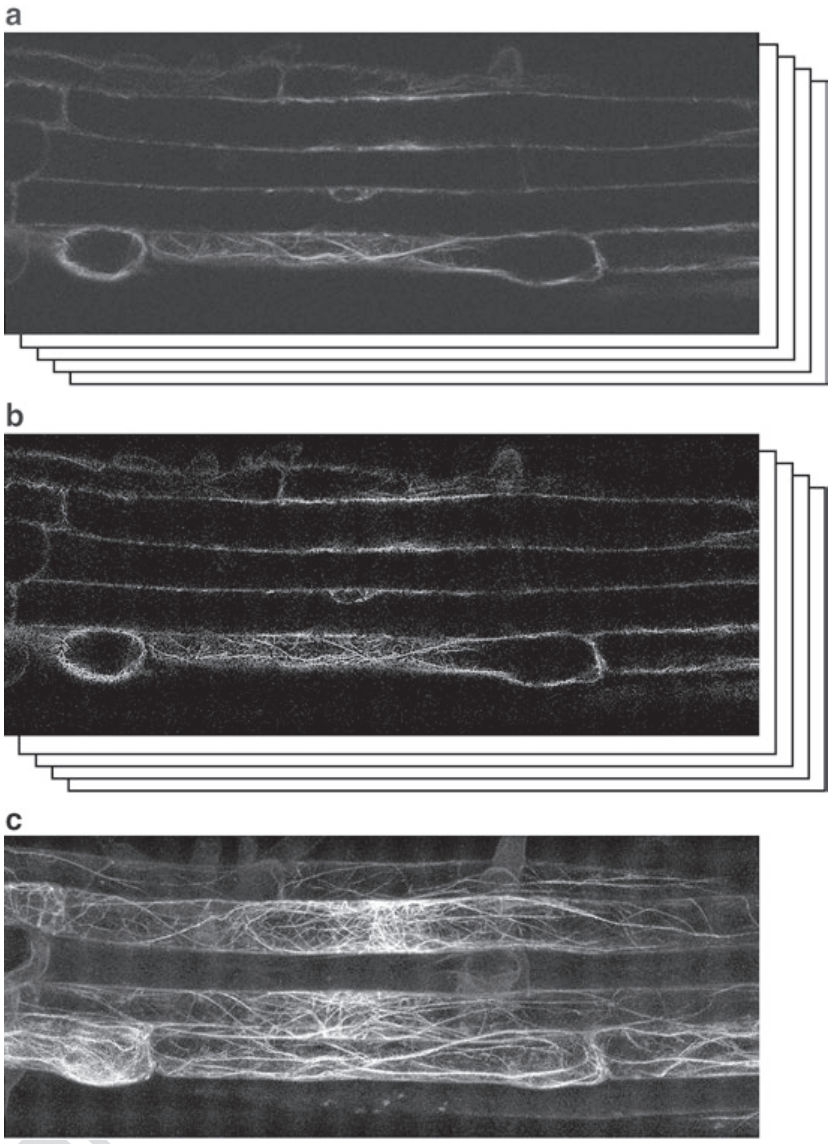


**Fig. 1** Stages of image processing prior to determining actin density and bundling using ImageJ. (**a**) Serial optical sections from CSLM. (**b**) Skeletonization of serial optical sections. (**c**) Single image from maximum intensity projections



with inhibitors, such as latrunculin B [28] or by gene mutations ([25, 33, 34]; *see* **Note 10**).

5. The size and organization of microtubules make their analysis easier than in the case of actin; microtubule density can be estimated in small specific area also by direct manual counting [25].

### *3.4 Evaluating Actin Bundle Thickness by Measuring the Skewness of Fluorescence Distribution*

1. Record an image stack and prepare a skeletonized image of a maximum intensity projection as described in Subheading 3.3, **steps 1** and **2**.
2. Open the image in ImageJ and measure the skewness of the fluorescence intensity distribution (a measure of the degree of asymmetry of a distribution, correlated with microfilament

bundling because bundles exhibit brighter fluorescence) in the microfilament-containing pixels using the macro: hig_skewness.txt (Plugins > hig skewness).

### 3.5 Evaluating Actin Bundle Thickness Using the Histogram Method

1. From original stack of optical sections obtained by CLSM, prepare a maximum intensity projection (Image > Stacks > Zproject) and save it as an 8 bits *.tif image (Image > type > 8bits).
2. Define a specific line length by ROI selection (Plugins > ROI > SpecifyLine); put the line across a representative area of the image (across a well-focused part of a cell; *see* **Note 11**).
3. Generate a profile of GFP fluorescence intensity (Analyze > Plot profile) and record the brightness values of all peaks corresponding to microfilament bundles crossed by the line (values appear on mouse over or generate a list of values by pressing "List"). Record also background values in an area devoid of actin filaments.
4. Using the table calculator, subtract the average background value from the peak values and generate a histogram of the distribution of the resulting net peak values into three or four equally broad classes of gray level (in arbitrary units). The resulting plot documents microfilament bundling, as low intensity represents weakly labeled bundles or single filaments and high intensity corresponds to brightly labeled bundles.

### 3.6 Quantifying Filament Dynamics from VAEM Image Series

1. Acquire temporal series of single-plane optical sections (XYT) of the cortical cytoplasm of a cell expressing a suitable marker by VAEM. We aim towards imaging at least five plants per sample, with 15–20 movies per sample evaluated (*see* **Note 9**).

[AU1]

2. To measure microfilament dynamics, select randomly ten actin bundles per sample and measure their pause duration (for monitoring over time, use multipoint selection tool in ImageJ and register manually the time when the filament end shows a change in behavior). Values and distribution of pause duration can serve, e.g., as an indicator of differences either in bundle size or in the degree of actin cross-linking ([25]; *see* **Note 12**).
3. To quantify microtubule turnover, select randomly 10–20 microtubule ends per sample and monitor their behavior over time (2 min); use the pen or brush tool in ImageJ to mark the already evaluated ends. Count microtubules in the four distinct phases (growing, shrinking, pausing, and alternating between growth and shrinkage).
4. To estimate of microtubule growth and shrinkage rates, select randomly 5–10 microtubule ends per cell and measure their distances from the starting position during specific time using ImageJ.

### 3.7 Kymograph Construction from VAEM Image Series

Kymographs can be used to visualize aspects of microfilament and microtubule dynamics that are not easily observed in the video sequences.

1. Open the *.lif file generated by VAEM by dragging it onto the ImageJ window; use the "open as hyperstack" option in the dialog box, and select the desired image to evaluate.
2. Define a specific line length by ROI selection (Plugins > ROI > SpecifyLine) and locate the line across a representative area of the image (across a well-focused part of a cell).
3. Generate the kymographs using the plug-in Multiple Kymograph (Plugins > MultipleKymograph with linewidth: 3).
4. The image generated shows velocity, movement, and different phases of microfilament or microtubule turnover (*see* **Note 13**).

## 4 Notes

1. Use the culture media and protocols established in the laboratory; any medium and culture setup that allows easy removal of intact seedlings from plates should work. Alternatively, seedlings may be grown on a medium-covered slide surface in situ to avoid disturbance of, e.g., root hairs.
2. Any tissue that can be positioned flat towards the cover slip surface ought to be accessible to CLSM and VAEM; especially for the latter, tight contact with the cover slip is critical. Leaves of glabrous mutants and petals may be especially worth exploring.
3. Ideally, the measurements should be done at least in a single-blind manner to eliminate observer bias (i.e., the person performing quantitative image analysis should not know which image series belongs to which genotype or experimental treatment.
4. In our case, both microscopes are in the inverted configuration. For an upright microscope, sample preparation may have to be modified.
5. This software exists also in versions for other operation systems such as Linux.
6. Take care to treat all the seedlings equally, since mechanical stress may elicit modification of cytoskeletal organization and dynamics during the plant manipulation, media exchange, or even cover slip placement. For longer observation, edges of the cover slip may be sealed with nail polish, but this is usually not necessary. Do not use too much water, as the cover slip should be held in place by capillary forces rather than move around on excess liquid (this is easier to achieve with large cover slips).

7. If working carefully, live seedlings can be recovered from the slide after observation and transferred ex vitro for further cultivation, but do not expect 100 % survival.
8. In case of high autofluorescence background, the window should be narrowed (i.e., longer wavelengths should be cut off in the Beam Path settings).
9. Cytoskeletal structure and dynamics varies dramatically with anatomical location; therefore, imaged cells should be located consistently (e.g., at the bottom of the root tip elongation zone or in the middle of the cotyledon).
10. Maximum intensity projections from the serial optical sections can serve also for determining cytoskeletal filament orientation. Reference [28] describes a procedure employing noise reduction, conversion of the images to binary, and skeletonization. The resulting skeletonized image is used to evaluate cytoskeletal architecture in guard cells of the stomata. Mean angular difference between microfilament pixel pairs and the nearest pixel pairs of a specific cell edge (the stomatal pore) is used as a measure of microfilament orientation. The procedure can be checked by obtaining synthesized images. Analogously, microtubule orientation can be determined with respect to the cell's specific axis, e.g., the longitudinal axis of the hypocotyl [35].
11. It is recommendable to maintain a constant location/direction of the sampling line within a cell, e.g., along the longitudinal axis in case of rhizodermis.
12. Additional data about actin assembly rates, filament origin, and severing frequency can be obtained by the analysis of stochastic dynamics as described in ref. 20, where actin filaments are tracked manually through the time-lapse stack of images and different actin dynamic parameters are estimated by overlapping images or monitoring breaks along the filament over time.
13. Choose the length and location of the sampling line consistently (e.g., parallel to the longitudinal axis in roots and hypocotyls; *see* ref. 29). While 1 min is usually enough to document microfilament dynamics, in the case of the less mobile microtubules 2 min provides a more informative result.

## Acknowledgments

This work has been supported by the GAČR P305/10/0433 project. We thank Boris Voigt and Richard Cyr for transgenic *Arabidopsis* lines; Ondřej Šebesta, Ondřej Horváth, and Aleš Soukup for expert microscopy advice; and Marta Čadyová for technical assistance.

## References


1. Crowell EF, Gonneau M, Vernhettes S et al (2010) Regulation of anisotropic cell expansion in higher plants. C R Biol 333(4):320–324
2. Blanchoin L, Boujemaa-Paterski R, Henty JL et al (2010) Actin dynamics in plant cells: a team effort from multiple proteins orchestrates this very fast-paced game. Curr Opin Plant Biol 13:714–723
3. Szymanski DB (2005) Breaking the WAVE complex: the point of Arabidopsis trichomes. Curr Opin Plant Biol 8:103–112
4. Pei W, Du F, Zhang Y et al (2012) Control of the actin cytoskeleton in root hair development. Plant Sci 197:10–18
5. Fu Y, Gu Y, Zheng Z et al (2005) Arabidopsis interdigitating cell growth requires two antagonistic pathways with opposing action on cell morphogenesis. Cell 120:687–700
6. Žárský V, Cvrčková F, Potocký M et al (2009) Exocytosis and cell polarity in plants: exocyst and recycling domains. New Phytol 183:255–272
7. Ueda K, Matsuyama T, Hashimoto T (1999) Visualization of microtubules in living cells of transgenic *Arabidopsis thaliana*. Protoplasma 206:201–206
8. Nakamura M, Naoi K, Shoji T et al (2004) Low concentrations of propyzamide and oryzalin alter microtubule dynamics in Arabidopsis epidermal cells. Plant Cell Physiol 45:1330–1334
9. Marc J, Granger CL, Brincat J et al (1998) A GFP-MAP4 reporter gene for visualizing cortical microtubule rearrangements in living epidermal cells. Plant Cell 10:1927–1939
10. Van Damme D, Van Poucke K, Boutant E et al (2004) In vivo dynamics and differential microtubule-binding activities of MAP65 proteins. Plant Physiol 136:3956–3967
11. Chan J, Calder G, Fox S et al (2005) Localization of the microtubule end binding protein EB1 reveals alternative pathways of spindle development in Arabidopsis suspension cells. Plant Cell 17:1737–1748
12. Dhonukshe P, Gadella TWJ (2003) Alteration of microtubule dynamic instability during preprophase band formation revealed by yellow fluorescent protein-CLIP170 microtubule plus-end labeling. Plant Cell 15:597–611
13. Kost B, Spielhofer P, Chua NH (1998) A GFP-mouse talin fusion protein labels plant actin filaments in vivo and visualizes the actin cytoskeleton in growing pollen tubes. Plant J 16:393–401
14. Sheahan MB, Staiger CJ, Rose RJ et al (2004) A green fluorescent protein fusion to actin-binding domain 2 of Arabidopsis fimbrin highlights new features of a dynamic actin cytoskeleton in live plant cells. Plant Physiol 136:3968–3978
15. Voigt B, Timmers ACJ, Šamaj J et al (2005) GFP-FABD2 fusion construct allows in vivo visualization of the dynamic actin cytoskeleton in all cells of Arabidopsis seedlings. Eur J Cell Biol 84(6):595–608
16. Era A, Tominaga M, Ebine K et al (2009) Application of Lifeact reveals F-actin dynamics in *Arabidopsis thaliana* and the liverwort, Marchantia polymorpha. Plant Cell Physiol 50:1041–1048
17. Hashimoto T (2002) Molecular genetic analysis of left-right handedness in plants. Philos Trans R Soc Lond B Biol Sci 357:799–808
18. Ketelaar T, Anthony RG, Hussey PJ (2004) Green fluorescent protein-mTalin causes defects in actin organization and cell expansion in Arabidopsis and inhibits actin depolymerizing factor's actin depolymerizing activity in vitro. Plant Physiol 136:3990–3998
19. Cvrčková F, Grunt M, Žárský V (2012) Expression of GFP-mTalin reveals an actin-related role for the Arabidopsis Class II formin AtFH12. Biologia Plantarum 56:431–440
20. Staiger CJ, Sheahan MB, Khurana P et al (2009) Actin filament dynamics are dominated by rapid growth and severing activity in the Arabidopsis cortical array. J Cell Biol 184: 269–280
21. Smertenko A, Deeks MJ, Hussey P (2010) Strategies of actin reorganisation in plant cells. J Cell Sci 123:3019–3028
22. Vizcay-Barrena G, Webb S, Martin-Fernandez M et al (2011) Subcellular and single-molecule imaging of plant fluorescent proteins using total internal reflection fluorescent microscopy (TIRFM). J Exp Bot 62:5419–5428
23. Wan Y, Ash WM 3rd, Fan L et al (2011) Variable-angle total internal reflection fluorescence microscopy of intact cells of *Arabidopsis thaliana*. Plant Methods 7:27
24. Sparkes I, Graumann K, Martiniere A et al (2011) Bleach it, switch it, bounce it, pull it: using laser to reveal plant cell dynamics. J Exp Bot 62:1–7
25. Rosero A, Žárský V, Cvrčková F (2013) AtFH1 formin mutation affects actin filament and microtubule dynamics in *Arabidopsis thaliana*. J Exp Bot 64:585–597
26. van der Honing H, Kieft H, Emons A et al (2012) Arabidopsis VILLIN2 and VILLIN3 are required for the generation of thick actin filament bundles and for directional organ growth. Plant Physiol 58:1426–1438
27. Higaki T, Kutsuna N, Sano T et al (2008) Quantitative analysis of changes in actin microfilament contribution to cell plate development in plant cytokinesis. BMC Plant Biol 8:80

28. Higaki T, Kutsuna N, Sano T et al (2010) Quantification and cluster analysis of actin cytoskeletal structures in plant cells: role of actin bundling in stomatal movement during diurnal cycles in Arabidopsis guard cells. Plant J 61:156–165
29. Sampathkumar A, Lindeboom J, Debolt S et al (2011) Live cell imaging reveals structural associations between the actin and microtubule cytoskeleton in Arabidopsis. Plant Cell 23:2302–2313
30. Ketelaar T, Allwood EG, Anthony RG et al (2004) The actin-interacting protein AIP is essential for actin organization and plant development. Curr Biol 14:149
31. Abramoff MD, Magelhaes PJ, Ram SJ (2004) Image processing with ImageJ. Biophotonics International 11:36–42
32. Collins T (2007) ImageJ for microscopy. Biotechniques 43:S25–S30
33. Henty JL, Bledsoe S, Khurana P et al (2011) Arabidopsis actin depolymerizing factor 4 modulates the stochastic dynamic behavior of actin filaments in the cortical array of epidermal cells. Plant Cell 23:3711–3726
34. Li J, Henty JL, Huang S et al (2012) Capping protein modulates the dynamic behavior of actin filaments in response to phosphatidic acid in Arabidopsis. Plant Cell 24:3742–3754
35. Yao M, Wakamatsu Y, Itoh T et al (2008) Arabidopsis SPIRAL2 promotes uninterrupted microtubule growth by suppressing the pause state of microtubule dynamics. J Cell Sci 121:2372–2381

# 4. DISCUSION

Angiosperm FH2 proteins form a large family of paralogs: A. thaliana has 21 formin-encoding genes divided in two groups according to clade-specific domain structure, Class I and II (Deeks et al., 2002; Grunt et al., 2008). The phenotypic characterization of T-DNA mutants with insertions in the main housekeeping Arabidopsis Class I membrane-targeted formin AtFH1 (At3g25500) and its closest relative, AtFH2 (At2g43800) grown on standard or cytoskeletal inhibitors (LatB or Oryz) medium allowed us to uncover the role of formins in cytoskeleton organization and dynamics, and in the cellular-tissue development.

## 4.1. Role of AtFH1and AtFH2 in actin and microtubule organization and dynamics

Altered balance between fine actin filaments and bundles was observed in formin mutants; thicker, more compact and less dynamic actin bundles were observed in roots of fh1 mutant plants (Rosero et al., 2013), similar to some actin regulators mutants, such as adf4 (Henty et al., 2011) or aip1 (Ketelaar et al., 2004). AtFH1 was previously proposed to participate in regular actin nucleation and elongation (Michelot et al., 2005; Michelot et al., 2006) and in actin filaments anchoring across the plasmalemma into the cell wall (Martiniere et al., 2011), which may effectively constrain bundling. Our observations in roots (Rosero et al., 2013) were confirmed in cotyledon pavement cells of both fh1 and fh2 mutants (Rosero et al., 2013 submitted). Decreased availability of these proteins might thus disrupt

the association between actin and cell wall, by reduction of new filaments polymerization from cell membrane and rendering some fine cortical actin filaments free to move and bundle (perhaps with participation of other members of the formin family), with the net effect being a shift in the balance between fine, presumably cortically anchored filaments and massive, to more stable bundles (Rosero et al., 2013 submitted). The less dense and more dynamic microtubules found in the formin mutants are the subsequent response to the absence or reduction of the restrictions on their distribution or movement imposed by cell wall-anchored formin-actin complexes (Martiniere et al., 2011). Consistent with AtFH1 participating in actin-microtubule cross-talk, LatB aggravated or phenocopied also the presumably microtubule-related cell expansion phenotypes in roots (Rosero et al., 2013).

### 4.2. Formin inhibition mimics the mutant phenotype

The small molecule SMIFH2, a 2-Thiooxodihydropyrimidine-4,6-dione derivative, is an inhibitor of FH2 domain-mediated actin assembly, active in vitro against several formins, and eliciting actin-related phenotypes in yeast and mammalian cells (Rizvi et al., 2009).

In plants, SMIFH2 reduced root growth, increased microfilament bundling and decreased cortical microtubule density (Rosero et al., 2013), increased cell lobing and slowed down the movement of CLC-GFP (GFP-tagged clathrin light chain) dots (Rosero, 2013 submitted) comparable with the LatB effect on endosomal movements (Voigt et al., 2005). The use of SMIFH2 in plants was used as a tool

to confirme the phenotypes observed in formin mutants and to understand their role in cytoskeleton arrangement and turnover, their downstreaming effect in cell membrane recycling.

### 4.3. Role of AtFH1 in root isotropic growth

Consistent with primarily actin-related formin function, fh1 mutants showed increased sensitivity to the actin polymerization inhibitor Latrunculin B (LatB). Low doses of LatB, inhibiting primary root growth and causing radial swelling in young seedlings, and enhancing the phenotype of some cytoskeletal mutations (Collings et al., 2006). The "synthetic phenotype" in roots and/or root hairs induced by LatB in AtFH8 (Xue et al., 2011) and AtFH12 (Cvrčková et al., 2012) formin mutants was also observed in the fh1 mutants. Low doses of LatB seem to altere cell expansion rather than cell division (Baluška et al., 2001), shorter and thicker roots of LatB-treated mutants consisted of shorter and wider cells were observed. LatB can also disrupt intracellular membrane trafficking (Zhang et al., 2010), it is crucial for polar auxin transport and auxin-mediated effects on root growth (Rahman et al., 2007). LatB-treated fh1 mutants exhibited also malformed root hairs, in our experiments mainly root hair bases were affected, resembling the phenotype of actin (act2) mutants (Gilliland et al., 2002; Nishimura et al., 2003) and suggesting defective focusing of exocytosis during the bulge stage.

Disruption of microtubules affected fh1 mutants and wt similarly. However, mutants exhibit increased sensitivity to Oryz in the presence of LatB and showed altered microtubule organization and dynamics, suggesting that AtFH1 may

participate in a cross-talk between microfilaments and microtubules. Mutants had more dynamic microtubules and were partially resistant towards the root growth inhibition, radial root swelling and root twisting induced by the GFP-MAP4 marker and Taxol (Rosero et al., 2013), which can stabilize and bundle microtubules (Granger and Cyr, 2001; Hashimoto, 2002).

### 4.4. Role of AtFH1and AtFH2 in interdigitating pavement cell growth

At early steps of lobed epidermal cell development, elongated polygons are generated by cell elongation taking place preferentially along the leaf axis (Zhang et al., 2011a). This polarity is regulated by the interplay of ROP-GTPases, cytoskeleton and auxin transport (Xu et al., 2010; see Pietra and Grebe, 2010). Mutation AtFH1 and AtFH2 or formin inhibition by SMIFH2 reduced the leaf polarity affecting the planar pavement cell expansion by increasing cell size and lobing (Rosero et al., 2013 submitted).

The currently accepted model of interdigitating growth highlights the role of microtubule bands in neck formation, while lobe expansion depends on patches of microfilaments (Fu et al., 2005; Fu et al., 2009; Xu et al., 2010). Many proteins that regulate actin–microtubule arrangement and dynamics which are involved in pavement cells morphogenesis (see Mathur, 2006). The Rho of plant (ROP) GTPases and their RIC family interactors play an important role, microtubule bands in neck regions are induced by the RIC1/ROP6 pathway which antagonizes the RIC4/ROP2 pathway, promoting microfilament assembly in the lobes (Fu et al., 2005; Fu et al., 2009). Recently, the important role of microtubule turnover

induced by ROP6 GTPase for organizing paralleled cortical microtubule arrays was reported (Lin et al., 2013). Changes of spatial distribution of either cortical diffuse F-actin or actin bundles in Arabidopsis leaf pavement cells in mutants of Arp2/3 subunit genes (arp2-1, arp2-2, arp3-1, and arpc5-1) dramatically reduced lobe height (Li et al., 2003). Formins modulate cytoskeleton arrangement and dynamics, changes in actin filament density and reduction in their dynamics that probably affect the microtubules stability were observed in fh1 mutant which also showed alterations in pavement cell size and lobing (Rosero et al., 2013 submitted).

Absence of AtFH1 and AtFH2 showed to decreased membrane turnover by analogy with other systems via modulating actin filament arrangement and turnover, probably due the role of microfilament assembly anchorage to plasmalemma (Martiniere et al., 2011), both vesicle formation and transport could be affected. The inhibition of PIN1 endocytosis results in PIN1 polarization that enhances the lobe growth (Nagawa et al., 2012), thus both accumulation of cortical actin filaments and reduction of single actin filaments affect endocytosis.

In the other hand, cell expansion, in general, depends upon microtubule turnover (Shaw et al., 2003; Wang et al., 2007) which affects cellulose microfibrils arrangement (Sugimoto et al., 2003; Panteris and Galatis, 2005; Bringmann et al., 2012) and formation of the neck bands in fact requires reorganization of branched microtubules (Lin et al., 2013). Microtubule stabilization generally decreases growth anisotropy (Bibikova et al., 1999; Mathur, 2004), and in pavemental cells it reduces cell lobing as observed in GFP-MAP4 expressing plants. Thus, formin mutations appear to destabilize microtubules, or counter the stabilizing effect of

GFP-MAP4 (Rosero et al., 2013). Observations using cytoskelelal inhibitors LatB and Oryz support the notion that the effects of formin mutations on pavement cell lobing are at least in part due to alterations in microtubule dynamics that themselves may be secondary to changes in the actin architecture (Rosero et al., 2013 submitted), consistent with previous reports of actin-microtubules crosstalk (Collings et al., 2006; Sampathkumar et al., 2011; Smertenko et al., 2010).

### 4.5. Gametophytic function of AtFH1 and AtFH2

AtFH1 and/or AtFH2 formins are required for normal gametophytic development, both defective pollen grains and aborted seeds were observed in siliques of self-pollinated FH1/fh1FH2/fh2 or fh1/fh1 FH2/fh2 plants. This observation was confirmed in crosses of fh1 with plants tagged by GFP-mTalin, an actin marker known to perturb actin cytoskeleton dynamics (Ketelaar et al., 2004b) that also exhibits synthetic lethality with a mutation in another formin gene, AtFH12 (Cvrcková et al., 2012). The observed pollen grain defects included nuclear abnormalities which are associated with microtubule-mitosis defects (Pastuglia et al., 2006) and interestingly, mutants in a microtubule-binding Class II formin, AtFH14, exhibit defects in meiosis (Li et al., 2010). Ultrastructural aberrations in tapetum and endothecial cells of the formin-impaired plants, including detachement of the plasma membrane from the cell wall and presence of amorphous lipid bodies suggest a possible downstream effects on intracellular dynamics including the endomembrane system (Rosero et al., 2013 submitted).

## 4.6. Formins contribute to membrane trafficking and tissue and organ development

In mammalian and yeast cells, the participation of actin cytoskeleton in endocytosis is well described (see Kaksonen et al., 2006; Mooren et al., 2012). F-actin and its nucleators such as Arp2/3 contribute to vesicle formation (Yarar et al., 2005; Ferguson et al., 2009) and formins regulate endosomes motility by stabilizing their association with the actin cytoskeleton (Gasman et al., 2003), by modulation of actin and microtubule organization (Gachet and Hyams, 2005) and actin cable nucleation and elongation which are required for Rho1-mediated endocytosis (Prosser et al., 2011). These reported roles of actin cytoskeleton and formins suggest a way how the disruption of formin function might also affect membrane trafficking, as a downstream response to modifications of cytoskeletal organization and dynamics, which is involved in gametophyte development and interdigitating cell growth (Rosero et al., 2013 submitted).

The role of endocytosis during interdigitating cell growth was probed using TyrA23, an endocytosis inhibitor, which increased cell lobing and its effect was stronger in fh1 plants. The formin inhibitor SMIFH2 slowed down the movement of CLC-GFP dots comparable with the LatB effect on endosomal movements (Voigt et al., 2005), confirming thus the important role of cytoskeleton in cell membrane recycling. The ultrastructure of fh1/fh1 FH2/fh2 pavement cells showed plasma membrane invaginations and thickened cell walls similar to the phenotype of dynamin mutants drp1(Carter et al., 2004) and adl1A-2 (Kang et al., 2003), which may be due of inhibited membrane recycling. AtFH1 and AtFH2 participate in endocytosis via modulating actin filament arrangement and

turnover, probably due the role of microfilament assembly anchorage to plasmalemma (Martiniere et al., 2011), both vesicle formation and transport could be affected; thus insufficient formin function results in decreased membrane trafficking that also affect the distribution of PIN auxin carriers. Thus, alterations in cytoskeleton turnover affect pavement cell lobe development as reported previously by localized inhibition of PIN1 endocytocis induces PIN1 polarization in the lobing region (Nagawa et al., 2012), affect auxin transport and auxin-carriers recycling (Geldner et al., 2001; Dhonukshe et al., 2008) and auxin-dependent developmental processes as vascular tissue patterning (Rosero et al., 2013 submitted). The role of cytoskeleton in vascular pattern was observed in formin mutants and using SMIFH2, LatB and Oryz treatments. Auxin maxima visualized by DR5-GFP expression were altered in formin mutants (Rosero et al., 2013 submitted), consistent with possible defects in PIN polarity due to alterations in their recycling (Geldner et al., 2001; Dhonukshe et al., 2008).

# 5. CONCLUSIONS

Formin AtFH1 (At3g25500) and its closest relative, AtFH2 (At2g43800) modulate both actin and microtubule organization and dynamics and their mutations produced root growth sensitivity to LatB, defects in interdigitating cell expansion, abnormal gametophyte development and alterations in the vascular pattern. These defects are associated with the downstream effect of formin mutations in membrane trafficking. This phenotype was mimicked by SMIFH2 Formin inhibitor.

# 6. REFERENCES


Abe, T., and Hashimoto, T. (2005). Altered microtubule dynamics by expresion of modified alfa-tubulin protein causes right-handed helical growth in transgenic Arabidopsis plants. The plant Journal 43: 191-204.

Adamo, J., Rossi, G., and Brennwald, P. (1999). The Rho GTPase Rho3 has a direct role in exocytosis that is distinct from its role in actin polarity. Mol. Bio. Cell 10: 4121-4133.

Ambrose, S., Shoji, T., Kotzer, A., Pighin, J., and Wasteneys, G. (2007). The Arabidopsis CLASP Gene Encodes a Microtubule-Associated Protein Involved in Cell Expansion and Division. The plant Cell 19: 2763-2775.

Aspenstrom, P. (2010). Formin-binding proteins: Modulators of formin-dependent actin polimerization. Biochimica et Biophysica Acta (BBA) 1803: 174-182.

Baluska, F., Jasik, J., Edelmann, H., Salajova, T., and Volkmann, D. (2001). Latrunculin B-Induced Plant Dwarfism: Plant Cell Elongation Is F-Actin-Dependent. Developmental Biology 231: 113-124.

Banno, H., and Chua, N. (2000). Characterization of the Arabidopsis Formin-Like Protein AFH1 and Its Interacting Protein. Plant Cell Physiology 41: 617-626.

Bendezu, F., and Martin, S. (2011). Actin cables and the exocyst form two independent morphogenesis pathways in the fission yeast. Mol. Bio. Cell 22: 44-53.

Bibikova, T., Blancaflor, E., and Gilroy, S. (1999). Microtubules regulate tip growth and orientation in root hairs of Arabidopsis thaliana. The Plant Journal 17: 657-665.

Blanchoin, L., Boujemaa-Paterski, R., Henty, J., Khurana, P., and Staiger, C. (2010). Actin dynamics in plant cells: a team effort from multiple proteins orchestrates this very fast-paced game. Curr. Opinion Plant Biol. 13: 714-723.

Bringmann, M., Li, E., Sampathkumar, A., Kocabek, T., Hauser, M., and Persson, S. (2012). POM-POM2/CELLULOSE SYNTHASE INTERACTING1 is essential for the functional association of cellulose synthase and microtubules in Arabidopsis. The Plant Cell 24: 163-177.

Carter, C., Bednarek, S., and Raikhel, N. (2004). Membrane trafficking in plants: new discoveries and approaches. Curr. Opinion Plant Biol. 7: 701-707.

Collings, D., Lill, A., Himmelspach, R., and Wasteneys, G. (2006). Hypersensitivity to cytoskeletal antagonists demonstrates microtubule-microfilament cross-talk in the control of root elongation in Arabidopsis thaliana. New Phytologist 170: 275-290.

Cvrcková, F., Grunt, M., and Zarsky, V. (2012). Expression of GFP-mTalin reveals an actin-related role for the arabidopsis class II formin AtFH12. Biologia Plantarum 3: 431-440.

Cvrckova, F. (2012). Formins: emerging players in the dynamic plant cell cortex. Scientifica.ID: 712605: doi: 10.6064/2012/712605

Deeks, M., Fendrych, M., Smertenko, A., Bell, K., Oparka, K., Cvrcková, F., Zarsky, V., and Hussey, P. (2010). The plant formin AtFH4 interacts with both actin and microtubules, and contains a newly identified microtubule-binding domain. J. Cell Sci. 123: 1209-1215.

Deeks, M., Hussey, P., and Davies, B. (2002). Formins: intermediates in signal-transduction cascades that affect cytoskeletal reorganization. Trends in Plant Science 7: 492-498.

DeWard, A., and Alberts, A. (2008). Microtubule stabilization: Formins assert their independence. Current Biology 18: 605-608.

Dhonukshe, P., Grigoriev, I., Fischer, R., Tominaga, M., Robinson, D., Hasek, J., Paciorek, T., Petrasek, J., Seifertova, D., Tejos, R., Meisel, L., Zazimalova, E., Gadella,T., Stierhof, Y., Ueda, T., Oiwaf, K., Akhmanova, A., Brock, R., and

Spang, A. (2008). Auxin transport inhibitors impair vesicle motility and actin cytoskeleton dynamics in diverse eukaryotes. PNAS 105: 4489-4494.

Dobrak, B., Franklin-Tong, V., and Staiger, C. (2004). The role of the actin cytoskeleton in plant cell signaling. New Phytologist 163: 13-30.

Dong, Y., Pruyne, D., and Bretscher, A. (2003). Formin-dependent actin assembly is regulated by distinct modes of Rho signaling in yeast. J. cell Biol. 161: 1081-1092.

Evangelista, M., Pruyne, D., Amber, D., Boone, C., and Bretscher, A. (2002). Formins direct Arp2/3-independent actin filament assembly to polarize cell growth in yeast. Nat. Cell Biol. 4: 260-269.

Ferguson, S., Raimondi, A., Paradise, S., Shen, H., Mesaki, K., Ferguson, A., Destaing, O., Ko, G., Takasaki, J., Cremona, O., Toole, E., and De Camilli, P. (2009). Coordinated actions of actin and BAR proteins upstream of dynamin at endocytic Clathrin-coated pits. Developmental Cell 17: 811-822.

Fu, Y., Xu, T., Wen, M., and Yang, Z. (2009). A ROP GTPase signaling pathway controls cortical microtubule ordering and cell expansion in Arabidopsis. Current Biology 19: 1827-1832.

Fu,Y., Gu, Y., Zheng, Z., Wasteneys, G., and Yang, Z. (2005). Arabidopsis Interdigitating Cell GrowthRequires Two Antagonistic Pathways withOpposing Action on Cell Morphogenesis. Cell 120: 687-700.

Gachet, Y., and Hyams, J. (2005). Endocytosis in fission yeast is spatially associated with the actin cytoskeleton during polarised cell growth and cytokinesis. J. Cell Sci. 118: 4231-4242.

Gasman, S., Kalaidzidis, Y., and Zerial, M. (2003). RhoD regulates endosome dynamics through Diaphanous-related Formin and Src tyrosine kinase. Nature Cell Biol. 5: 195-204.

Geldner, N., Friml, J., Stierhof, Y., Jurgens, G., and Palme, K. (2001). Auxin transport inhibitors block PIN1 cycling and vesicle trafficking. Nature 413: 425-428.

Gilliland, L., Pawloski, L., Kandasamy, M., and Meagher, R. (2003). Arabidopsis actin gene ACT7 plays an essential role in germination and root growth. The Plant Journal 33: 319-328.

Guimil, S., and Dunand, C. (2007). Cell growth and differentiation in Arabidopsis epidermal cells. J. Exp. Bot. 58: 3829-3840.

Henty, J., Bledsoe, S., Khurana, P., Meagher, R., Day, B., Blanchoin, L., and Staiger, C. (2011). Arabidopsis Actin Depolymerizing Factor4 Modulates the Stochastic Dynamic Behavior of Actin Filaments in the Cortical Array of Epidermal Cells. The Plant Cell 23: 3711-3726.

Hussey, P., Ketelaar, T., and Deeks, M. (2006). Control of the Actin Cytoskeleton in Plant Cell Growth. Annu. Rev. Plant. Biol. 57: 109-125.

Chen, H., Bernstein, B., and Bamburg, J. (2000). Regulating actin-filament dynamics in vivo. Trends in Biochemical Sciences 25: 19-23.

Chesarone, M., DuPage, A., and Goode, B. (2010). Unleashing formins to remodel the actin and microtubules cytoskeletons. Nature Reviews. Molecular Cell Biology 11: 62-74.

Cheung, A., and Wu, H. (2004). Overexpression of an Arabidopsis Formin Stimulates Supernumerary Actin Cable Formation from Pollen Tube Cell Membrane. The Plant Cell 16: 527-269.

Kaksonen, M., Toret, C., and Brubin, D. (2006). Harnessing actin dynamics for clathrin-mediated endocytosis. Nature Reviews. Molecular Cell Biology 7: 404-414.

Kang, B., Busse, J., and Bednarek, S. (2003). Members of the Arabidopsis Dynamin-Like Gene Family, ADL1, are essential for plant cytokinesis and polarized cell growth. The Plant Cell 15: 899-913.

Ketelaar, T., Allwood, E., Anthony, R., Voigt, B., Menzel, D., and Hussey, P. (2004a). The actin-interacting protein AIP is essential for actin organization and plant development. Current Biol. 14: 145-149.

Ketelaar, T., Anthony, R., and Hussey, P. (2004b). Green Fluorescent Protein-mTalin causes defects in actin organization and cell expansion in Arabidopsis and inhibits actin depolymerizing factor's actin depolymerizing activity in Vitro. Plant Physiology 36: 3990-3998.

Kotzer, A., and Wasteneys, G. (2006). Mechanism behind the puzzle: microtubule-microfilament cross-talk in pavement cell formation. Can. J. Bot. 84: 594-603.

Li, J., Henty-Ridilla, J., Huang, S., Wang, X., Blanchoin, L., and Staiger, C. (2012). Capping protein modulates the dynamic behavior of actin filaments in response to phosphatidic acid in Arabidopsis. The Plant Cell 24: 3742-3754.

Li, S., Blanchoin, L., Yang, Z., and Lord, E. (2003). The putative Arabidopsis Arp2/3 complex controls leaf cell morphogenesis. Plant Physiology 132: 2034-2044.

Li, Y., Shen, Y., Cai, C., Zhong, C., Zhu, L., Yuan, M., and Ren, H. (2010). The Type II Arabidopsis Formin 14 Interacts with Microtubules and Microfilaments to Regulate Cell Division. The Plant Cell 22: 2710-2726.

Lin, D., Cao, L., Zhou, Z., Zhu, L., Ehrhardt, D., Yang, Z., and Fu, Y. (2013). Rho GTPase signaling activates microtubule severing to promote microtubule ordering in Arabidopsis. Current Biology 23: 290-297.

Martiniere, A., Gayral, P., Hawes, C., and Runions, J. (2011). Building bridges: formin 1 of Arabidopsis forms a connection between the cell wall and the actin cytoskeleton. The Plant Journal 66: 354-365.

Mathur, J., Mathur, N., Kernebeck, B., and Hulskamp, M. (2003). Mutations in Actin-Related Proteins 2 and 3 Affect Cell Shape Development in Arabidopsis. The Plant Cell 15:, 1632-1645.

Mathur, J. (2004). Cell shape development in plants. Trends in Plant Science 9: 583-590.

Mathur, J. (2006). Local interactions shape plant cells. Current Opinion in Cell Biology 18: 40-46.

Michelot, A., Derivery, E., Paterski-Boujemma, R., Guerin, C., Huang, S., Parcy, F., Staiger, C., and Blanchoin, L. (2006). A novel mechanism for the formation of actin-filament bundles by a nonprocessive formin. Current Biology 16: 1924-1930.

Michelot, A., Guerin, C., Huang, S., Ingouff, M., Richard, S., Rodiuc, N., Staiger, C., and Blanchoin, L. (2005). The formin homology 1 domain modulates the actin nucleation and bundling activity of Arabidopsis Formin 1. The Plant Cell 17: 2296-2313.

Mooren, O., Galletta, B., and Cooper, J. (2012). Roles of actin assembly in endocytosis. Annu. Rev. Biochem. 81: 661-686.

Nagawa, S., Xu, T., Lin, D., Dhonukshe, P., Zang, X., Friml, J., Scheres, B., Fu, Y., and Yang, Z. (2012). ROP GTPase-dependent actin microfilaments promote PIN1 polarization by localized inhibition of Clathrin-dependent endocytosis. PLOS Biology 10: e1001299, doi:10.1371/journal.pbio.1001299.

Nakano, K., Imai, J., Arai, R., Toh-E, A., Matsui, Y., and Mabuchi, I. (2002). The small GTPase Rho3 and the diaphanous/formin For3 function in polarized cell growth in fission yeast. J. Cell Sci. 115: 4629-4639.

Palazzo, A., Cook, T., Alberts, A., and Gundersen, G. (2001). mDia mediates Rho-regulated formation and orientation of stable microtubules. Nat Cell Biol. 3: 723-729.

Panteris, E., and Galatis, B. (2005). The morphogenesis of lobed plant cells in the mesophyll and epidermis: organization and distinct roles of cortical microtubules and actin filaments. New Phytologist 167: 721-732.

Parton, R., Fischer-Parton, S., Watahiki, M., and Trewavas, A. (2001). Dynamics of the apical vesicle accumulation and the rate of growth are related in individual pollen tubes. J. Cell Sci. 114: 2685-2695.

Pastuglia, M., Azimzadeh, J., Goussot, M., Camilleri, C., Belcram, K., Evrard, J., Schmit, A., Guerche, P., and Bouchez, D. (2006). γ-Tubulin Is Essential for Microtubule Organization and Development in Arabidopsis. The Plant Cell 18: 1412-1425.

Petrasek, J., and Schwarzerova, K. (2009). Actin and microtubule cytoskeleton interactions. Current Opinion in Plant Biology 12: 728-734.

Pietra, S., and Grebe, M. (2010). Auxin paves the way for planar morphogenesis. Cell 43: 29-31.

Pollard, T., and Cooper, J. (2009). Actin, a central player in cell Shape and movement. Science 326: 1208-1212.

Prosser, D., Drivas, T., Maldonado, L., and Wendland, B. (2011). Existence of a novel clathrin-independent endocytic pathway in yeast that depends on Rho1 and formin. J. Cell Sci. 195: 657-671.

Pruyne, D., and Bretscher, A. (2000). Polarization of cell growth in yeast II. The role of the cortical actin cytoskeleton. J. Cell Sci. 113: 571-585.

Qiu, J., Jilk, R., Marks, M., and Szymanski, D. (2002). The Arabidopsis SPIKE1 Gene is Requiered for Normal Cell Shape Control and Tissue Development. The Plant Cell 14: 101-118.

Rahman, A., Bannigan, A., Sulaman, W., Pechter, P., Blancaflor, E., and Baskin, T. (2007). Auxin, actin and growth of the Arabidopsis thaliana primary root. The Plant Journal 50: 514-528.

Ridley, A. (2006). Rho GTPases and actin dynamics in membrane protrusions and vesicle trafficking. Trends in Cell Biol. 6: 522-529.

Rosero, A., Zarsky, V., and Cvrckova, F. (2013). AtFH1 formin mutation affects actin filament and microtubule dynamics in Arabidopsis thaliana. J. Exp. Bot. 64: 585-597.

Rosero, A.; Grunt, M.; Schiebertová, P.; Žárský, V.; Cvrčková, F. Arabidopsis FH1 and FH2 formins affect pavement cell shape and vascular patterning by modulating cytoskeleton and membrane dynamics. Plant Cell (Submitted).

Samaj, J., Muller, J., Beck, M., Bohm, N., and Menzel, D. (2006). Vesicular trafficking, cytoskeleton and signalling in root hairs and pollen tubes. Trends in Plant Sci. 11: 594-600.

Sampathkumar, A., Lindeboom, J., Debolt, S., Gutierrez, R., Ehrhardt, D., Ketelaar, T., and Persson, S. (2011). Live cell imaging reveals structural associations between the actin and microtubule cytoskeleton in Arabidopsis. The Plant Cell 23: 2302-2313.

Shaw, S., Kamyar, R., and Ehrhardt, D. (2003). Sustained Microtubule Treadmilling in Arabidopsis Cortical Arrays. Science 300: 1715-1718.

Schmidt, A., and Hall, M. (1998). Signaling to the actin cytoskeleton. Annu. Rev. Cell Dev. Biol. 14: 305-338.

Smertenko, A., Deeks, M., and Hussey, P. (2010). Strategies of actin reorganisation in plant cells. J. Cell Sci. 123: 3019-3028.

Smith, L., and Oppenheimer, D. (2005). Spatial control of cell expansion by the plant cytoskeleton. Annu. Rev. Cell Dev. Biol. 21: 271-295.

Staiger, C., and Blanchoin, L. (2006). Actin dynamics: old friends with new stories. Current Opinion in Plant Biol. 9: 554-562.

Staiger, C., Sheahan, M., Khurana, P., Wang, X., McCurdy, D., and Blanchoin, L. (2009). Actin filament dynamics are dominated by rapid growth and severing activity in the Arabidopsis cortical array. J. Cell Biol. 182: 269-280.

Sugimoto, K., Himmelspach, R., Williamson, R., and Wasteneys, G. (2003). Mutation or drug-dependent microtubule disruption causes radial swelling without altering parallel cellulose microfibril deposition in Arabidopsis root cells. The Plant Cell 5: 1414-1429.

Szymanski, D., and Cosgrove, D. (2009). Dynamic coordination of cytoskeletal and cell wall systems during plant cell morphogenesis. Current Biol. 19: 800-811.

Thitamadee, S., Tuchihara, K., and Hashimoto, T. (2002). Microtubule basis for left-handed helical growth in Arabidopsis. Nature 417: 193-196.

van Gisbergen, P., and Bezanilla, M. (2013). Plant formins: membrane anchors for actin polymerization. Trends in Cell Biology 23: 227-233.

Vaskovicova, K., Žárský, V., Rosel, D., Nikolic, M., Buccione, R., Cvrčkova, F., and Brabek, J. (2013). Invasive cells in animals and plants: searching for LECA machineries in later eukaryotic life. Biology Direct 8. Doi: 101186/1745-6.

Vaughn, L., Baldwin, K., Jia, G., Verdonk, J., Strohm, A., and Masson, P. (2010). The cytoskeleton and root growth behavior. In: The Plant Cytoskeleton: Advances in plant biology, B. Liu, ed ( Springer), pp. 307-326.

Voigt, B., Timmers, A., Samaj, J., Hlavacka, A., Ueda, T., Preuss, M., Nielsen, E., Mathur, J., Emans, N., Stenmark, H., Nakano, A., Baluska, F., and Menzel, D. (2005). Actin-based motility of endosomes is linked to the polar tip growth of root hairs. Europ. J. Cell Biol. 84: 609-621.

Wang, X., Zhu, L., Liu, B., Wang, C., Jin, L., Zhao, Q., and Yuan, M. (2007). Arabidopsis MICROTUBULE-ASSOCIATED PROTEIN18 functions in directional cell growth by destabilizing cortical microtubules. The Plant Cell 9: 877-889.

Wen, Y., Eng, C., Shmoranzer, J., Cabrera, N., Morris, E., Chen, M., Wallar, B., Alberts, A., and Gundersen, G. (2004). EB1 and APC bind to mDia to stabilize microtubules downstream of Rho and promote cell migration. Nature Cell Biology 6: 820-830.

Xu, T., Wen, M., Nagawa, S., Fu, Y., Chen, J., Wu, M., Perrot-Rechenmann, C., Friml, J., Jones, A., and Yang, Z. (2010). Cell Surface -and Rho GTPase- Based Auxin Signaling Controls Cellular Interdigitation in Arabidopsis. Cell 143: 99-110.

Yalovsky, S., Bloch, D., Sorek, N., and Kost, B. (2008). Regulation of membrane trafficking, cytoskeleton dynamics, and cell polarity by ROP/RAC GTPases. Plant Physiology 147: 1527-1543.

Yarar, D., Waterman-Storer, C., and Shmid, S. (2005). A dynamic actin cytoskeleton functions at multiple stages of Clathrin-mediated endocytosis. Mol. Biol. Cell 16: 964-975.

Žárský, V., Cvrčkova, F., Potocký, M., and Hala, M. (2009). Exocytosis and cell polarity in plants – exocyst and recycling domains. New Phytologist 183: 255-272.

Zhang, C., Halsey, L., and Szymanski, D. (2011). The development and geometry of shape change in Arabidopsis thaliana cotyledon pavement cells. BMC Plant Biol. 11: doi 10.1186/1471-2229-11-2.

Zhang, X., Bi, E., Novick, P., Kozminski, K., Lipschutz, J., and Guo, W. (2001). Cdc42 interacts with the exocyst and regulates polarized secretion. J. Biol. Chem. 76: 46745-46750.

Zhang, Y., He, J., and McCormick, S. (2010). Interdependence of endomembrane trafficking and actin dynamics during polarized growth of arabidopsis pollen tubes. Plant Physiology 152: 2200-2210.

Zhang, Z., Zhang, Y., Tan, H., Wan, Y., Li, G., Liang, W., Yuan, Z., Hu, J., Ren, H., and Zhang, D. (2011b). RICE MORPHOLOGY DETERMINANT encodes the type II formin FH5 and regulates rice morphogenesis. The Plant Cell 23: 681-700.